

**IFS DOCUMENTATION – Cy47r3**  
**Operational implementation 12 Oct 2021**

**PART I: OBSERVATIONS**

© Copyright 2020-

European Centre for Medium-Range Weather Forecasts  
Shinfield Park, Reading, RG2 9AX, UK

The content of this document is available for use under a Creative Commons Attribution 4.0 International Public License. See the terms at <https://creativecommons.org/licenses/by/4.0>.

## REVISION HISTORY

### Changes since CY43R1

- Minor change to text in subsection 'Conventional observations'.
- New subsection on 'Additional error inflation for dropsondes'.

### Changes since CY41R2

- Major rewrite and restructure of the observation documentation reflecting OOPS developments for CY43R1, removal of outdated material and identification of deprecated areas of code.

## Chapter 1

# Overview: the observation world

### Table of contents

- 1.1 Introduction**
- 1.2 Concepts**
  - 1.2.1 Observation groupings, reports and datums
  - 1.2.2 Observation sets
  - 1.2.3 Timeslots
  - 1.2.4 Events and status
  - 1.2.5 The screening trajectory
  - 1.2.6 Observation Database usage in IFS
  - 1.2.7 Parallel aspects (scalability)
- 1.3 Dataflow through processing and screening**
- 1.4 Observation groupings in the IFS**
  - 1.4.1 Obstype and codetype
  - 1.4.2 SQNO - *[DEPRECATED]*
  - 1.4.3 Physical variable: varno
  - 1.4.4 Observation operator codes: NVAR - *[DEPRECATED]*
  - 1.4.5 Satgrp\_table and friends
  - 1.4.6 'Area' type - *[DEPRECATED]*
  - 1.4.7 VarBC bias groups

## 1.1 INTRODUCTION

The handling of observations is one of the most complex parts of the IFS data assimilation system. Observations come in diverse forms and, depending on their type, they are treated in very different ways. The observations themselves ( $y$ ) and the observation operator  $H()$ , which converts from the model state  $x$  to an observation equivalent  $H(x)$ , are just part of a wider infrastructure of processing, quality control, thinning, and assigning observation errors. The metadata associated with each observation can run into hundreds of variables, all needing to be stored in an observation database (ODB). Thus the observation world encompasses:

- **Observation operators** as described in [Chapter 3](#). The input to the observation operator is the ODB, plus the the model state at observation locations. Observation operators, as well as generating  $H(x)$ , may put additional information into the ODB in some cases including observation error and quality control decisions.
- **Model state interpolated to observation location** or **GOM\_PLUS** is described in Part 2 (Data Assimilation). This contains vertical profiles of atmospheric variables (temperature, humidity etc.), surface variables and any other information required from the model. Using the '2D GOM' facility, instead of a single vertical profile, the GOM\_PLUS can contain a slant-path, a set of profiles along a limb path (e.g. for GPSRO) or just all the nearby model columns (which is used in the Bayesian radar retrieval at Météo-France).
- **ODB** is a collection of data formats and metadata describing the observations.
  - In the core of the IFS, processing is based on ODB-1, a hierarchical table format capable of running in a parallel environment, manipulated and accessed using Structured Query Language (SQL). Documentation on ODB-1 can be found at <https://software.ecmwf.int/wiki/display/ODB/ODB+User+Guide>.

- However, most interactions with ODB in the IFS use an additional layer of code known as ODB-IFS which is in the process of being completely rewritten. See Sec. 1.2.6.
  - For some pre-processing, and for archiving to MARS, the ODB-2 format is used: <https://software.ecmwf.int/wiki/display/ODB/ODB+API>.
  - The variables and codes used in the ODB are governed by a committee, and can be browsed at <http://apps.ecmwf.int/odbgov>.
  - At a more detailed level, some parts of the ODB contents are described in the current documentation, mainly in Chapter 6.
- **Observation processing** is a chain that leads from the ingestion of raw data (as BUFR files and other data formats) to the archiving of ODBs in MARS containing diagnostics from the assimilation run (traditionally known as feedback files). Apart from running the observation operators in the data assimilation, observation processing has two main components that can be described as ‘preparation’ and ‘screening’, described next.
  - **Preparation** generates all the parameters needed to run the observation operator in the assimilation system. This is everything from format conversions (e.g. BUFR to ODB-1) to the retrieval of surface emissivities or cloud top pressure from satellite radiances. It is also necessary to apply coordinate transforms (for example from windspeed and direction to horizontal wind components) or to run a retrieval prior to assimilation (for example from backscatter to ocean surface wind). This stage may include simple thinning (such as discarding some satellite observations) This stage also sets up observation errors and other parameters such as the settings for quality control. All this is described in Chapter 2.
  - **Screening** includes all the decisions whether or not to use a certain data. Screening decisions are made throughout the processing chain. They includes blacklisting and other quality control decisions that can only be made when a first guess is available, or in the presence of all observations (‘dependent’ screening). See Chapter 4.
  - **Observation errors:** the diagonal part of the observation error matrix  $\mathbf{R}$  is created during observation processing. For conventional observations, it is done in COPE; for other observations it may be created in DEFRUN or the first time the observation operator is called, particularly if the observation error is situation-dependent. This observation error is eventually stored in the ODB for later use by the data assimilation system. Correlated parts of the observation error model are described in Part 2 (Data assimilation).
  - **Bias correction** Some bias correction is performed as part of pre-processing (such as for radiosondes, done in COPE) but most is now handled inside the 4D-Var minimisation using variational bias correction (VarBC). This is more properly part of the data assimilation, so it is also left to Part 2.
  - **Other auxiliary control variables** Similar to VarBC, other auxiliary control variables are used for satellite radiance assimilation. These include a skin temperature sink variable and a cloud top height variable, and are partly described in Part 2, but their main documentation is here, in Chapter 3.
  - **Variational quality control** This is part of the data assimilation algorithm, so again it is found in Part 2. However, it is the responsibility of the observation processing to provide the parameters that control these tests, such as for example the Huber norm parameters; these are stored in the ODB for use during the assimilation.
  - **Diagnostic Jo table** Although this is another Part 2 concept, the diagnostic Jo table has a detailed structure that breaks down observations into smaller groups, such as observation type and variable for the conventional observations (e.g. radiosonde wind) and satellite instrument for radiances (e.g. AMSU-A). This fine structuring of observations is known only by the observation world, and is described here.

As with the rest of the IFS, the observation world has built up over more than 20 years and is still in constant development. Processing takes place in different layers of code, from ancient parts of the original IFS, through to more OOPS encapsulations. We are constantly working to remove and refactor the older layers of code, but this is an ongoing task. Many areas and concepts are now ‘deprecated’, in other words they still provide important functions but they are expected to disappear in future cycles and they should not be involved in new developments. Where possible, this is clearly stated in the current documentation, and their descriptions have been moved to a special section: Chapter 5. More broadly, the exercise of documenting code is a good way to understanding its inadequacies and indicating ways its design could be improved; thus it also tries to identify areas that could be rationalised in future cycles. To understand the code as it stands, it is worth knowing the

history of such developments. For example, before the ODB was introduced, observations were stored in a data structure called CMA, and concepts from the CMA live on in many places, some good, others outdated and in the process of being refactored. Parts of the processing for conventional observations have been exported into the COPE project, and the ability to call observation operators has now been encapsulated for OOPS, but areas such as setup and screening have not seen so much development.

## 1.2 CONCEPTS

### 1.2.1 Observation groupings, reports and datums

Observations are organised into a hierarchical structure which is reflected in ODB-1. At the broadest level, observations can be organised into meaningful groupings, such as the data from a sensor on one satellite, or all drifting buoys. There are a number of schemes for grouping used in the IFS, and many of these groupings overlap, since they make sense in some areas but not others. Lower down is the concept of a 'report', encompassing for example a single radiosonde ascent or a satellite observation that spans multiple frequencies. Each report thus contains multiple observations, often referred to as datums. Strictly, the plural of datum is data, but 'datum' or 'datums' emphasises that this is the lowest quantum of observational information. In the ODB each datum is associated with a vertical position (`vertco_reference_1@body`, given in terms of pressure, height or channel number) and a variable number (`varno@body`). Datums are grouped into reports to take advantage of their common characteristics: for satellite observations, we often loosely think of the report level as the 'observation'; the datums in the report (measurements at different frequencies) relate to a single location and were made using the same observational parameters, such as scan angle or instrument temperature. Hence it is more precise to talk about datums and reports than 'observations'.

### 1.2.2 Observation sets

To allow efficient parallel computation in the IFS, reports are usually processed together in a small groups known as sets. The maximum number of reports in a set is given by `NMXLEN` (`yomdim0`; default 511 but currently set to 64 by `namelist`). To balance the parallel processing, sets are handled in order from the most computationally expensive to the least. The observation sets may span several 4D-Var timeslots, though in the current operational context this is not the case. Sets are generated by the class `OBSOP_SETS` with their detailed organisation being handled by `ECSET`. Satellite observation sets (e.g. radiances, AMVs, limb radiances, scatterometer) must not contain data from more than one instrument. This is controlled by the misnamed 'area' parameter, which for radiance data is an indicator of satellite ID and instrument, determined in `SUOBAREA`.

### 1.2.3 Timeslots

Timeslots are sub-divisions of the 4D-Var window into which observations are grouped for processing, typically of length 30 minutes. For interpolation from model to observation space, one timestep of the model is chosen to represent the model state in that timeslot. Timeslots are useful because they isolate the observation grouping from the model time resolution, which varies within 4D-Var. However, timesteps may be eliminated in future to simplify the code and to use the most appropriate model timestep for the observation.

### 1.2.4 Events and status

The results of observational processing are stored in the ODB, at the report and datum level, in columns called `REPORT_STATUS`, `DATUM_STATUS`, `REPORT_EVENT1` and `DATUM_EVENT1` (Secs. 6.8 and 6.9). The status summarises whether (and how) the observations should be used in the assimilation system; the event columns are bitfields that record the causes of data rejection, plus some other processing events. Many processing decisions are unique to a particular observation type. For this reason, the `REPORT_EVENT2` and `DATUM_EVENT2` columns can be customised according to the observation type, although in practice this facility is rarely used. All-sky radiance observations use their own event bitfield called `DATUM_TBFLAG` (Sec. 3.3.3).

### 1.2.5 The screening trajectory

Most observations rely on the 'screening trajectory' to perform one-off initialisations that may require the model's first guess. Hence a large part of the observation processing runs only once, in the pre-processing chain, or in the first trajectory under the screening flag `LSCREEN = .TRUE`. This leads to some confusion over what 'screening' means. This documentation makes the distinction between 'preparation' (some of which takes place when the screening is being done, but is not screening) and true screening, which selects data to go into the assimilation algorithm, and is applied at or after the stage the observation operator is run.

### 1.2.6 Observation Database usage in IFS

ODB-1 is an MPI-parallel distributed in-memory, hierarchical database developed at ECMWF. The IFS uses ODB-1 to access observational data and store feedback data (for example, to store first guess departures and information on whether a particular observation was rejected by screening).

Typically, when IFS needs to access observational data, an SQL query is run to retrieve a subset of the data. The queries themselves can be found in the `odb/ddl` directory. The results from the query are returned in 2D arrays. The IFS then uses and manipulates these data arrays, before the modified data is put back into the ODB again. Often, separate queries are run for the report-level data (stored in `ROBHDR`) and the datum-level data (stored in `ROBODY`). In a typical screening trajectory, each MPI task performs  $O(10,000)$  separate SQL queries on the database.

Although IFS uses ODB-1, there are no direct calls to the ODB library from the IFS source code. Instead, IFS accesses ODB through an interface layer. The original IFS-ODB interface is contained in the `odb/cma2odb` directory. Subroutines such as `GETDB()` and `PUTDB()` wrap up the lower level `ODB_get()` and `ODB_put()` library calls, and perform other tasks such as setting up column index variables.

An improved, IFS-ODB interface layer (named `ifsobs`) is being developed. While the old interface relied heavily on global variables and C pre-processor macros, the new interface is more modern and flexible, taking advantage of the object-oriented features of Fortran 2003. The new interface provides more transparency on what SQLs are being run, and which columns are being accessed (aspects which were previously obscured). It also has the advantage that it allows for other database backends to be plugged in seamlessly. The new `ifsobs`-based interface is in the process of being rolled out in IFS, and in `CY43R1` is confined to the observation operator code.

### 1.2.7 Parallel aspects (scalability)

The IFS is multi-process multi-threaded parallel. For running the forecast model, each process holds the state variables for a small part of the globe. In contrast observations are (roughly randomly) distributed across all processors with the aim of avoiding any geographical link. Each processor works with a selection of observations from across the globe. This is why the interpolation from model space to observation space (the GOMs) is one of the more demanding parallel-processing tasks in the IFS. An alternative strategy of keeping the relevant observations on the processor that owns the model data would fall down in two ways: First, a horizontal interpolation, and even more so a limb or slant path interpolation, will often need access to model data located on multiple processors, so multi-process communication would be needed anyway. Second, the computational burden would be unequally distributed, concentrated in whichever processors have satellites overhead on that particular timestep: maybe a dozen out of hundreds.

The top level for running the observation operator is `TASKOB` (or its tangent-linear and adjoint equivalents) which loops over the available observation sets on that processor. This loop is multi-threaded, which means that many sets will be processed in parallel. Moreover, given that the IFS is also multi-process parallel, each processor will be handling different sets of observations. Running the observation operator is thus almost perfectly scalable, as long as the workload is evenly distributed across all processors and threads.

The next level down is `TASKOB_THREAD` which handles the parallel parts of the observation loop. For each observation set, it calls `YDGOM5%MODEL_AT_OBS` to get the `GOM_PLUS` (the model state at observation locations) and then calls the per-set observation operator `HOP`, which is where [Chapter 3](#) (Observation operators) takes over. The screening uses a similar framework of a parallel loop over observation sets.

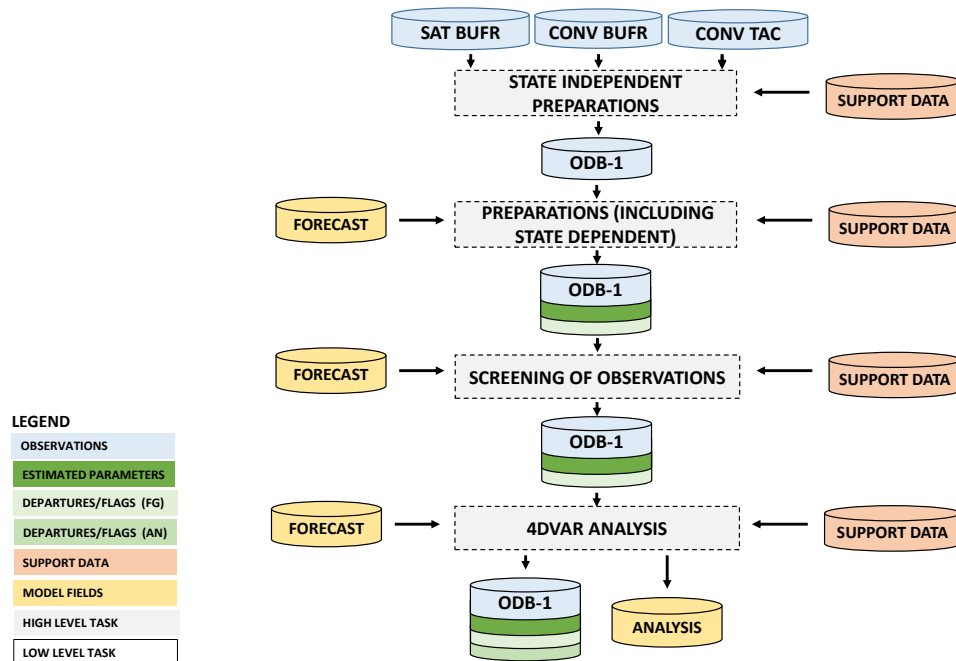


**Figure 1.1** Simplified IFS observation processing flow diagram, with the disc icons representing data stores and the rectangles representing processing stages. Further details can be found in Fig. 2.1 for the state-independent preparations, Fig. 2.2 for the main preparations, Fig. 4.1 for the screening and Fig. 3.1 for 4D-Var.

### 1.3 DATAFLOW THROUGH PROCESSING AND SCREENING

Observation processing happens at many different stages during the journey through the IFS. For computational reasons it can be helpful to reduce observation numbers early on, when the data is stored compactly, and before too much computational time has been expended on unwanted data. However, the cost of observation processing in the current operational system is small, and these computational limitations are not as important as they have been (Lean *et al.*, 2016). Also, much of the screening needs to be left until later stages because it cannot be done in isolation. It is often necessary to have access to:

- The first guess (FG) model state
- The first guess departure, i.e.  $y - H(x)$
- The results of screening decisions from other observations

The last of these points leads to an important distinction in the IFS: between ‘independent’ and ‘dependent’ screening decisions. The dependent decisions are things like checking for redundant observations and thinning, where a selection is made among all the observations that passed earlier quality checks. For example, clear-sky satellite radiance thinning takes as input all observations that passed quality control and blacklisting, and it selects observations with the warmest brightness temperature, as a way of filtering otherwise undetected cloud.

There is thus an opposition between wanting to discard data early for performance reasons, and keeping it until enough supporting information is available, such as the FG model state, or the FG departure. For this reason, and also to perform actions in the easiest place, as well as just for historical reasons, there is a complex and multi-stranded flow of data through the IFS. Figure 1.1 illustrates how some of the data formats are used, and how the ODB-1 data is progressively augmented with additional information as the observations flow through the system. It also acts as a key to more detailed figures, found throughout this document, that summarise these steps in more detail (see figure caption).

However, the complexity of dataflow in the IFS makes it hard to summarise in a compact, well-structured way. Table 1.1 uncovers a little more of this complexity, and also summarises the structure used in this document. Chapter 2 covers observation preparations (defined in Sec. 1.1) which may take place before the main IFS,

when it has historically been called preprocessing, or inside the main IFS code. The only place that has access to the atmospheric state is the main IFS, so we can identify the pre-processing stages as 'state-independent', as in Fig. 1.1. Note that the observation operators themselves are often responsible for processing and data selection decisions, so some preparations are described under Chapter 3, on the observation operators. Chapter 4 then covers the generic screening, i.e. the decisions on observation usage made inside the IFS (bearing in mind that some decisions have already been made during 'preparation' and are described in chapter 2 or 3). The generic screening is split into independent screening and dependent screening, such as redundancy checks and combined thinning. Finally, 4D-Var itself can update the status of observations, such as by downweighting outlying observations using VarQC.

## 1.4 OBSERVATION GROUPINGS IN THE IFS

Observations are associated with various different identifiers and grouping structures. Some illustrative though out-of-date tables are provided in Chapter 6; more current information is found in the ODB governance database at <http://apps.ecmwf.int/odbgov>. Of the groupings described there, the reportype defines the structure of the ODB data archived in MARS, but is not used anywhere inside the IFS. Externally-defined identifiers, such as WMO codes for satellite and instruments, and the BUFR type and subtype, are used in only a few parts of the IFS. Instead a set of internally-defined codes are used most widely. Of these the obstype, codetype and varno are documented by ODB governance. There are further, less well-known IFS groupings including the 'SQNO', the group tables and VarBC bias groups. Those groupings most relevant to the IFS will be discussed in the following sections. A long-term design goal must be to rationalise or eliminate some of these groupings. Each grouping is associated with a considerable code and maintenance overhead, and moreover, badly-structured or overlapping groupings can be confusing.

### 1.4.1 Obstype and codetype

There are currently 16 obstypes used in the IFS, and as such this is one of the coarsest possible groupings for the data. For example, obstype 7, 'SATEM' covers clear-sky radiances as well as satellite retrievals including some atmospheric composition observations. Although confusing, obstype is widely used to route observations through the more established parts of the IFS, in areas such as thinning, and to identify observations for special treatment. For example, in the horizontal interpolation from model to observation space (the GOMs) the choice of variable to interpolate, and how that interpolation is done, is dependent on the obstype. The diagnostic costfunction (the Jo table) is structured by obstype at its broadest level.

Codetype is sometimes used to provide a finer level of structure in areas that use obstypes. However, its meaning is not well defined. Codetypes are often used for conventional observations: they appear to be useful in distinguishing instrument types, for example radiosondes launched from land or ship ('Land TEMP' vs 'TEMP SHIP'), as well as coding practices ('Land TEMP' vs. 'BUFR Land TEMP'). For satellite data, they help distinguish radiances from retrievals, but this distinction would be better made at obstype level, or by using the varno (see later). Satellite codetypes are largely superfluous and could be deprecated in the future.

See <http://apps.ecmwf.int/odbgov> and Sec. 6.3 for more information.

### 1.4.2 SQNO - [DEPRECATED]

Not to be confused with the sequence number assigned to datums in the ODB, the 'SQNO' is a pair of indices that maps onto the obstype and codetype, used in a limited number of contexts in the IFS:

- Huber norm error definitions
- REPORT\_EVENT2 and DATUM\_EVENT2 categories
- Internal structure of the diagnostic Jo table

There is a one-to-one mapping between obstype and codetype and their SQNO equivalent, provided by the hardcoded routines and definitions in [CMOCTMAP](#), [CMOCTMAP\\_INV](#) and [SUCOCTP](#). The historical benefit of the SQNO is to provide a compressed index over the small set of codetypes being used for any obstype. Given the limited use cases, the annoyance of having to hardcode this information, and how easy it would be



Table 1.1 *Observation processing stages in the IFS.*

Name	Format	Requirements		
<b>State-independent preparations (pre-processing) - Chapter 2</b>				
<b>Ingestion:</b> in SAPP, before the IFS	BUFR, HDF	None		
<b>prepare_obs:</b> e.g. simple thinning, reject obviously bad data, superobbing	BUFR	None		
<b>cope_conv:</b> pre-processing and observation error assignment for conventional data	ODB-2	None		
<b>BUFR to ODB:</b> not just conversion, but some processing too	BUFR, ODB-1	None		
<b>Preparations (including state dependent) - Chapter 2; Chapter 3</b>				
<b>setup:</b> Many things including defining observation groupings like the satgrp table	ODB-1	None		
<b>defrun:</b> Define some observation errors, QC paramers including VarQC and (for conventional data) Huber norm	ODB-1	None		
<b>Make CMA replacement</b> [ <i>DEPRECATED</i> ]: No longer used for conventional data, but important for satellite data, especially scatterometers, which retrieve wind from backscatter	ODB-1	FG		
<b>hretr:</b> Mainly for satellite radiance data, including cloud and surface emissivity retrievals.	ODB-1	FG	$H(\mathbf{x})$	
<b>observation operator:</b> Many screening decisions and observation error assignments are handled when the observation operator is called, when LSCREEN=.TRUE.	ODB-1	FG	$H(\mathbf{x})$	
<b>Independent screening - Chapter 4</b>				
<b>blacklist:</b> utilisation decisions, e.g. excluding a particular sensor over sea-ice	ODB-1	FG	$H(\mathbf{x})$	
<b>BgQC:</b> background quality control, based on the first-guess departure and the observation errors	ODB-1	FG	$H(\mathbf{x})$	
<b>Dependent screening - Chapter 4</b>				
<b>redundancy checks:</b> (conventional observations)	ODB-1	FG	$H(\mathbf{x})$	other obs
<b>thinning:</b> the ‘best’ remaining observation can be selected from among multiple candidates within a certain thinning box area	ODB-1	FG	$H(\mathbf{x})$	other obs
<b>4D-Var:</b> observations may be removed by VarQC; analysis departures and other assimilation diagnostics are recorded	ODB-1	FG	$H(\mathbf{x})$	other obs
<b>Archiving</b>				
<b>Convert and archive:</b> move to the ODB-2 format and archive to MARS	ODB-2	None		

to eliminate it using modern code, this is deprecated and should be replaced in a future cycle. An opportunity to do this is when the diagnostic Jo table is refactored for OOPS.

### 1.4.3 Physical variable: varno

The varno, or variable number, describes the type of variable being assimilated. This is the fundamental physical description, for example: '2m temperature in Kelvin'. As such the varno is well-defined and very useful. It is used throughout the screening and for selecting the appropriate observation operator. See <http://apps.ecmwf.int/odbgov> and Sec. 6.4 for more information.

### 1.4.4 Observation operator codes: NVAR - [DEPRECATED]

As further detailed in Sec. 6.5, conventional observation operators, and some other operators, have been given a number (NVAR) that maps directly onto a varno through `MAP_VARNO_TO_NVAR`. These codes are used to select conventional observations, to structure the observation error and QC settings for conventional observations in `DEFRUN` and as the third and lowest level of structure in the diagnostic Jo-table. Given that NVARs form an alternative indexing scheme for an incomplete subset of the varnos, they will be eliminated in future, with the intention that the varno be used directly, and that where compact indexing schemes are needed, they are generated automatically.

### 1.4.5 Satgrp\_table and friends

For most satellite data, including limb radiances, ordinary radiances, AMVs, radio-occultation and scatterometers, the most useful groupings are by satellite ID and instrument. For example the instrument AMSU-A on satellite Metop-A forms one group. For satellite radiances, this structure is encoded in the `satgrp_table` by `YOMSATS` and `SURAD`. Similar tables are maintained for other satellite obtypes in `SUREO3`, `SULIMB`, etc. One very visible function in the IFS is to provide the relevant satellite groupings for the diagnostic Jo-table, and the descriptive names to go with that. A lot of other observation settings are encoded in the table, including those that help access the correct radiative transfer coefficient files for RTTOV. An important aspect of these tables is that they are dynamically created and only contain those satellite/instrument combinations available from the current observational data. Given the great similarities between the `satgrp_table` and those tables used by other satellite types, a design goal should be to provide a unified framework for creating these groups.

### 1.4.6 'Area' type - [DEPRECATED]

An overlapping concept to the `satgrp_table` is the misnamed 'area' type, maintained by `SUOBAREA`. It is only used for grouping satellite data when creating observation sets. Its original role related to the geographical area of conventional observations, long since superseded. Given its limited use, it should be eliminated in a future cycle.

### 1.4.7 VarBC bias groups

It's worth noting that VarBC maintains its own 'bias groups' distinct from any of the above grouping systems.

## Chapter 2

# Preparation of observations

### Table of contents

- 2.1 Introduction**
- 2.2 Non-COPE state-independent preparations (preprocessing)**
  - 2.2.1 Clear-sky satellite radiances
  - 2.2.2 All-sky microwave radiances
  - 2.2.3 Ground-based radar precipitation composites
- 2.3 Continuous Observation Processing Environment (COPE)**
- 2.4 Variable conversions including retrievals**
  - 2.4.1 Conventional observations:
  - 2.4.2 Scatterometer winds
  - 2.4.3 Adjusted variables
  - 2.4.4 Other conversions
- 2.5 Observation errors**
  - 2.5.1 Conventional observations
  - 2.5.2 Satellite observations
  - 2.5.3 Ground-based radar precipitation composites
- 2.6 Background error estimates for screening**
- 2.7 Other preparations**
  - 2.7.1 Surface emissivity for microwave radiances
  - 2.7.2 Cloud affected infrared radiances
  - 2.7.3 AMV height reassignment

## 2.1 INTRODUCTION

This chapter describes the processing required before a normalised first guess departure can be computed. This is best referred to as ‘observation preparation’ as it combines the ‘pre-processing’ tasks upstream of the main IFS code and the preparations that takes place within the IFS during the initial ‘screening’ run (i.e. when `LSCREEN=.TRUE.`). Although the observation operator is part of this process, it is used more widely so it is left for the next chapter. Figure 1.1 and Table 1.1 show how this fits into the processing chain as a whole. Many of these preparations have historically been thought of as ‘screening’ simply because they have been performed during the screening run. This new documentation tries to make a clear distinction between ‘preparations’, which are described in this chapter, and ‘screening’, described in Chapter 4. Screening properly refers to what happens once the normalised first guess departures are available, as decisions on what goes into the assimilation are made at almost every stage of processing.

Historically, the upstream observation pre-processing (described here as ‘state-independent preparations’) have not been part of the IFS documentation. The aim is to bring this more fully into the documentation, but because these tasks are in the process of re-factoring under COPE, they will not be covered in great detail. Fig. 2.1 illustrates these tasks but is far from comprehensive.

Figure 2.2 summarises broadly the preparations that take place inside the IFS and are mostly ‘state-dependent’. However, viewing the processing in this way is not always helpful. For example, variable conversions, such as from wind-speed and direction to horizontal wind components, take place in COPE (in prescreening) for conventional data but in the IFS for satellite-derived AMVs. This chapter is hence mostly structured by the scientific procedure (e.g. parameter conversions, prior retrievals, observation error) rather than the technical location in which the science is achieved.

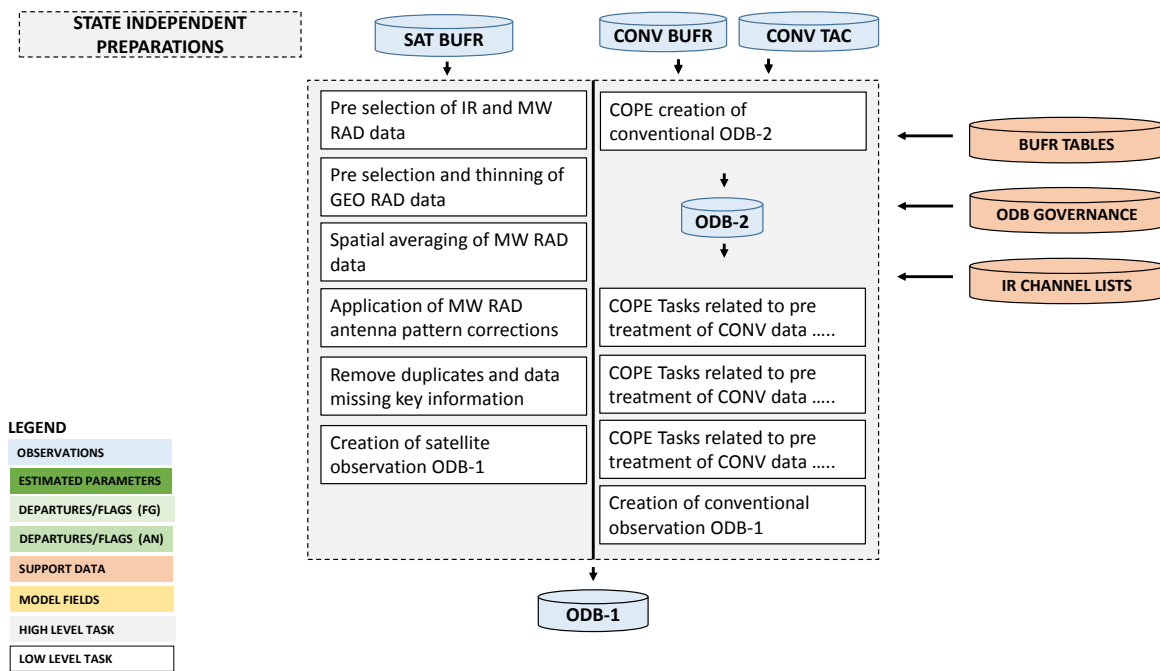


**Figure 2.1** Simplified IFS flow diagram for state-independent observation preparations (alternatively known as preprocessing). The disc icons representing data stores and the rectangles representing processing stages. This is an illustrative, rather than comprehensive, description of the processing. See Fig. 1.1 for the wider observation processing context.

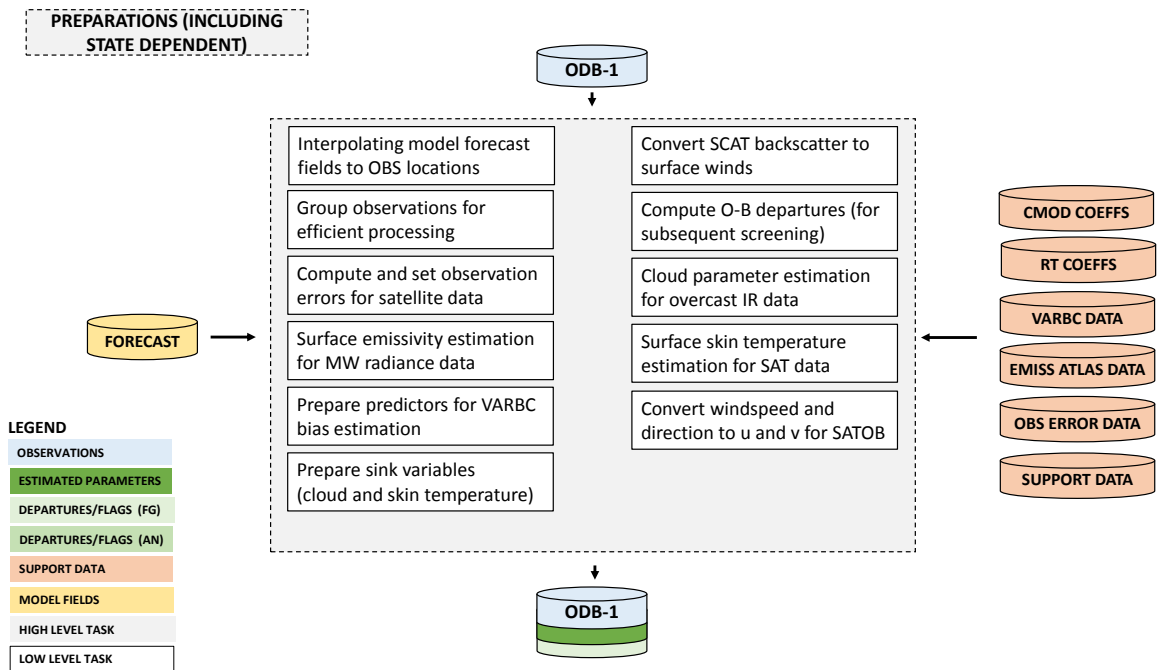


**Figure 2.2** Simplified IFS flow diagram for observation preparations which may be state dependent: more broadly, processing which takes place inside the main IFS. The disc icons representing data stores and the rectangles representing processing stages. This is an illustrative, rather than comprehensive, description of the processing. See Fig. 1.1 for the wider observation processing context.

## 2.2 NON-COPE STATE-INDEPENDENT PREPARATIONS (PREPROCESSING)

Processing external to COPE still accounts for the majority of data going into the IFS. All satellite data goes through the long-established path of BUFR preprocessing (the `PREPARE_OBS` tasks) and BUFR to ODB-2 conversion (the `BUFR2ODB` tasks). In this area, data undergo some rudimentary quality controls, e.g. a check for the observation format and position, and for the climatological limits. These jobs are multi-tasked running in parallel on multiple nodes. Several or all observation types can run synchronously.

### 2.2.1 Clear-sky satellite radiances

Radiance observations undergo a pre-screening process before being loaded into the ODB for input to the main IFS screening. Firstly, this is used to reduce the data volume and thus the computational burden of the main screening. Secondly, this rejects observations that fail to contain crucial header information and/or the correct number of channels that could potentially cause a computational run-time failure in the main screening. Observations in BUFR are decoded and checked inside `SCREEN_1C` where, additionally, data measured at particular scan lines and or scan positions may be removed to reduce the data volume (by setting `LINE_THIN`, `FOV_THIN` in the calling script `PRE_1CRAD`). Observations which survive the checking and thinning process are then re-encoded in BUFR and supplied to the ODB loader. A key consideration for rejecting data in the pre-screening is that removed observations will NOT be passed through the IFS screening and thus will NOT accrue feedback quality information. Currently all pre-screening tasks are scalar (i.e. not parallel). However, for IASI (by far the largest data volume) the process is effectively parallelized by splitting the input BUFR file and launching multiple scalar tasks simultaneously.

### 2.2.2 All-sky microwave radiances

Observations are received in BUFR format and are pre-processed by `SCRIPTS/GEN/premwing` for conical-scanning imagers and `SCRIPTS/GEN/pre1crad*` for sounders. Observations part of the all-sky path are given codetype 215 (see `ODB/CMA2ODB/bufr2cmat_new`).

For imagers, `SATRAD/PROGRAMS/bufr_grid_screen` is called to do superobbing. Observations are put onto a Gaussian grid corresponding to T255 resolution, but with every second point removed to reduce data volumes. Observations within 60 km of the grid point centres are averaged together to form a superob. This brings the relatively high observation resolution of microwave imagers (up to 10 km) down to roughly the scale of clouds in the IFS model. The superobbing is done by computing the numerical mean of all BUFR fields, except longitude and latitude, which are taken to be those of the grid-point, and the observation time, which comes from the last observation mean. This program also allows a further thinning of the data by keeping only observations associated with grid points at every  $n$ th longitude and  $m$ th latitude.

For sounders, there is data thinning but no superobbing. Thinning is done after any antenna pattern corrections are applied, performed in one hour time slots. AMSU-A is a special case, with thinning performed at T159 resolution and in 30 minute time slots considering all AMSU-A sensors together. For humidity sounders thinning is done on a T255 resolution grid, retaining every other point.

### 2.2.3 Ground-based radar precipitation composites

Prior to their assimilation, the original hourly 4-km NCEP Stage IV surface precipitation composites (based on NEXRAD ground-based radars and (some) rain gauges over the United States; Lopez, 2011) are averaged over the model grid at trajectory resolution to reduce possible representativeness issues. In addition, only observations that are located east of 105°W are selected. This is to avoid the likely degradation of ground-radar-based measurements over the Rocky Mountains due to beam blocking, precipitation enhancement or the need for a proper correction of vertical profiles of reflectivity at higher radar beam angles. For similar reasons, observations located over high ( $z_{\text{orog}} > 1500$  m) or rugged terrain ( $\sigma_{\text{orog}} > 100$  m) are rejected. The observations are then accumulated over the period NPRACCL, currently set to 21600 seconds in namelist NAEPHY. All this pre-screening is performed by routine `BUFR_SCREEN_NEXRAD`. Pre-processed observations are then converted to  $\log(\text{RR}[\text{mm/h}]+1)$  space in routine `B20_CONVERT_RAIN_RATES`.

## 2.3 CONTINUOUS OBSERVATION PROCESSING ENVIRONMENT (COPE)

Preparation of conventional in-situ observations is now handled in the COPE environment, prior to the IFS.

The main objective of COPE project has been to consolidate various observation processing tasks that are either carried out in IFS screening, BUFR2ODB conversion or in preobs tasks, into a unified modular framework. The first phase of the project was focused on tasks that do not require model information and thus can be externalized from IFS. Decoupling observation pre-processing from the actual assimilation run has many benefits. Perhaps the most important being to free computational resources in time critical path and to increase resilience against anomalies in observing systems.

So far, only conventional in-situ observation pre-processing has been fully externalized from IFS, replacing the functionality of `MKCMARPL`. To activate COPE framework, one needs to set `LCOPE` option to `true` in `PrepIFS` (this is default since 40r3). Activating COPE will automatically disable `MKCMARPL` worker subroutines for all conventional observations (e.g. `AIREPIN`, `METARIN`, etc.). This is done in `ifstraj` script using `LMKCMARPL` logical array in `NAMOBS` namelist to deactivate processing for selected observation types.

More information on the transition from `MKCMARPL` to COPE can be found in [Chapter 5](#). COPE now handles conventional, in-situ data in configuration files and new COPE routines, e.g:

- `airep.json`
- `dribu.json`
- `temp.json`
- `pilot.json`
- `pgps.json`
- `synop.json`
- `ship.json`
- `awp.json`
- `ewp.json`
- `DateTimeValidator`, `LocationValidator`
- `error_statistics.csv`
- `PrescribedErrorAssigner`
- `FinalErrorAssigner`
- `SpecificHumidityAssigner`
- `InstrumentTypeAssigner`
- `HeightToPressureConverter`
- `RadiosondeBiasCorrector`

The JSON configuration files describe processing pipeline for the given observation type in declarative way. This allows to modify or even construct new pipelines at runtime, reusing existing filters, without having to recompile the source. Conceptually, every pipeline is composed of a chain of filters that are sequentially applied on each observation report. All JSON configuration files can be found in the standard IFS scripts directory.

Since COPE is a collaborative project involving several external partners, its source code is managed under common Git repository: <https://software.ecmwf.int/stash/projects/COPE/repos/cope>.

For SYNOP, SHIP and BUOY reports the usual humidity variable reported is dewpoint temperature and for many years this was the only one extracted. However some (particularly in cold regions) report relative humidity and from 47R1 there is an option (`B2O_EXTRACT_RH2M`, default false) to extract this and another option (`COPE_OVERRIDE_RH2M`) which determines which is used if both are reported.

## 2.4 VARIABLE CONVERSIONS INCLUDING RETRIEVALS

Most observations are used in their original form as this is usually the most optimal use of the data. However, some are transformed, either with a change of variable, but also there may be a retrieval from satellite data if they are independent from the background model fields. The original variables may be kept with the derived ones so that first guess departures can be assigned for both.

### 2.4.1 Conventional observations:

Variables which are transformed for further use by the analysis are as follows.

- (i) Wind direction ( $DDD$ ) and force ( $FFF$ ) are transformed into wind components ( $u$  and  $v$ ) for SYNOP, AIREP, SATOB, DRIBU, TEMP and PILOT observations.
- (ii) Temperature ( $T$ ) and dew point ( $Td$ ) are transformed into relative humidity ( $RH$ ) for SYNOP and TEMP observations, with a further transformation of the  $RH$  into specific humidity ( $Q$ ) for TEMP observations.

The wind components are worked out as

$$u = -FFF \sin\left(DDD \frac{\pi}{180}\right)$$

$$v = -FFF \cos\left(DDD \frac{\pi}{180}\right)$$

The  $RH$  is derived using

$$RH = \frac{F(Td)}{F(T)}$$

where function  $F$  of either  $T$  or  $Td$  is expressed as

$$F(T) = a \frac{R_{\text{dry}}}{R_{\text{vap}}} e^{b \frac{T-T_0}{T-c}}$$

where  $T_0 = 273.16$  K,  $a = 611.21$ ,  $b = 17.502$ ,  $c = 32.19$ ,  $R_{\text{dry}} = 287.0597$  and  $R_{\text{vap}} = 461.5250$  are constants.

The specific humidity  $Q$  is worked out by using

$$Q = RH \frac{A}{1 - RH \left( \frac{R_{\text{vap}}}{R_{\text{dry}}} - 1 \right) A}$$

with function  $A$  is expressed as

$$A = \min \left[ 0.5, \frac{F(T)}{P} \right]$$

where  $P$  is pressure.  $Q$  is assigned in the **RH2Q** subroutine.

These transformations are (probably) now done in COPE (see Sec. 2.3) except for the SATOB/AMV transformations, which are still performed underneath the deprecated MKCMARPL (Sec. 5.3)

### 2.4.2 Scatterometer winds

For ASCAT and possibly some other scatterometers, the retrieval from backscatter to wind is performed internally to the IFS. This is one of the remaining tasks carried out by the deprecated 'Make CMA replacement' process (Sec. 5.3).

Dedicated observation operators exist for scatterometer ambiguous surface winds (Stoffelen and Anderson, 1997; Isaksen and Janssen, 2004). Backscatters ( $\sigma^0$ 's) are transformed into several pairs of ambiguous wind components ( $u$  and  $v$ ); this actually involves a retrieval according to some model function describing the relationship between winds and  $\sigma^0$ 's and requires a fair bit of computational work. The screening of scatterometer data involves the conversion of the backscatter measurements acquired by the instrument (triplets for ERS and ASCAT and quadruplets for NSCAT and QuikSCAT) into ambiguous  $u$  and  $v$  wind components that will actually be assimilated into the IFS (see Section 3.2.9). The (empirical) relation between wind and backscatter is described by a geophysical model function (GMF). Although in principle inverted wind components are provided as a level 2 product, at ECMWF the wind inversion is performed in house. In this way any drifts in backscatter levels can be corrected in a direct manner.

Data from the AMI instrument on ERS-2 have been used from June 1996 (with an interruption from January 2001 till March 2004), data from the SeaWinds instrument on-board QuikSCAT was used from January 2002 until November 2009 (when QuikSCAT failed), and data from ASCAT on MetOp have been assimilated from June 2007 onwards. Data from NSCAT have never been used in an operational setup, although offline assimilation experiments have been performed. From November 2010 onwards scatterometer data is assimilated as equivalent-neutral 10-metre wind, rather than (real) 10-metre wind, since the former model winds are closer related to scatterometer observations.

(a) *Wind retrieval*

Since geometry and measurement principle of ERS and ASCAT are alike, data from these instruments is processed in a similar way. The procedure for wind inversion closely follows the wind retrieval and ambiguity removal scheme originally developed for the ERS-1 scatterometer (Stoffelen and Anderson, 1997), though the original geophysical model function CMOD4 has been replaced by CMOD5 (Hersbach *et al.*, 2007) in March 2004, by CMOD5.4 in June 2007, and by CMOD5.n (Hersbach, 2010b) in November 2010, after which scatterometer winds are assimilated as equivalent-neutral wind (Hersbach, 2010a).

For QuikSCAT the task of wind inversion is performed in the pre-screening (PRESCAT). Data are like ERS and ASCAT, provided at a resolution of 25 km. Rather than data thinning (see Subsection 4.5.6), for QuikSCAT a 50 km product is created which contains information about backscatter from the four underlying original sub-cells. The weight of the scatterometer cost function (defined in routine HJO) of each 50 km wind vector cell is reduced by a factor four, which effectively mimics the assimilation of a 100 km product. It is the re-sampled 50 km product that is stored in ODB. Original backscatter observations at 25 km are not available within the assimilation.

In general, the wind retrieval is performed by minimizing the distance between observed backscatter values  $\sigma_{oi}^0$  and modelled backscatter values  $\sigma_{mi}^0$  given by

$$D(u) = \sum_i^n \frac{[(\sigma_{oi}^0)^p - \sigma_{mi}^0(u)^p]^2}{k_p \left[ \sum_j^n \sigma_{mj}^0(u)^p \right]^2} \quad (2.1)$$

For ERS and ASCAT data, the sum is over triplets, while for QuikSCAT the sum may extend to 16 values (four 25 km sub-cells with each four observations). The quantity  $p$  is equal to unity for NSCAT and QuikSCAT. For ERS and ASCAT data, a value of  $p = 0.625$  was introduced because it makes the underlying GMF more harmonic, which helps to avoid direction-trapping effects (Stoffelen and Anderson, 1997). The noise to signal ratio  $k_p$  provides an estimate for the relative accuracy of the observations.

The simulation of  $\sigma_m^0$  is for ERS and ASCAT data based on the CMOD5.4 model function. For NSCAT data the NSCAT-2 GMF has been utilized. For QuikSCAT data, the choice of GMF is handled by a logical switch LQTABLE. By default LQTABLE = .TRUE. and the QSCAT-1 model function is used, otherwise, modelled backscatter values are based on the NSCAT-2 GMF. The minimization is achieved using a tabular form of the GMF, giving the value of the backscatter coefficient for wind speeds, direction and incidence angles discretized with, for ERS and ASCAT data, steps of  $0.5 \text{ ms}^{-1}$ ,  $5^\circ$  and  $1^\circ$ , respectively. For NSCAT and QuikSCAT data the corresponding values are  $0.2 \text{ ms}^{-1}$ ,  $2.5^\circ$  and  $1^\circ$ . ERS and ASCAT use the same table, which is read in the initialisation subroutine INIERSCA. For QuikSCAT, inversion takes place in the QSCAT25TO50KM program in the PRESCAT task.

(b) *Quality control*

The wind inversion involves some quality control. For ERS (ERS1IF),  $k_p$  must for each antenna be below 10%, and a missing packet number must be less than 10 to ensure that enough individual backscatter measurements have been averaged for estimating the value.

For ASCAT (ASCATIF) a in the product provided land fraction must be zero for each backscatter measurement. No restriction on  $k_p$  is imposed, other than that values should be non missing. It is checked whether two other provided quality flags ('sigma0 usability' and 'kp quality') have acceptable values. However, no quality control decisions are made on these two indicators for the moment, since so far, they have not been fully calibrated and validated by EUMETSAT.



For QuikSCAT, from 38 across-track 50 km cells, the outer 4 at either side of the swath are, due to their known reduced quality rejected. In addition, for QuikSCAT, it is verified whether inverted winds are well-defined, i.e. whether minima  $D(u)$  are sufficiently sharp. In practise this is mainly an issue for cells in the central part of the swath. Data is rejected when the angle between the most likely solution and its most anti-parallel one is less than  $135^\circ$  (routine **SCAQC**).

After wind inversion, a further check is done on the backscatter residual associated to the rank-1 solution (also called 'distance to the cone'). This misfit contains both the effects of instrumental noise and of GMF errors. Locally, these errors can become large when the measurements are affected by geophysical parameters not taken into account by the GMF, such as sea-state or intense rainfall. For ERS, a triplet is rejected when the cone distance exceeds a threshold of three times its expected value. For QuikSCAT and ASCAT data such a test is not performed.

In addition to a distance-to-cone test on single observations, a similar test is performed for averages for data within certain time slots. If these averages exceed certain values, all data within the considered time slot is suspected to be affected by an instrument anomaly, since geophysical fluctuations are expected to be averaged out when grouping together large numbers of data points. For ERS and ASCAT, cell-wise averages are calculated for the default 4D-Var observation time slot (30 minutes) in the IFS routine **SCAQC**, and its rejection threshold (1.5 times average values) are defined in the IFS routine **SUFGLIM**. For QuikSCAT averages are considered over six-hourly data files and are evaluated in the pre-screening (**DCONE\_OC**), using a threshold of 1.45 for any of cells between 5 and 34.

#### (c) *Rain contamination*

Thanks to the usage of C-band frequency, rain contamination is mild for ERS and ASCAT. For QuikSCAT and NSCAT, which operate in Ku band, rain contamination is a serious issue.

For QuikSCAT the check on rain contamination occurs in the pre-screening and is imposed on the original 25 km observations. Any 25 km rejected cell is not used in the determination of the 50 km wind product. When more than one 25 km sub-cell is rejected, the entire 50 km product is rejected (decision made in **SCAQC**).

Since February 2000, the BUFR product provides a rain flag. This flag, which was developed by NASA/JPL, is based on a multidimensional histogram (MUDH) incorporating various quantities that may be used for the detection of rain ([Huddleston and Stiles, 2000](#)). Examples of such parameters are *mp\_rain\_probability* (an empirically determined estimate for the probability of a columnar rain rate larger than  $2 \text{ m}^2 \text{ hr}^{-1}$ ; typically values larger than 0.1 indicate rain contamination) and *nof\_rain\_index* (a rescaled normalized objective function – values larger than 20 give a proxy for rain). Since at the time of implementation, the quality of the JPL rain flag had not been fully confirmed, an alternative (more aggressive) flag was established in house. Based on a study in which QuikSCAT winds were compared to collocated ECMWF first guess winds, a quality flag was introduced. It is given by

$$L_{\text{rain}} = \{ \text{nof\_rain\_index} + 200 \text{ mp\_rain\_probability} > 30 \}.$$

Both *mp\_rain\_probability* and *nof\_rain\_index* are provided in the original 25 km BUFR product (for details see [Leidner et al., 2000](#)). When one of these quantities is missing, the above mentioned condition for the remaining quantity is used.

#### (d) *Bias corrections*

For ASCAT and ERS, bias corrections are applied, both in terms of backscatter (before wind inversion) and wind speed (after inversion), particularly to compensate for any change in the instrumental calibration and to ensure consistency between the retrieved and model winds. The backscatter and wind-speed bias corrections are defined by dedicated files read in the initialization subroutine **INIERSCA**. Files are in principle model-cycle and date dependent. Currently for ERS-2, the appropriate files have no effect (i.e. containing only unity correction factors and zeros), since the CMOD5.4 GMF was tuned on ERS-2. For ASCAT, though, the usage of bias corrections is essential, since the backscatter product for this instrument has been calibrated differently from ERS. The bias correction file for backscatter has been updated every time a change in the calibration of ASCAT was imposed by EUMETSAT.

For QuikSCAT data no bias corrections in  $\sigma^0$  space is applied, though, wind-bias corrections are made. This also takes place in the pre-screening. Corrections are performed in three steps. First of all, wind speeds are slightly reduced according to:

$$v' = 0.2 + 0.96 v.$$

Where  $v$  is the wind speed as obtained from inversion (2.1) The addition of  $0.2 \text{ ms}^{-1}$  is used in the operational configuration, where scatterometer data is assimilated as equivalent neutral wind. In case this is not desired (expressed by `LSCATT_NEUTRAL=false`) only the rescaling factor of 0.96 is used. It was observed that the residual bias between QuikSCAT winds and ECMWF first guess winds depends on the value of `mp_rain_probability`. The motivation is that, for higher amounts of precipitation, a larger part of the total backscatter is induced by rain, leaving a smaller part for the wind signal. The correction applied is

$$v'' = v' - 20 \langle mp\_rain\_probability \rangle,$$

where  $\langle \rangle$  denotes the average value over the 25 km sub-cells that were taken into account in the inversion (i.e. over rain-free sub-cells). The maximum allowed correction is  $2.5 \text{ ms}^{-1}$ , which is seldom reached. Finally, for strong winds, QuikSCAT winds were found to be quite higher than their ECMWF first guess counterparts. In order to accommodate this, for winds stronger than  $19 \text{ ms}^{-1}$  the following correction is applied:

$$v''' = v'' - 0.2(v'' - 19.0).$$

### 2.4.3 Adjusted variables

The only observed quantity which is adjusted is the SYNOP's surface pressure ( $P_s$ ). This is done by using pressure tendency ( $P_t$ ) information, which in turn may be first adjusted.  $P_t$  is adjusted only in the case of SYNOP SHIP data for the ship movement.

The ship movement information is available from input data in terms of ship speed and direction, which are first converted into ship movement components  $U_s$  and  $V_s$ . The next step is to find pressure gradient ( $\partial p / \partial x$  and  $\partial p / \partial y$ ) given by

$$\begin{aligned} \frac{\partial p}{\partial x} &= C(A_1 u - A_2 v) \frac{1}{2} \\ \frac{\partial p}{\partial y} &= -C(A_1 u + A_2 v) \end{aligned}$$

where  $u$  and  $v$  are observed wind components, and  $A_1 = 0.94$  and  $A_2 = 0.34$  are the sine and cosine of the angle between the actual and geostrophic winds.  $C$  is the Coriolis term multiplied by a drag coefficient ( $D$ ) so that

$$C = 2\Omega D \sin \theta$$

where,  $\theta$  is the latitude and  $\Omega = 0.7292 \times 10^{-4} \text{ s}^{-1}$  is the angular velocity of the earth and  $D$  is expressed as

$$D = GZ$$

$G = 1.25$  is an assumed ratio between geostrophic and surface wind over sea and  $Z = 0.11 \text{ kgm}^{-3}$  is an assumed air density. Now the adjusted pressure tendency ( $P_t^a$ ) is found as

$$P_t^a = P_t - \left( U_s \frac{\partial p}{\partial x} + V_s \frac{\partial p}{\partial y} \right)$$

Finally, the adjusted surface pressure ( $P_s^a$ ) is found as

$$P_s^a = P_s - P_t^a \Delta t$$

where,  $\Delta t$  is a time difference between analysis and observation time. Of course in the case of non-SHIP data  $P_t^a \equiv P_t$ .

These transformations are (probably) now done in COPE (see Sec. 2.3)

#### 2.4.4 Other conversions

It is worth mentioning the superobbing of all-sky microwave radiances from their raw resolution into a superob more representative of the cloud and precipitation scales in the forecast model. Currently, all raw observations within a 60 km radius of a chosen central point are averaged together. This is done in the BUFR stages of pre-processing.

## 2.5 OBSERVATION ERRORS

The diagonal part of the observation errors are written, at some point during the observation processing, into the ODB column MDBFOE for use by the data assimilation algorithm. However, the source of these error estimates is varied.

### 2.5.1 Conventional observations

Three types of observation errors are dealt with at the observation pre-processing level. These steps are now done under COPE, external to the IFS. The errors assigned at this stage are persistence observation error, prescribed observation error, and the combination of the two above called the final observation error. These are described in the following sections, as well as the additional error inflation for dropsondes, which is done within the data assimilation system, as a function of the FG departure.

#### (a) Persistence observation error

The persistence error is formulated in such a way to reflect its dependence on the following.

- (i) Season.
- (ii) Actual geographical position of an observation.

Seasonal dependency is introduced by identifying three regimes.

- (i) Winter hemisphere.
- (ii) Summer hemisphere.
- (iii) Tropics.

The positional dependency is then introduced to reflect the dependence on the precise latitude within these three regimes.

The persistence error calculation is split into two parts. In the first part the above dependencies are expressed in terms of factors  $a$  and  $b$  which are defined as

$$a = \sin\left(2\pi\frac{d}{365.25} + \frac{\pi}{2}\right)$$

and

$$b = 1.5 + a\left\{0.5 \min\left[\frac{\max(\theta, 20)}{20}\right]\right\}$$

where  $d$  is a day of year and  $\theta$  is latitude.

The persistence error for time difference between analysis and observation  $\Delta t$  is then expressed as a function of  $b$  with a further dependence on latitude and a maximum persistence error  $E_{\max\text{pers}}$  for 24 hour given by

$$E_{\text{pers}} = \frac{E_{\max\text{pers}}}{6} [1 + 2 \sin(|2\theta|b\Delta t)]$$

where  $\Delta t$  is expressed as a fraction of a day. The  $E_{\max\text{pers}}$  have the values shown in [Table 2.1](#).

Subroutine **SUPERERR** is used to define all relevant points in order to carry out this calculation, and is called only once during the general system initialization. The calculation of the actual persistence error is dealt with by **OBSPERR**.

**Table 2.1** Observation persistence errors of maximum 24-hour wind ( $u, v$ ), height ( $Z$ ) and temperature ( $T$ ).

Variable (unit)	1000–700 hPa	699–250 hPa	249–0 hPa
$u, v$ ( $\text{ms}^{-1}$ )	6.4	12.7	19.1
$Z$ (m)	48	60	72
$T$ (K)	6	7	8

(b) *Prescribed observation errors*

Prescribed observational errors have been derived by statistical evaluation of the performance of the observing systems, as components of the assimilation system, over a long period of operational use. Currently, observational errors are defined for each observation type that carries the following quantities.

- (i) Wind components.
- (ii) Height.
- (iii) Temperature.
- (iv) Humidity.

As can be seen from the tables of prescribed observation errors, they are defined at standard pressure levels but the ones used are interpolated to the observed pressures. The interpolation is such that the observation error is kept constant below the lowest and above the highest levels, whereas in between it is interpolated linearly in  $\ln p$ . Several subroutines are used for working out the prescribed observation error: **SUOBSERR**, **OBSERR**, **FIXERR**, **THIOERR** and **PWCOERR**.

- **SUOBSERR** defines observation errors for standard pressure levels.
- **OBSERR** and **FIXERR** calculate the actual values.
- **THIOERR** and **PWCOERR** are two specialised subroutines to deal with thickness and PWC errors.

Relative humidity observation error  $RH_{\text{err}}$  is either prescribed or modelled. More will be said about the modelled  $RH_{\text{err}}$  in [Subsection \(c\)](#).  $RH_{\text{err}}$  is prescribed only for TEMP and SYNOP data.  $RH_{\text{err}}$  is preset to 0.17 for TEMP and 0.13 for SYNOP. However, if  $RH < 0.2$  it is increased to 0.23 and to 0.28 if  $T < 233$  K for both TEMP and SYNOP.

(c) *Derived observation errors*

Relative humidity observation error,  $RH_{\text{err}}$ , can also be expressed as function of temperature  $T$  so that

$$RH_{\text{err}} = \min[0.18, \min(0.06, -0.0015T + 0.54)]$$

This option is currently used for assigning  $RH_{\text{err}}$ .

Specific humidity observation error,  $Q_{\text{err}}$ , is a function of  $RH$ ,  $RH_{\text{err}}$ ,  $P$ ,  $P_{\text{err}}$ ,  $T$  and  $T_{\text{err}}$ , and formally can be expressed as

$$Q_{\text{err}} = Q_{\text{err}}(RH, RH_{\text{err}}, P, P_{\text{err}}, T, T_{\text{err}})$$

or

$$Q_{\text{err}} = RH_{\text{err}} F_1(RH, P, T)$$

where function  $F_1$  is given by

$$F_1(RH, T, P) = \frac{A}{\left[1 - RH \left(\frac{R_{\text{vap}}}{R_{\text{dry}}} - 1\right) A\right]^2}$$

Subroutine **RH2Q** is used to evaluate  $Q_{\text{err}}$ .

Surface pressure observation error  $P_{s_{\text{err}}}$  is derived by multiplying the height observation error  $Z_{\text{err}}$  by a constant:

$$P_{s_{\text{err}}} = 1.225 Z_{\text{err}}$$

However, the  $P_{s_{\text{err}}}$  may be reduced if the pressure tendency correction is applied. For non-SHIP data the reduction factor is 4, whereas for SHIP data the reduction factor is either 2 or 4, depending on if the  $P_t$  is adjusted for SHIP movement or not.

The thickness observation error ( $DZ_{\text{err}}$ ) is derived from  $Z_{\text{err}}$ .

(d) *Final (combined) observation error*

In addition to the prescribed observation and persistence errors, the so called final observation error is assigned at the COPE stage too. This is simply a combination of observation and persistence errors given by

$$F_{\text{OE}} = \sqrt{O_{\text{E}}^2 + P_{\text{E}}^2}$$

where  $F_{\text{OE}}$ ,  $O_{\text{E}}$  and  $P_{\text{E}}$  are final, prescribed and persistence observation errors, respectively. The subroutine used for this purpose is **FINOERR**.

(e) *Additional error inflation for dropsondes*

Dropsonde errors can be inflated further as a function of the first guess departure  $d$ , in order to prevent problems in tropical cyclones, where the representation error can be large. This is done in **FGWND**. A brief summary is given here; more details can be found in [Bonavita et al. \(2017\)](#). If the 'final' observation error is  $F_{\text{OE}}$  then a new and more final observation error  $F_{\text{OE}2}$  is computed by adding a component for representation error  $R_{\text{O}}$ :

$$F_{\text{OE}2}^2 = F_{\text{OE}}^2 + R_{\text{O}}^2$$

where for  $d^2 \leq F_{\text{OE}}^2 + B_{\text{O}}^2$

$$R_{\text{O}}^2 = 0$$

and for  $d^2 > F_{\text{OE}}^2 + B_{\text{O}}^2$

$$R_{\text{O}}^2 = d^2 - F_{\text{OE}}^2 - B_{\text{O}}^2$$

Here,  $B_{\text{O}}$  represents an estimate of background error in observation space.

## 2.5.2 Satellite observations

(a) *Clear-sky radiances*

The setup routine **DEFRUN** sets up initial defaults for clear-sky radiance observation errors, set by sensor and channel in the variable **ROERR\_RAD1C**. Observation errors for 1C radiances are then written to the ODB in a call to **RAD1COBE** (from **HRETR\_RAD**, which runs under the observation operator). However, these values are sometimes superseded by situation-dependent error schemes, such as those for the microwave sounders in **MW\_CLEARSKY\_OBERROR\_MOD**. This is also done within the observation operator code.

For hyperspectral infrared sounder data, **DEFRUN** first specifies the default observation errors, and then overrides these by reading in ASCII files **rmtberr\_airs**, **rmtberr\_iasi** and **rmtberr\_cris**. These files specify observation error separately for each channel. For IASI and CrIS, these files also specify the matrices of observation error correlations. The observation error specifications for IASI and CrIS are based on background and analysis departure diagnostics as explained in [Bormann et al. \(2016\)](#). Those for AIRS are more conservative and only loosely based on observation minus background departure data.

(b) *All-sky microwave radiances*

The observation error is determined using a 'symmetric' observation error model which is driven by the observed and first guess equivalent brightness temperatures. This can only be computed once the observation operator has been run, so it is computed within the observation operator code under the screening flag **LSCREEN=.TRUE**. As this is done within the observation operator code, more details are given in [Chapter 3](#).

(c) *AMVs*

Situation-dependent observation errors are computed in `AMV_OBERR`. These are generated within the AMV observation operator when `LSCREEN=.TRUE`.

(d) *GPSRO*

Observation errors are computed in `GPSRO_OBERROR`. These are generated within the observation operator when `LSCREEN=.TRUE`.

### 2.5.3 Ground-based radar precipitation composites

In the direct assimilation of NCEP Stage IV surface precipitation composites (using NEXRAD ground-based radars over the United States), observation error is expressed in  $\log(\text{RR}[\text{mm/h}]+1)$  space and is assumed to have a constant value of 0.2 (resp. 0.1) for rainfall (resp. snowfall). This roughly corresponds to errors of 20% (resp. 10%) in terms of actual precipitation amounts. Practically, these errors are set in routines `GBRAD_PUT` and `GBRAD_PUT_TL`.

## 2.6 BACKGROUND ERROR ESTIMATES FOR SCREENING

All observations are assigned an estimate of the background error in observation space for later use in the background quality control (see 4.4.3), and this estimate is stored in the ODB under `fg_error`. This estimate is only used to determine the expected variance of the background departures in the quality control against the background, and it is technically separate from the background error used during the assimilation for the control variables to determine the weighting of observations.

The assignment of the `fg_error` is performed in the routine `GEFGER`, and the method applied depends on the variable number `varno`. For the majority of geophysical variables the estimate is based on fields of situation-dependent estimates of the background error, calculated from the spread of the EDA. The fields are hence consistent with the derivation of the situation-dependent estimate of the background error used in the assimilation. The fields are available in MARS (scaled ensemble spread, SES), and they are read into variable `RZEGRID` in the routine `INIFGER`. In `GEFGER`, these fields are horizontally and - if required - vertically interpolated to observation locations. This method is applied for all standard geophysical variables (ie, T, q, TCWV, etc), and hence applies, for instance, to conventional observations and AMVs. Scaling of the error fields by `REDNMC` used in the assimilation is included. Note, however, that the SES fields are strictly only applicable for the initial time of the assimilation window, and no attempt is made to account for the temporal evolution of the background error pattern.

For observations with more complex observation operators, modifications of the above approach are used, dependent on whether estimates of the EDA spread have previously been calculated for the observed quantity. These result in estimates that may or may not be closely related to values of the actual statistical background error. This is, for instance, the case for:

**Clear-sky radiances:** For some clear-sky radiances, background error estimates based on the EDA spread (for a given zenith angle) are available as SES fields, and these are treated similar to the values for standard geophysical variables. SES fields are available for clear-sky simulations of HIRS, MSU, SSU, AMSU-A, AMSU-B/MHS and SSMI (Bormann and Bonavita, 2013). Where needed, these values are interpolated to the observation locations. For some other sensors (e.g., geostationary imagers, ATMS, MWTS-2), background error estimates from equivalent channels of the previously named sensors are assigned. While these estimates are not the same as a mapping of the actually used control vector background error into observation space they will capture similar spatial structures.

For hyperspectral infrared instruments (IASI, AIRS, CrIS), the background error estimate is set to 3 K. For most spectral regions this is a severe over-estimation of the uncertainty in the background, and the implication is that the background error quality control for these instruments is very loose.

**All-sky radiances:** All-sky radiances do not use situation-dependent estimates from the EDA spread, but rather employ a parametric model, as defined in `MWAVE_ERROR_MODEL`.

**Bending angles:** The background error is set to the same value as the observation error.

## 2.7 OTHER PREPARATIONS

### 2.7.1 Surface emissivity for microwave radiances

#### (a) *Clear-sky microwave*

Microwave (`EMIS.MW.N`) and infrared (`EMIS.IR`) surface emissivities are set during the screening phase in `RAD1CEMIS` (called from `HRETR.RAD`) and stored in the ODB for later use by RTTOV. Setting the emissivity to values outside the range of 0 and 1 prompts the calculation of surface emissivity within RTTOV, using FASTEM ([Deblonde and English, 2001](#)) for the microwave and ISEM-6 ([Sherlock, 1999](#)) for the infrared. This is done for all microwave and infrared radiances over sea.

For microwave radiances over land, several options exist to specify the surface emission, following the methods described in [Karbou et al. \(2006\)](#). The surface emissivity can be specified through an atlas, or it can be dynamically retrieved from window channel observations and FG estimates of skin temperature and atmospheric profiles, or the skin temperature can be retrieved given an emissivity atlas value and FG estimates of atmospheric profiles. Default choices are made by sensor in `SUEMIS.CONF` (including which channel is used for the last two options) and can be overwritten through the namelist `NAMEMIS.CONF` or controlled through the PreIFs switch `AMSU.LAND` in the Satellites window in the case of AMSU-A/B/MHS. For the two options with dynamic retrieval of emissivity or skin temperature, the required radiative transfer calculations are performed in the routine `satrat/rttov/ifs/rttov.ec` when called from `HRETR.RAD` via `RADTR` or `RADTR.ML` (see also next section). The atlas values and the retrieved emissivities or skin temperatures are written to the ODB, and used as fixed input in subsequent calls to RTTOV. If atlas values are required, these are read in the routine `DEFRUN`. The default for AMSU-A/B/MHS over land is to use the dynamic retrieval of surface emissivity, using an evolving emissivity atlas to quality-control the retrieved emissivities.

For some microwave sounders such as AMSU-A, a Kalman Filter is used to produce an evolving emissivity atlas from past dynamically retrieved emissivity values, as summarised in [Krzeminski et al. \(2009a\)](#) and [Bormann \(2014\)](#). The atlas is updated using the programs `EMISKF.UPDATE` in the `satrad` project (together with `emiskf*` and `kfgrid*` routines that can be found in the `emiss` directory of the `satrad` project). The program accesses the ODB and reads the required retrieved emissivity values. Only emissivity values that have the datum status flag “`use_emiskf_only`” set during the blacklisting are considered. Routine `EMISKF.INIT` specifies the resolution of the atlas and other configuration settings. Routine `EMISKF.INIT.ATLAS` is used to read the atlas values, `EMISKF.TRAJ` to evaluate the new emissivity values against the atlas values, `EMISKF.PREDICT` to predict forward in time the evolution of the errors in the atlas emissivity, and `EMISKF.UPDATE.ATLAS` to perform the update of the emissivity parametrization using the Kalman Filter equations, and `EMISKF.WRITE.ATLAS` to output the updated atlas. To use the atlas with a new sensor/channel, include the new sensor/channel in the look-up table of known emissivity channels in `EMISKF.INIT`, and provide a new ODBsql view in `EMISKF.UPDATE`. The cycling of the atlas information is done through the files `emiskf.cycle*` which are stored as tar-ball in ECFS. The routine `EMISKF.INIT.ATLAS` is also used to read the atlas under `DEFRUN` during the application stage in the screening run. If no atlas is available a “coldstart” is performed, setting the atlas values and their errors to pre-specified values.

#### (b) *All-sky microwave*

A similar framework exists for all-sky microwave radiances, but with the use of a fixed emissivity atlas (`TELSEM`) instead of an evolving Kalman Filter atlas. A dynamic emissivity retrieval is performed, taking into account the presence of light cloud and precipitation ([Baordo and Geer, 2016](#)). If the retrieval fails, which generally happens if the surface is not fully visible due to heavy cloud or precipitation, then a value is taken from the emissivity atlas. This process happens in the observation operator code under `MWAVE.EMIS`, when `LSCREEN=.TRUE.`

### 2.7.2 Cloud affected infrared radiances

For infrared data from HIRS, AIRS and IASI simplified cloud parameters (cloud top pressure and effective cloud fraction) are estimated for each field of view. Background values are computed during the screening in routine `CLOUD.ESTIMATE` using a method described in [McNally \(2009\)](#).

### 2.7.3 AMV height reassignment

#### (a) Legacy height reassignment scheme for diagnostics

A framework exists to perform height reassignment for AMVs when `LSCREEN=.TRUE.`. This is not used operationally. The reassignment is done using the routine `AMV.REASSIGN`, called from `HRETR.CONV`.

#### (b) Operational reassignment of low-level AMVs

In order to mitigate height assignment problems of AMVs in cases of high wind shear, some AMVs have their heights reassigned to the model cloud layer average. The scientific motivation for the height reassignment scheme, and evidence of its beneficial impact on forecast skill, are explained in [Lean and Bormann \(2021\)](#). The height reassignment scheme is used via the `LAMV_HEIGHT_ADJUST=.TRUE.` switch.

Model cloud tops and cloud bases are provided by the routine `AMV.GET.MODCLOUD`, called from `HRETR.CONV`. A model level is considered cloudy if its model cloud fraction is above 1%, and the sum of its cloud liquid and ice water content is greater than  $10^{-6}$  kg/kg. Three consecutive levels must meet the cloudy criteria for the routine to record a cloud top and cloud base and therefore for the height reassignment to be applied to a given AMV.

The reassignment of AMV heights is performed in the routine `HRETR.CONV`. Within this routine further conditions are checked before the reassignment scheme is applied: the AMV must be between 700 and 900 hPa, and must be above the model cloud top. Finally, the scheme is only applied for dates later than 31 December 2009, this date cut-off ensures that the height reassignment scheme is only operating when low level clouds are sufficiently represented in the model.

The pre-reassignment AMV height is copied to the variable `VERTCO.REFERENCE.2` while the height stored in `VERTCO.REFERENCE.1` is modified. The model u and v wind values at the pre-reassignment height are stored in ODB columns `UMOD.OLD` and `VMOD.OLD`; this is so that O-B statistics can be derived at either height. Optionally, the model cloud-top and cloud-base pressure can be written to the ODB in the `CT.P` and `CB.P` columns.



## Chapter 3

# Observation operators

### Table of contents

#### 3.1 Introduction

- 3.1.1 Top-level observation operator: HOP
- 3.1.2 Tangent-linear and adjoint code
- 3.1.3 Data selection controls: NOTVAR
- 3.1.4 Test harness
- 3.1.5 Other tests of the observation operator

#### 3.2 Conventional observation operators

- 3.2.1 General aspects
- 3.2.2 Geopotential height
- 3.2.3 Wind
- 3.2.4 Humidity
- 3.2.5 Temperature
- 3.2.6 Surface observation operators
- 3.2.7 Atmospheric Motion Vectors
- 3.2.8 Gas retrievals
- 3.2.9 Scatterometer winds

#### 3.3 Satellite radiance operators

- 3.3.1 Common aspects for the setup of nadir radiance assimilation
- 3.3.2 Clear-sky nadir radiances and overcast infrared nadir radiances
- 3.3.3 All-sky nadir radiances
- 3.3.4 Clear-sky limb radiances

#### 3.4 GPS Radio Occultation bending angles

#### 3.5 Ground-based radar precipitation composites

#### 3.6 Atmospheric composition

### 3.1 INTRODUCTION

The observation operators provide the link between the analysis variables and the observations (Lorenc, 1986; Pailleux, 1990). The observation operator is applied to components of the model state to obtain the model equivalent of the observation, so that the model and observation can be compared. The operator  $H$  signifies the ensemble of operators transforming the control variable  $x$  into the equivalent of each observed quantity,  $y^o$ , at observation locations.

From a data assimilation perspective, the job of the observation operator is to interpolate the model state to the observation location, and then to convert from state variables to observed variables. In the IFS, this job is divided into two or three parts. The horizontal interpolation to observation locations is handled by the GOMs; this is a complex task requiring multi-process communication to interpolate and to get the model data from whichever processors it is located onto the processors where the observation data resides (see part 2). From a dataflow point of view, the observation operator is needed in the context of observation preparation, screening and 4D-Var. Figure 3.1 summarises the operations relevant to observations in 4D-Var. In this observation operator documentation, we consider a more limited part of the observation operator: the vertical part of the interpolation (where relevant) and the transformation into observed variables.

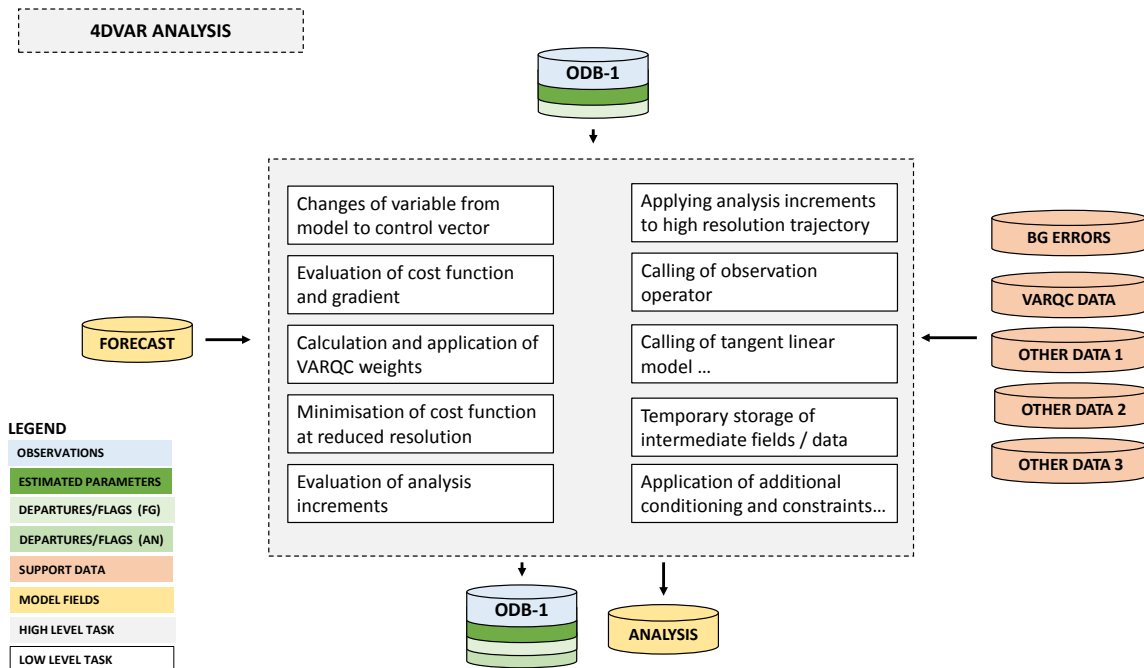


**Figure 3.1** Simplified IFS flow diagram for observation-related processing in 4D-Var. This is an illustrative, rather than comprehensive, description of the processing. See Fig. 1.1 for the wider observation processing context.

The IFS observation operators are generic in the sense that the same routine is often used for several different data types. For example, the radiance operator (RTTOV) simulates measurements from a large number of satellite radiometers (microwave and infrared), and the temperature operator (PPT) is used for TEMP, AIREP, and other data types. Similarly the routine PPQ is used for interpolation of specific humidity to given pressures, but it can also be used for any other atmospheric mixing ratio constituents, such as ozone and carbon dioxide. Note that many of the PP-routines were developed for the model’s pressure-level post-processing package and are used also in that context.

### 3.1.1 Top-level observation operator: HOP

HOP runs the observation operator for one set (see Sec. 1.2.2) of observations. The inputs are:

- the GOM\_PLUS (YDGP5) containing the model state at observation locations;
- the ODB, currently an implicit input through a Fortran module; as OOPS develops further the ODB will become an explicit input too;
- the VarBC object YDVARBC, representing the bias correction coefficients;
- the implicit (communicated-by-module) results of a variety of setup routines (see later).

The outputs are:

- the observation equivalent  $H(\mathbf{x})$ ;
- the bias correction in observation space;
- the ODB is updated (mainly only when LSCREEN=.TRUE.) to store the results of operator-level screening, prior retrievals (done in HRETR routines, e.g. surface emissivity) and operator-level observation error assignments.

The main job of HOP is first to open an ODB view, i.e. to give access to the contents of the ODB relevant to this set of observations, and second, to call a lower level observation operator depending on what observational data is in the set. This is determined by the varnos (see Sec. 6.4) of the reports and datums in the set. The

varno determines what physical observation operator is required, for example radiance simulation using RTTOV or a vertical interpolation of humidity. Because observation sets often contain multiple variables, it is possible for more than one physical observation operator to be called for the same set. The main physical operators are:

- **Conventional observations** (`OBSOP_CONV`): this covers surface and upper-air observations, as well as in-situ data and satellite retrievals that include AMVs and scatterometer winds. What links these observations is the observed variables are closely related to the model state, so that the main part of the observation operator is usually only a vertical interpolation or integration (for example interpolating to the vertical level of an aircraft observation, or integrating over many model levels for total or partial column ozone observations). All the necessary conventional operators are handled by 'PP' or post-processing routines, and are accessed through the top-level PP interface to the observation operator, `PPNEW`. Section 3.2 covers these observation operators.
- **Nadir radiances** (`OBSOP_RAD`): this covers both clear-sky and all-sky radiance observations. At a lower level, these use either RTTOV or (for all-sky microwave) RTTOV\_SCATT. See section 3.3
- **Limb radiances** (`OBSOP_LIMB`): the 2-dimensional model state and 2-dimensional observation operator for limb radiances is not handled by RTTOV, so limb radiances need their own operator. This code is dormant and not used operationally. See section 3.3
- **GPS bending angles** (`OBSOP_GPSRO`): this covers satellite radio-occultation, and it usually requires 2-D slice through the model to compute the tangent path through the earth's atmosphere, including the computation of the bending angles. See section 3.4
- **GPS path delays (ground-based GPS)** (`OBSOP_APDSS`): Currently only active at Météo-France, so not discussed further.
- **Ground-based radar observations** (`OBSOP_RADAR`): This implements the 1D-Bayesian retrieval of [Wattrelot et al. \(2014\)](#) used at Météo-France, and not discussed further here.
- **Precipitation accumulations**, (`OBSOP_PRECIP_ACCUM`): This enables the assimilation of NEXRAD rain radar and rain gauges. The model-equivalent precipitation accumulations are computed inside the model physics and then stored directly to ODB, circumventing the normal process of the observation operator. The main job of the observation operator under HOP is to extract the pre-computed observation equivalent from the ODB. This approach is DEPRECATED and will become impossible in OOPS.
- **Atmospheric composition** (`OBSOP_COMPOSITION`): This handles observations mainly used in the Copernicus atmospheric monitoring service, and it covers retrieved constituent variables as well as aerosol optical depth and some other advanced experimental operators. Composition variables would normally be expected to go through the conventional observation route (`OBSOP_CONV`). However, the composition route allows proper treatment of the averaging kernels. A more technical link among the composition operators is their use of the 'GEMS' input model variables, split into greenhouse gases (GHG), reactive gases (CHEM) and aerosols (AERO). Nevertheless, there is much overlap at a scientific and technical level between the conventional and composition parts of the observation operator, so a long-term design goal should be to unify them.

### 3.1.2 Tangent-linear and adjoint code

In the upper levels of the observation operator, tangent-linear (TL) and adjoint (AD) routines are often merged with the direct (i.e. nonlinear) version. The top-level observation operator routine, `HOP` is one example. Within each of these routines the mutually exclusive logicals LLDIRECT, LLTL and LLAD indicate the mode of operation. TL or adjoint mode is activated by the presence of optional arguments containing the additional data structures needed in a TL or adjoint context. Whether present or not, these optional arguments can cascade down the calling tree. For example, the GOM.PLUS\_TL structure (model increment at observation locations) is an optional argument to HOP, which is then optionally passed down to the lower level operators.

In the lower levels of the code, and particularly those that do extensive numerical computation, the direct, TL and adjoint will usually be three separate routines. Merging the three options together into one routine makes sense in areas where little numerical computation is done: in many of the routines that have been merged, 90% of code was common across the direct, TL and adjoint. Merging the routines reduces the maintenance overhead (preventing changes having to be implemented three times over) and makes it easier to keep the

direct, TL and adjoint routines consistent. For example, if a new feature is added in the direct version, it is more obvious that the TL and adjoint should be updated to reflect this.

Where direct and TL or adjoint variables are present in the same routine, the usual IFS naming convention applies:

- VARIABLE5 is the nonlinear (direct) variable;
- VARIABLE is the TL or adjoint variable, with its meaning depending on the context (e.g. LLTL or LLAD);

### 3.1.3 Data selection controls: NOTVAR

Most data selection criteria are kept in the blacklist or are performed in observation operator code under the `LSCREEN=.TRUE.` switch. (see later). However, classes of data can also be switched on and off in the observation operator using the NOTVAR array in `NAMJO`. The second dimension in this array is the observation type. The first dimension is the variable number (`varno`, see later). The elements of the NOTVAR array can take either of two values: 0, means that the data will be used; -1, means that it won't. NOTVAR is only intended for operational emergencies or debugging, as uniquely it can stop some observations going through the observation operators. The blacklist only stops observations going into the 4D-Var minimisation. If an observation is crashing the observation operator in the screening trajectory, NOTVAR is a temporary solution; later the code should be re-written to prevent the crash, or the data should be blacklisted in the usual way.

### 3.1.4 Test harness

The test harness for HOP, `HOP_DRIVER`, is a program that can be run independently of the IFS with suitable input files:

- GOM\_PLUS\_DUMP files containing the model state at observation locations;
- ODB-1 files (ECMA and CCMA) containing the ODB;
- VARBC.cycle file containing the VarBC coefficients;
- HOP\_RESULTS files containing reference HOP output, for comparison;
- All the data files required to run the observation operator, such as RTTOV coefficient files, channel mappings etc.

To produce these files it is necessary to run the IFS with `LHOP_RESULTS=true` and `LGOM_PLUS_DUMP=true` in the TESTVAR namelist. Also it is necessary to restrict the amount of observational data to make it feasible to run the test harness interactively on a single node. Further details can be found in the test harness `README.run` file.

In direct mode the test harness runs the observation operator and computes the VarBC bias correction; these are compared to the reference output and should be bit-identical between offline and online runs of the same code. In TL and adjoint mode the TL-adjoint consistency test is run, along with a comparison of the TL results with reference results from a run of the IFS. There is not yet the facility to test VarBC TL or adjoint or the auxiliary control variables like the skin-temperature sink variable.

### 3.1.5 Other tests of the observation operator

The adjoint test of the whole 4D-Var operator chain (change of variable, forecast model, interpolation, observation operator) can be activated with `NTESTVAR = 1` and `LADTEST = .TRUE.` There are actually two tests of adjoint triggered here; the relevant one for observations is coded under `ADJOTEST`. The results of this test are printed to the logfiles after 'Adjoint test obs. operator 1.234567890123456789'.

An adjoint test of the RTTOV clear-sky observation operator, on a per-set basis, can be activated with `NTESTVAR = 1` and `LRTTOV_ADTEST = .TRUE.`

## 3.2 CONVENTIONAL OBSERVATION OPERATORS

### 3.2.1 General aspects

This section describes the great variety of observation operators handled by `OBSOP_CONV` and underneath, `PPNEW`, which is a wrapper for all the PP routines.

The vertical operations depend on the variable. The vertical interpolation is linear in pressure for temperature (`PPT`) and specific humidity (`PPQ`), and it is linear in the logarithm of pressure for wind (`PPUV`). The vertical interpolation of geopotential (`PPGEOP`) is similar to wind (in order to preserve geostrophy) and is performed in terms of departures from the ICAO standard atmosphere for increased accuracy ([Simmons and Chen, 1991](#)). The current geopotential vertical interpolation together with the temperature vertical interpolation are not exactly consistent with hydrostatism. A new consistent and accurate vertical interpolation has been devised by Météo-France, which may be important for intensive use of temperature information. The new routines have been tested by ECMWF and as the results were not unambiguously positive the new routines have not yet been adopted – and they are not described in this documentation. In the meantime, the old routines are still used (switch `LOLDPP = .TRUE.` in `namct0`), under the names `PPT_OLD`, `PPGEOP_OLD` and `PPUV_OLD`, with tangent linear `PPTTL_OLD`, `PPGEOPTL_OLD` and `PPUVTL_OLD` and adjoint `PPTAD_OLD`, `PPGEOPAD_OLD` and `PPUVAD_OLD`.

The vertical interpolation operators for SYNOP 10-metre wind (`PPUV10M`) and 2-metre temperature (`PPT2M`) match an earlier version of the model's surface layer parametrization. The vertical gradients of the model variables vary strongly in the lowest part of the boundary layer, where flow changes are induced on very short time and space scales, due to physical factors such as turbulence and terrain characteristics. The vertical interpolation operator for those data takes this into account following Monin–Obukhov similarity theory. Results using such operators, which follow [Geleyn \(1988\)](#) have been presented by [Cardinali et al. \(1994\)](#). It was found that 2-metre temperature data could not be satisfactorily used in the absence of surface skin temperature as part of the control variable, as unrealistic analysis increments appeared in the near-surface temperature gradients. The Monin–Obukhov based observation operator for 10-metre wind, on the other hand, is used for all surface winds (SYNOP, DRIBU, TEMP, PILOT and SCAT), where interpolation is not confined to only 10 m, but is performed to the actual observation height (in practice ranging from 4 to 10 m).

Relative humidity is assumed constant in the lowest model layer to evaluate its 2-metre value (`PPRH2M`), see [Subsection \(e\)](#). Model equivalents of total column water vapour data are obtained by vertical integration of  $q$  (in `GPPWC` and `PPPWC`). The routine `PPPWC` is also used for vertical integration of GEMS/MACC trace gasses. Observation operators exist for precipitable water content (also using `PPPWC`) and thicknesses (`PPGEOP`).

The details regarding observation operators for conventional data can be found in [Vasiljevic et al. \(1992\)](#), [Courtier et al. \(1998\)](#), and in the following sections.

### 3.2.2 Geopotential height

The geopotential at a given pressure  $p$  is computed by integrating the hydrostatic equation analytically using the ICAO temperature profile and vertically interpolating  $\Delta\phi$ , the difference between the model level geopotential and the ICAO geopotential ([Simmons and Chen, 1991](#)). The ICAO temperature profile is defined as

$$T_{\text{ICAO}} = T_0 - \frac{\Lambda}{g}\phi_{\text{ICAO}} \quad (3.1)$$

where  $T_0$  is 288 K,  $\phi_{\text{ICAO}}$  is the geopotential above 1013.25 hPa and  $\Lambda$  is 0.0065 K m<sup>-1</sup> in the ICAO troposphere and 0 in the ICAO stratosphere (the routine `PPSTA`). The ICAO tropopause is defined by the level where the ICAO temperature has reached 216.5 K (`SUSTA`). Using this temperature profile and integrating the hydrostatic equation provides  $T_{\text{ICAO}}$  and the geopotential  $\phi_{\text{ICAO}}$  as a function of pressure (`PPSTA`). We may then evaluate the geopotential  $\phi(p)$  at any pressure  $p$  following

$$\phi(p) - \phi_{\text{surf}} = \phi_{\text{ICAO}}(p) - \phi_{\text{ICAO}}(p_{\text{surf}}) + \Delta\phi \quad (3.2)$$

where  $p_{\text{surf}}$  is the model surface pressure and  $\phi_{\text{surf}}$ , the model orography.  $\Delta\phi$  is obtained by vertical interpolation from the full model level values  $\Delta\phi_k$ . The interpolation is linear in  $\ln(p)$  up to the second

model level (**PPINTP**) and quadratic in  $\ln(p)$  for levels above it (**PPITPQ**, see below). Following [Simmons and Burridge \(1981\)](#) the full model level values are obtained by integrating the discretized hydrostatic equation using the routine **GPGE0** of the forecast model to give

$$\Delta\phi_k = \sum_{j=L}^{k+1} R_{\text{dry}}(T_{v_j} - T_{\text{ICAO}_j}) \ln\left(\frac{p_{j+1/2}}{p_{j-1/2}}\right) + \alpha_k R_{\text{dry}}(T_{v_k} - T_{\text{ICAO}_k}) \quad (3.3)$$

with

$$\alpha_k = 1 - \frac{p_{k-1/2}}{p_{k+1/2} - p_{k-1/2}} \ln\left(\frac{p_{k+1/2}}{p_{k-1/2}}\right)$$

for  $k > 1$  and  $\alpha_1 = \ln(2)$ .

(a) *Quadratic vertical interpolation near the top of the model*

Above the second full level of the model, the linear interpolation (**PPINTP**) is replaced by a quadratic interpolation in  $\ln p$ , performed in the routine **PPITPQ** using

$$z(\ln p) = a + b(\ln p) + c(\ln p)^2 \quad (3.4)$$

where  $a$ ,  $b$  and  $c$  are constants determined so that the above equation fits the heights at the top levels ( $k = 1, 2$  and  $3$ ). The interpolation formula is

$$\phi(\ln p) = z_2 + \frac{(z_2 - z_1)(\ln p - \ln p_2)(\ln p - \ln p_3)}{(\ln p_2 - \ln p_1)(\ln p_1 - \ln p_3)} - \frac{(z_2 - z_3)(\ln p - \ln p_1)(\ln p - \ln p_2)}{(\ln p_2 - \ln p_3)(\ln p_1 - \ln p_3)} \quad (3.5)$$

where 1,2 and 3 refer to levels  $k = 1, 2$  and  $3$ , respectively.

(b) *Below the model's orography*

The extrapolation of the geopotential below the model's orography is carried out as follows: Find  $T^*$  (surface temperature) by assuming a constant lapse rate  $\Lambda$ , from the model level above the lowest model level (subscript  $l - 1$ ), see the routine **CTSTAR**, using

$$T^* = T_{l-1} + \Lambda \frac{R_{\text{dry}}}{g} T_{l-1} \ln \frac{p_{\text{surf}}}{p_{l-1}} \quad (3.6)$$

$$T^* = \frac{\{T^* + \max[T_y, \min(T_x, T^*)]\}}{2} \quad (3.7)$$

Find the temperature at mean sea level,  $T_0$  (also in **CTSTAR**) from

$$T_0 = T^* + \Lambda \frac{\phi_{\text{surf}}}{g} \quad (3.8)$$

$$T_0 = \min[T_0, \max(T_x, T^*)] \quad (3.9)$$

where  $T_x$  is 290.5 K and  $T_y$  is 255 K. The geopotential under the model's orography is (in **PPGEOP**) calculated as

$$\phi = \phi_{\text{surf}} - \frac{R_{\text{dry}} T^*}{\gamma} \left[ \left( \frac{p}{p_{\text{surf}}} \right)^\gamma - 1 \right] \quad (3.10)$$

where  $\gamma = \frac{R_{\text{dry}}}{\phi_{\text{surf}}}(T_0 - T_{\text{surf}})$ .

### 3.2.3 Wind

In **PPUV** a linear interpolation in  $\ln p$  (**PPINTP**) is used to interpolate  $u$  and  $v$  to the observed pressure levels up to the second full model level, above which a quadratic interpolation is used (**PPITPQ**). Below the lowest model level wind components are assumed to be constant and equal to the values of the lowest model level.

### 3.2.4 Humidity

Specific humidity  $q$ , relative humidity  $U$  and precipitable water content  $PWC$  are linearly interpolated in  $p$ , in **PPQ**, **PPRH** and **PPPWC**, respectively. Upper air relative humidity data are normally not used, but could be used, if required. The use of surface relative humidity data is described in [Subsection \(e\)](#).

#### (a) Saturation vapour pressure

The saturation vapour pressure  $e_{\text{sat}}(T)$  is calculated using Tetens's formula given by

$$e_{\text{sat}}(T) = a_1 \exp^{a_3 \left( \frac{T-T_3}{T-a_4} \right)} \quad (3.11)$$

using FOEEWM (mixed phases, water and ice) in the model and FOEEWMO (water only) for observations. The use of water-phase only is in accordance with the WMO rules for radiosonde and SYNOP reporting practices. Note that these statement functions compute  $(R_{\text{dry}}/R_{\text{vap}})e_{\text{sat}}(T)$ , with the parameters set according to [Buck \(1981\)](#) and the AERKi formula of [Alduchov and Eskridge \(1996\)](#), i.e.  $a_1 = 611.21$  hPa,  $a_3 = 17.502$  and  $a_4 = 32.19$  K over water, and for FOEEWM  $a_3 = 22.587$  and  $a_4 = -0.7$  K over ice, with  $T_3 = 273.16$  K. Furthermore in FOEEWM the saturation value over water is taken for temperatures above  $0^\circ\text{C}$  and the value over ice is taken for temperatures below  $-23^\circ\text{C}$ . For intermediate temperatures the saturation vapour pressure is computed as a combination of the values over water  $e_{\text{sat}(\text{water})}$  and  $e_{\text{sat}(\text{ice})}$  according to the formula

$$e_{\text{sat}}(T) = e_{\text{sat}(\text{ice})}(T) + [e_{\text{sat}(\text{water})}(T) - e_{\text{sat}(\text{ice})}(T)] \left( \frac{T - T_i}{T_3 - T_i} \right)^2 \quad (3.12)$$

with  $T_3 - T_i = 23$  K.

#### (b) Relative humidity

In **GPRH** relative humidity  $U$  is computed from

$$U = \frac{pq \frac{R_{\text{vap}}}{R_{\text{dry}}}}{\left[ 1 + \left( \frac{R_{\text{vap}}}{R_{\text{dry}}} - 1 \right) q \right] e_{\text{sat}}(T)} \quad (3.13)$$

and then in **PPRH** interpolated to the required observed pressure levels (using **PPINTP**). Below the lowest model level and above the top of the model is  $U$  assumed to be constant. Saturation vapour pressure is calculated using FOEEWMO if **GPRH** has been called from the observation operator routines, and using FOEEWM if called from the model post processing.

#### (c) Precipitable water

In **GPPWC** precipitable water is calculated as a vertical summation from the top of the model by

$$PWC_k = \frac{1}{g} \sum_{i=1}^k q_i (p_i - p_{i-1}) \quad (3.14)$$

and then in **PPPWC** interpolated to the required observed pressure levels (using **PPINTP**).  $PWC$  is assumed to be zero above the top of the model. Below the model's orography  $PWC$  is extrapolated assuming a constant  $q = q_l$ .

#### (d) Specific humidity

Specific humidity  $q$  is in **PPQ** interpolated to the required observed pressure levels (using **PPINTP**). Below the lowest model level and above the top of the model is  $q$  assumed to be constant and equal to  $q_l$  and  $q_1$ , respectively.

### 3.2.5 Temperature

Temperature is interpolated linearly in pressure (**PPINTP**), in the routine **PPT**. Above the highest model level the temperature is kept constant and equal to the value of the highest model level. Between the lowest model

level and the model's surface the temperature is interpolated linearly, using

$$T = \frac{(p_{\text{surf}} - p)T_l + (p - p_l)T^*}{p_{\text{surf}} - p_l} \quad (3.15)$$

Below the lowest model level the temperature is extrapolated by

$$T = T^* \left[ 1 + \alpha \ln \frac{p}{p_{\text{surf}}} + \frac{1}{2} \left( \alpha \ln \frac{p}{p_{\text{surf}}} \right)^2 + \frac{1}{6} \left( \alpha \ln \frac{p}{p_{\text{surf}}} \right)^3 \right] \quad (3.16)$$

with  $\alpha = \Lambda R_{\text{dry}}/g$ , for  $\phi_{\text{surf}}/g < 2000$  m, but  $\alpha$  is modified for high orography to  $\alpha = R_{\text{dry}}(T'_0 - T^*)/\phi_{\text{surf}}$ , where

$$T'_0 = \min(T_0, 298) \quad (3.17)$$

for  $\phi_{\text{surf}}/g > 2500$  m, and

$$T'_0 = 0.002[(2500 - \phi_{\text{surf}}/g)T_0 + (\phi_{\text{surf}}/g - 2000) \min(T_0, 298)] \quad (3.18)$$

for  $2000 < \phi_{\text{surf}}/g < 2500$  m. If  $T'_0 < T^*$  then  $\alpha$  is reset to zero. The two temperatures  $T^*$  and  $T_0$  are computed using (3.6) to (3.9).

### 3.2.6 Surface observation operators

Preparations for the vertical interpolation of surface data are done in during the creation of the GOM\_PLUS. Here dry static energy (**SURBOUND**), Richardson number, drag coefficients and stability functions (**EXCHCO**) are computed. For scatterometer data, information on equivalent neutral 10-metre wind is directly fetched from the physics package (via the GOM arrays) which is preprocessed in routine **EXCHCO\_VDF**. The actual vertical interpolation is performed in **PPOBSAS**, which embraces routines for 10-metre vector-wind components (**PPUV10M**), 2-metre temperature (**PPT2M**) and 2-metre relative humidity (**PPRH2M**).

The routines mentioned above for 2-metre temperature and humidity and 10-m wind were superceded some years ago by **SPPCFL**, documented in Chapter 3.10 of Part 4 of the IFS documentation. At CY47R1 an option to use the newer routines in the surface observation operators was added (this is **L\_SCREEN\_LEVEL\_OBSOP** default false). The 2-metre temperature (or humidity) is interpolated between the value at the lowest model level and the surface value (and the fact that the 4D-Var control variable does not contain surface temperature may cause a problem). Note that this alternative does not use **PPNEW** but that values are set in **OBSOP\_CONV**. Also note that 2-metre relative humidity (which still uses the old observation operator) is replaced by 2-metre specific humidity as the assimilated variable. There is a technical issue in that model equivalents for the first time step (15 minutes) are not available so for now these values are blacklisted if the new option is used - the number of stations affected is quite small since most report "on the hour". There is another new namelist variable (**4DLAPSET2**, default 0.0065 K/m) which is the lapse rate used in 4D-Var for T2m to adjust for the difference between station height and model orography (if **L\_SCREEN\_LEVEL\_OBSOP** is true). Similar or identical adjustments are used in other NWP systems (eg [Ingleby \(2015\)](#)) and also in the verification against SYNOPs at ECMWF.

#### (a) Vertical interpolation

For wind and temperature an analytical technique ([Geleyn, 1988](#)) is used to interpolate values between the lowest model level and the surface. It is based on Monin–Obukhov theory in which simplified versions of stability functions  $\phi_M$  and  $\phi_H$  are used. The following equations are to be integrated:

$$\frac{\partial \mathbf{u}}{\partial z} = \frac{\mathbf{u}_*}{\kappa(z + z_0)} \phi_M \left( \frac{z + z_0}{L} \right), \quad (3.19)$$

$$\frac{\partial s}{\partial z} = \frac{s_*}{\kappa(z + z_0)} \phi_H \left( \frac{z + z_0}{L} \right), \quad (3.20)$$

$$L = \frac{c_p T u_*^2}{g \kappa s_*}, \quad (3.21)$$



were  $\mathbf{u}$ ,  $s$  are wind and energy variables,  $\mathbf{u}_*$ ,  $s_*$  are friction values,  $u_* = |\mathbf{u}_*|$ , and  $\kappa = 0.4$  is von Kármán's constant. Note that  $\mathbf{u}$  denotes the vector wind relative to a surface current  $\mathbf{u}_0$ ,

$$\mathbf{u} = \mathbf{u}_a - \mathbf{u}_0, \quad (3.22)$$

with  $\mathbf{u}_a$  the wind in the absolute (model) frame. In default configuration (global variable LECURR is false) surface current is zero, in which case the distinction between absolute and relative wind is irrelevant.

The temperature is linked to the dry static energy  $s$  by

$$s = c_p T + \phi \quad (3.23)$$

$$c_p = c_{p\text{dry}} \left[ 1 + \left( \frac{c_{p\text{vap}}}{c_{p\text{dry}}} - 1 \right) q \right]. \quad (3.24)$$

The neutral surface exchange coefficient at the height  $z$  is defined as

$$C_N = \left[ \frac{\kappa}{\ln\left(\frac{z+z_0}{z_0}\right)} \right]^2, \quad (3.25)$$

where  $z_0$  is the surface roughness length. Drag and heat coefficients are defined as

$$C_M = \frac{u_*^2}{[u(z)]^2}, \quad (3.26)$$

$$C_H = \frac{u_* s_*}{u(z)[s(z) - \tilde{s}]}, \quad (3.27)$$

where  $u(z) = |\mathbf{u}(z)|$  and  $\tilde{s}$  is the dry static energy at the surface. Details on the estimation of the roughness length and transfer coefficients can be found in [Subsection \(c\)](#).

For convenience the following quantities are introduced:

$$B_N = \frac{\kappa}{\sqrt{C_N}}, \quad B_M = \frac{\kappa}{\sqrt{C_M}}, \quad B_H = \frac{\kappa\sqrt{C_M}}{C_H}. \quad (3.28)$$

For stable conditions the (simplified) stability function is assumed

$$\phi_{M/H} = 1 + \beta_{M/H} \frac{z}{L}, \quad (3.29)$$

and integration of (3.19) and (3.20) from 0 to  $z_1$  (the lowest model level) leads to values for relative wind  $\mathbf{u}(z)$  and static energy  $s(z)$  at observation height  $z$ :

$$\mathbf{u}(z) = \frac{\mathbf{u}(z_1)}{B_M} \left[ \ln\left(1 + \frac{z}{z_1}(e^{B_N} - 1)\right) - \frac{z}{z_1}(B_N - B_M) \right], \quad (3.30)$$

$$s(z) = \tilde{s} + \frac{s(z_1) - \tilde{s}}{B_H} \left[ \ln\left(1 + \frac{z}{z_1}(e^{B_N} - 1)\right) - \frac{z}{z_1}(B_N - B_H) \right]. \quad (3.31)$$

In unstable conditions the stability function is chosen as

$$\phi_{M/H} = \left(1 - \beta_{M/H} \frac{z}{L}\right)^{-1} \quad (3.32)$$

and the vertical profiles for relative wind and dry static energy are then given by

$$\mathbf{u}(z) = \frac{\mathbf{u}(z_1)}{B_M} \left[ \ln\left(1 + \frac{z}{z_1}(e^{B_N} - 1)\right) - \ln\left(1 + \frac{z}{z_1}(e^{B_N - B_M} - 1)\right) \right], \quad (3.33)$$

$$s(z) = \tilde{s} + \frac{s(z_1) - \tilde{s}}{B_H} \left[ \ln\left(1 + \frac{z}{z_1}(e^{B_N} - 1)\right) - \ln\left(1 + \frac{z}{z_1}(e^{B_N - B_H} - 1)\right) \right]. \quad (3.34)$$

In case the influence of stability is neglected, the following equivalent-neutral wind profile  $\mathbf{u}_n(z)$  is obtained:

$$\mathbf{u}_n(z) = \frac{\mathbf{u}(z_1)}{B_M} \ln \left( 1 + \frac{z}{z_1} (e^{B_N} - 1) \right). \quad (3.35)$$

For wind, the relevant routine **PPUV10M** embodies this method of [Geleyn \(1988\)](#) to estimate vector wind components at observation height  $z$  from provided lowest model level wind  $\mathbf{u}(z_1) = \mathbf{u}_a(z_1) - \mathbf{u}_0$ . For scatterometer data, by default, relative wind (3.30), (3.33) is returned, while for all other data the wind in the absolute frame is evaluated:

$$\mathbf{u}_a = \mathbf{u} + \mathbf{u}_0. \quad (3.36)$$

For scatterometer data, by default equivalent-neutral wind (3.35) is returned. In case non-neutral wind is to be assimilated (operational before November 2010), a variable `LSCATT_NEUTRAL` is to be set to false.

The temperature at observation height  $z = 2$  m is evaluated in **PPT2M**. It is obtained from  $s$  as

$$T(z) = s(z) - \frac{zg}{c_p}, \quad (3.37)$$

where  $s$  is interpolated according to (3.31) and (3.34).

The vertical interpolation relies on estimates for coefficients  $B_M, B_N$  for wind, and on coefficients  $B_H, B_N$  and dry static energy at the surface  $\tilde{s} = \tilde{s}(T_{\text{surf}}, q = 0)$ . These are provided in the routines **EXCHCO**, **EXCHCO\_VDF** and **SURBOUND**, and are described in the following two subsections.

#### (b) Surface values of dry static energy

To determine the dry static energy at the surface we use (3.23) and (3.24) where the humidity at the surface is defined by

$$\tilde{q} = q(z = 0) = h(C_{\text{snow}}, C_{\text{liq}}, C_{\text{veg}})q_{\text{sat}}(T_{\text{surf}}, p_{\text{surf}}) \quad (3.38)$$

where, according to [Blondin \(1991\)](#),  $h$  is given by

$$h = C_{\text{snow}} + (1 - C_{\text{snow}})[C_{\text{liq}} + (1 - C_{\text{liq}})\bar{h}] \quad (3.39)$$

with

$$\bar{h} = \max \left\{ 0.5 \left( 1 - \cos \frac{\pi \vartheta_{\text{soil}}}{\vartheta_{\text{cap}}} \right), \min \left( 1, \frac{q}{q_{\text{sat}}(T_{\text{surf}}, p_{\text{surf}})} \right) \right\} \quad (3.40)$$

where  $\vartheta_{\text{soil}}$  is the soil moisture content and  $\vartheta_{\text{cap}}$  is the soil moisture at field capacity (2/7 in volumetric units). Equation (3.39) assigns a value of 1 to the surface relative humidity over the snow covered and wet fraction of the grid box. The snow-cover fraction  $C_{\text{snow}}$  depends on the snow amount  $W_{\text{snow}}$  so that

$$C_{\text{snow}} = \min \left( 1, \frac{W_{\text{snow}}}{W_{\text{snow}_{\text{cr}}}} \right)$$

where  $W_{\text{snow}_{\text{cr}}} = 0.015$  m is a critical value. The wet skin fraction  $C_{\text{liq}}$  is derived from the skin-reservoir water content  $W_{\text{liq}}$  by

$$C_{\text{liq}} = \min \left( 1, \frac{W_{\text{liq}}}{W_{\text{liq}_{\text{max}}}} \right),$$

where

$$W_{\text{liq}_{\text{max}}} = W_{\text{layer}_{\text{max}}} \{ (1 - C_{\text{veg}}) + C_{\text{veg}} A_{\text{leaf}} \}$$

with  $W_{\text{layer}_{\text{max}}} = 2 \times 10^{-4}$  m being the maximum amount of water that can be held on one layer of leaves, or as a film on bare soil,  $A_{\text{leaf}} = 4$  is the leaf-area index, and  $C_{\text{veg}}$  is the vegetation fraction.

(c) *Transfer coefficients*

Comparing the (3.19) and (3.20) integrated from  $z_0$  to  $z + z_0$  with (3.25) to (3.27),  $C_M$  and  $C_H$  can be analytically defined:

$$\frac{1}{C_M} = \frac{1}{\kappa^2} \left[ \int_{z_0}^{(z+z_0)} \frac{\phi_M(z'/L)}{z'} dz' \right]^2 \quad (3.41)$$

$$\frac{1}{C_H} = \frac{1}{\kappa^2} \left[ \int_{z_0}^{(z+z_0)} \frac{\phi_M(z'/L)}{z'} dz' \int_{z_0}^{(z+z_0)} \frac{\phi_H(z'/L)}{z'} dz' \right] \quad (3.42)$$

Because of the complicated form of the stability functions, the former integrals have been approximated by analytical expressions, formally given by (coded in **EXCHCO**)

$$\begin{aligned} C_M &= C_N f_M \left( Ri, \frac{z}{z_0} \right) \\ C_H &= C_N f_H \left( Ri, \frac{z}{z_0} \right) \end{aligned} \quad (3.43)$$

where  $C_N$  is given by (3.25). The bulk Richardson number  $Ri$  is defined as

$$Ri = \frac{g \Delta z \Delta T_v}{c_p T_v |\Delta u|^2} \quad (3.44)$$

where  $T_v$  is the virtual potential temperature. The functions  $f_M$  and  $f_H$  correspond to the model instability functions and have the correct behaviour near neutrality and in the cases of high stability (Louis, 1979; Louis et al., 1982).

(i) *Unstable case  $Ri < 0$* 

$$f_M = 1 - \frac{2bRi}{1 + 3bcC_N \sqrt{\left(1 + \frac{z}{z_0}\right)(-Ri)}}, \quad (3.45)$$

$$f_H = 1 - \frac{3bRi}{1 + 3bcC_N \sqrt{\left(1 + \frac{z}{z_0}\right)(-Ri)}}, \quad (3.46)$$

with  $b = c = 5$ .

(ii) *Stable case  $Ri > 0$* 

$$f_M = \frac{1}{1 + 2bRi / \sqrt{(1 + dRi)}}, \quad (3.47)$$

$$f_H = \frac{1}{1 + 3bRi / \sqrt{(1 + dRi)}}, \quad (3.48)$$

with  $d = 5$ .

(d) *Extraction of stability information from the ECMWF surface-layer physics*

The estimation of transfer coefficients as described above (Louis, 1979; Louis et al., 1982) does not overlap well with the stability as evaluated in the full nonlinear surface layer physics parametrization, for two reasons. First, the method of Louis (1979); Louis et al. (1982) does not correspond anymore with the presently used parametrization. And second, the estimation of the neutral exchange coefficient (3.25) uses (for technical reasons) a roughness length  $z_0$  that is based on climatology, rather than on the actual roughness. Over oceans this embraces a value of  $z_0 = 1\text{mm}$ , which is typically one order of magnitude too high. The effect on the estimation on 10-metre wind appears to be negligible, however, for 10-metre equivalent neutral wind (used for scatterometer data) and wind at 4 or 5 metre height (typical buoy observation height) a systematic effect can be observed (Hersbach, 2010a).

As an alternative, the information on stability can be extracted from the 10-metre equivalent neutral wind  $u_n$  as evaluated in `SPPCFL_MOD` in the ECMWF surface-layer physics, which is activated by a switch `LVDFTRAJ=true`. In that case, over the ocean roughness length  $z_0$  is estimated from  $u_n$  and the ocean-wave Charnock parameter  $\alpha$ , by an approximate solution (Hersbach, 2011) of the following set of implicit equations (coded in `Z0SEA`):

$$z_0 = \alpha_M \frac{\nu}{u_*} + \alpha \frac{u_*^2}{g}, \quad (3.49)$$

$$u_n = \frac{u_*}{\kappa} \log(1 + z_{10}/z_0). \quad (3.50)$$

Here  $z_{10} = 10$  m,  $\alpha_M = 0.11$ ,  $\kappa = 0.4$  is the Von Kármán constant,  $g = 9.80665$  ms<sup>-2</sup> is the gravitational acceleration, and  $\nu = 1.5 \times 10^{-5}$  m<sup>2</sup>s<sup>-1</sup> the kinematic viscosity.

The coefficient  $C_N$  is, again evaluated by (3.25), but now using the improved estimate of  $z_0$ , while coefficient  $C_M$  for momentum is given by (`EXCHCO_VDF`):

$$C_M = B_M^2/\kappa, \quad B_M = \log(1 + z_{10}/z_0) \|\mathbf{u}(z_{10})\|/u_n. \quad (3.51)$$

In the operational configuration this method is only used for the assimilation of scatterometer wind. For other observables, the method of Louis (1979); Louis *et al.* (1982) (`LVDFTRAJ=false`) is used. Routine `EXCHCO_VDF` does not provide an estimate for the coefficient  $C_H$  for heat.

#### (e) Two-metre relative humidity

In `GPRH` relative humidity is computed according to (3.13). The relative humidity depends on specific humidity, temperature and pressure ( $q$ ,  $T$  and  $p$ , respectively) at the lowest model level. It is constant in the surface model layer, see `PPRH2M`.

### 3.2.7 Atmospheric Motion Vectors

Groups of AMVs (aka SATOBs) are set up in the routine `SUAMV`, one group per satellite, computational method, and codetype. The information is stored in the satob group table, residing in the module `YOMSATS`.

The group table also specifies what type of observation operator is to be used for the particular group (entry `obs_oper`). The default used in operations is to assimilate all AMVs as single-level wind observations (Tomassini *et al.*, 1998; Bormann *et al.*, 2003), in the same way as conventional data, using the same interpolation routine. Other options are treating AMVs as layer averages, with weights defined, for instance, by a boxcar weighting function.

### 3.2.8 Gas retrievals

Retrievals of atmospheric species such as ozone or water vapour are used in the form of integrated layers bounded by a top and bottom pressure which are given as a part of the observation. The same observation operator is used as for precipitable water (`PPPWC`). The same concept is applied to all data, whether it is total column data (like TOMS and GOME ozone data or MERIS total column water vapour) or data with higher vertical resolution (like SBUV). For ozone, variational bias correction is implemented (see Part II, class name "to3", module `VARBC_TO3`). SBUV data is currently used as anchor for the variational bias correction of ozone and therefore assimilated without bias correction.

### 3.2.9 Scatterometer winds

For ERS-2 and ASCAT normally two ambiguous pairs of  $u$ -component and  $v$ -component observations are found at each SCAT location – with directions approximately 180 degrees apart. QuikSCAT can have 2, 3 or 4 ambiguous winds. Up to the first `NSCAWSOLMAX` (4 by default, adaptable through the namelist `NAMSCC`) wind solutions are accepted. In case only one ambiguity is found, the report is rejected. If `LQSCATT = .TRUE.` (the default, modifiable through the namelist `NAMJO`), the normal quadratic  $J_o$  will be used. In this case only the SCAT wind nearest to the high resolution background will be used (which is determined in a section of `HOP`). For winds that are not closest to the first guess or analysis, global datum event flag 9, respectively

10 is set (see Table 6.25). For the latter case datum status is set to rejected as well (Table 6.24). When LQSCATT = .FALSE, the two first winds are used and the ambiguity removal takes place implicitly through a special SCAT cost-function (see part II), in HJO (Stoffelen and Anderson, 1997). In that case for QuikSCAT the most likely wind (highest *a priori* probability) and its most opposing ambiguity are selected.

Routine PPUV10M is like SYNOP, SHIP and DRIBU wind, also used also for SCAT data. Difference is that (in case account is taken for ocean current) the relative wind rather than the absolute wind is returned (not active in the operational suite, though), and the evaluation of equivalent-neutral wind rather than the real wind (which latter includes for scatterometer data undesired stability effects; operational since November 2011).

### 3.3 SATELLITE RADIANCE OPERATORS

The majority of satellite data assimilated currently is radiances, all of it going through the top-level observation operator OBSOP\_RAD. Radiances, rather than retrieved products, are assimilated directly (Andersson *et al.*, 1994), wherever possible. The current operational configuration uses clear level-1C radiances from a number of sensors, including ATOVS (McNally *et al.*, 1999), AIRS, IASI, ATMS, as well as geostationary water vapour clear-sky radiances (Munro *et al.*, 2004).

Clear, cloudy and precipitation-affected radiances from microwave imagers, humidity sounders, and temperature sounders (AMSU-A) are assimilated using an all-sky approach. Hence there are currently two observation operators active in the IFS to assimilate satellite radiances, one for clear-sky radiances and totally overcast infrared radiances, and one for all-sky microwave radiances. The observation operators for both routes are different flavours of the RTTOV radiative transfer model (Saunders and Matricardi, 1998; Matricardi *et al.*, 2001), currently using RTTOV version 12.1.

This section also covers the (non-operational) satellite limb radiances that are handled under OBSOP\_LIMB as they have many commonalities.

#### 3.3.1 Common aspects for the setup of nadir radiance assimilation

The operational radiance assimilation shares the following setup aspects for both radiance assimilation routes. The datasets are distinguished by a satellite ID, a sensor ID, and a codetype. The latter is used to distinguish clear-sky (codetype=210=NGTHRB) or all-sky radiances (codetype=215=NSSMI).

The main set-up routine for radiances is SURAD. It recognises BUFR satellite IDs (call to GETSATID), reads RTTOV coefficient files (call to RTSETUP), and builds a “satellite group table” containing information on which satellite groups are present.

##### (a) Satellite identifiers and sensors

Satellite identifiers are dealt with in the routine GETSATID, called from SURAD. The ODB contains the identifiers as given in the original BUFR messages. Lists of identifiers for which data exist in any given ODB are prepared in the routine SURAD. The routine GETSATID matches those BUFR satellite identifiers with the platform and satellite numbers used by the RT-code (e.g. platform 1, satellite 10 for NOAA-10). New satellite IDs need to be defined in GETSATID, but the id-conversion tables can also be modified through the namelist NAMSATS.

The various types of radiance data in the IFS are also classified by sensor. Each satellite sensor is assigned a number, defined in the module YOMSATS. The sensor number is used as index to various tables containing observation errors, BgQC thresholds, VarQC parameters, the  $J_o$ -table JOT, etc. See the routine DEFRUN.

##### (b) Satellite group table

Various satellite-related indices are gathered in the routine SURAD in the FORTRAN90 data structure called the ‘satellite group table’, satgrp\_t (defined in YOMSATS). The table contains elements such as the satellite ID, the sensor ID, the codetype, a sequence number for addressing the transmittance coefficients (rtcoef\_pos), the number of channels, a channel number list, etc. The various satellite-related indices are universally determined across all processors. There is one entry in the satellite group table per satellite, sensor, and codetype. A list

of all the satellite groups that were found in the ODBs can be found in the *ifstraj* output by searching for SATGRP.

(c) *Radiative transfer coefficients, pressure levels and validation bounds*

Various preparations for RTTOV calculations are set-up in the call to **RTSETUP** from **SURAD**. This includes reading of the various coefficient files required by RTTOV. The files can be found under `/home/rd/rdx/data/< cycle >/sat/rttov`. There is one file with the prefix `rtcoef_` containing coefficients for the general clear-sky radiative transfer for each instrument and satellite, and files with prefix `scldcoef_` used for a parametrization of cloud scattering effects for some infrared sensors. Both types of files are read via a call to **RTTVI** (in the `satrad` library) which also communicates other settings from the RTTOV code in the `satrad` library to the IFS side. Only the files that are required are read, i.e. only the files for which observations are present (for the clear-sky coefficients) or for which data is present and the calculation of cloudy radiances is requested through switching the flags `LCLD_RTCALC_SCREEN` or `LCLD_RTCALC_ASSIM` on in the module **SATS\_MIX** for the respective sensor. A third type of RTTOV coefficient files (prefix `mietable_`) is required for RTTOV\_SCATT computations in the all-sky system (see 3.3.3), read via a call to **MWAVE\_SETUP** under **RTSETUP**.

The transmittance coefficient file for different sensors can use any number of fixed pressure levels, and the number can be different for different sensors. However, interpolation to RTTOV pressure levels is performed inside RTTOV - see 3.3.2 - so the IFS does not need to know about that.

### 3.3.2 Clear-sky nadir radiances and overcast infrared nadir radiances

(a) *Bias correction*

The bias correction is performed through variational bias correction, see part II. The VarBC class is called "rad", and the class-specific routines for the generic VarBC code are in the module **VARBC\_RAD**. For most sounding radiances, the predictors used consist of four layer-thicknesses derived from the First Guess (as defined in **VARBC\_PRED**), but some window channels do not include such airmass predictors to avoid aliasing of cloud information into the bias correction. AMSU-A channel 14 and the equivalent ATMS channel 15 are assimilated with a constrained bias correction, in order to better anchor the stratospheric temperature analysis (Han and Bormann, 2016). Without such an anchor, the variational bias corrections tend to drift to unrealistic values as a result of model biases. This is done at script level, through the namelist `NAMVARBC_RAD`.

(b) *Calling the radiative transfer model*

The radiative transfer model RTTOV is called from the general observation operator routine **HOP** via **OBSOP\_RAD**, **RADTR\_ML** and **RTTOV\_EC**. More details on RTTOV can be found in Eyre (1991), updated by Saunders and Matricardi (1998).

RTTOV performs optical depth calculations on a number of fixed pressure levels, as specified in the `rtcoef_` coefficient file mentioned earlier. RTTOV includes the option to provide the atmospheric profile input either on this set of fixed pressure levels or on a set of different and variable pressure levels. In the latter case, RTTOV will perform the required interpolation internally, using an interpolation that provides smoother gradients than a simple linear interpolation. If this option is used, the radiative transfer computations are also performed on the input user levels, rather than the fixed RTTOV pressure levels.

The vertical interpolation to the RTTOV pressure levels is now performed by the RTTOV internal interpolation (Hocking, 2014). This was previously done using the same PP routines involved in conventional observation processing, but this caused a problem of 'missing levels' in the TL and adjoint. Because of the limited number of RTTOV coefficient levels compared to IFS model levels, some IFS model levels were not used in the vertical interpolation and for these, the gradient of the model values with respect to the observations was zero, leading sometimes to vertical oscillations in the temperature increments. RTTOV internal interpolation is more sophisticated and ensures that all model levels are used in the vertical interpolation, preserving adjoint sensitivity at every level.

Profile information is input to RTTOV on `NFLEVG+1` levels. These correspond to the `NFLEVG` model levels with an additional level set at the model's surface pressure, for which the temperature,

humidity, and other gas concentration values are taken from the lowest model level. A check against the validity bounds of the RTTOV transmittance parametrization is in this case done within RTTOV (routine `SATRAD/RTTOV/MAIN/RTTOV.CHECKINPUT.F90`), for the optical depth calculations only (switch `APPLY_REGRESSION_LIMITS` in `SATRAD/MODULE/RTTOV.CONST.F90`). Various radiance preparations are again performed in `HRADP_ML`.

In either case, the routine `OBSOP_RAD` constructs a list of requested channel numbers for each report from the observation array, and only model radiances for exactly those channels are then requested from the RT-code. The routine `RADTR_ML` packets the profiles into chunks of work of an appropriate maximum size for the RT-code (currently set to 8 in `SATRAD/MODULE/mod_cparam.F90`). The RT packet size has been communicated to IFS in the call to `RTSETUP`. The output is radiances for the channels requested.

The TL and the adjoint are done in the common routines `HOP` and `OBSOP_RAD`, with separate lower-level routines. The  $\dot{T}$  and  $\dot{q}$  have to be recomputed before the actual tangent linear and adjoint computations can start. The pointers to the radiance data in the observation array are obtained just as done in the direct code. Consistency of the TL and adjoint operator can be tested by turning on the switch `LRTTOV_ADTEST` in `preIFS`.

(c) *Skin-temperature 'sink-variable' at satellite FOVs*

In the case of 1C, or 'raw' radiance data, as used since May 1999 (McNally *et al.*, 1999) surface skin temperature is retrieved by 3D/4D-Var at each field of view, if the switch `LTOVSCV` is on (default is on), in namelist `NAMVAR`. This is done for all infrared and microwave satellite sensors and instruments. The handling of the skin temperature retrieval at the radiance FOVs is performed in the routine `HRADP/HRADPTL/HRADPAD`, called from `OBSOP_RAD`. The background skin temperature is provided by the model trajectory integration, and a background error of 1 K/5 K/7.5 K is assigned over sea/land/sea-ice, respectively (set in `SURAD`). The gradient with respect to the skin temperature obtained from RTTOV is temporarily stored in the `TOVSCVX` array and later transferred to its location in the distributed control vector. The next iteration of the minimisation provides updated skin temperature increments (also stored in `TOVSCVX`) that are used by `RTTOVTL` in subsequent iterations. The outer-loop iterations result in a new linearisation state, stored in `TOVSCVX5`. All the skin-temperature-related information at FOV locations that needs to be passed between job-steps, reside in the ODB, in the `skintemp` array. Here, `skintemp_1` is the background skin temperature, and subsequent values are the values at the end of each following minimisation. The approach has been adopted for  $\text{CO}_2$  retrieval at AIRS FOVs (Engelen *et al.*, 2004).

(d) *Cloud affected infrared radiances*

For infrared data from HIRS, AIRS and IASI simplified cloud parameters (cloud top pressure and effective cloud fraction) are estimated for each field of view. Background values are computed during the screening in routine `CLOUD_ESTIMATE` using a method described in McNally (2009). If the scene is diagnosed as overcast (i.e. cloud fraction equal to 1) then all channels are used (that would be used in a completely clear scene) and the cloud parameters become additional elements of the local control vector (as skin temperature). This is done by default, but can be disabled by setting the switch `LCLDSINK` to false in namelist `NAMVAR`. The cloud top pressure is assigned an error (`CTOPBGE` in `YOMVAR` currently equal to 5 hPa) but the cloud fraction is effectively fixed. The handling of the estimated cloud parameters is then performed in the routine `HRADP/HRADPTL/HRADPAD`, called from `OBSOP_RAD`. The gradient with respect to the cloud parameters is obtained from RTTOV (`TOVSCVX` array) and it is later transferred to its location in the distributed control vector. The next iteration of the minimisation provides updated cloud parameter increments (also stored in `TOVSCVX`) that are used by `RTTOVTL` in subsequent iterations. The outer-loop iterations result in a new linearisation state, stored in `TOVSCVX5`. All the cloud parameter information at FOV locations that needs to be passed between job-steps, resides in the ODB, in the satellite predictors table.

If the scene is not diagnosed as overcast, only channels flagged as clear are assimilated and the cloud parameters are essentially inactive.

The approach is also applied to SEVIRI all sky geostationary radiances to allow the additional assimilation of SEVIRI water-vapour overcast radiance observations in parallel with water-vapour clear sky radiances (Lupu and McNally, 2012).

### 3.3.3 All-sky nadir radiances

Observations from microwave imagers and sounders can be assimilated using an all-sky approach which unifies clear-sky, cloudy, and precipitation-affected radiances in one observation operator, using RTTOV-SCATT for the radiative transfer. RTTOV-SCATT is capable of modelling the effects of multiple scattering from hydrometeors. Three classes of microwave data are addressed by the all-sky route, with sometimes more than one class of data in the same instrument:

- (i) Microwave imagers—AMSR2, GMI, MWRI, and some channels of SSMIS are actively assimilated; WINDSAT and SSM/I are passively monitored, though only over oceans and only for latitudes equatorward of 60°
- (ii) Microwave humidity sounders—MHS, MWHS-2 channels 11-15, and some channels of SSMIS are actively assimilated over land, ocean and sea-ice
- (iii) Microwave temperature sounders—AMSU-A channels 5-14 and MWHS-2 channels 2-7 are assimilated over land, ocean and sea-ice with few exceptions

All-sky observations follow a path through the IFS code that is slightly different from that for clear-sky radiance observations, though the observation operator runs under `HOP` and `OBSOP_RAD` rather than under the model physics, as previously. However, the observation operator requires a number of diagnostic variables (e.g. precipitation flux and fraction) that come from the moist physics parametrizations and require a model timestep to have been run before they can be made available in observation space. These fields are generated in `CALLPAR`, stored in the `GFL` arrays and interpolated to observation space like any other model field required by an observation operator, using the `GOM` arrays. The main difference is that there is no interpolation: the observation operator gets the model profile at the grid point closest to the observation. An exception to this is temperature sounders such as AMSU-A, which use slant-path radiative transfer (Bormann, 2017) via 2D `GOM` arrays.

All-sky assimilation can be switched on in PrepIFS by means of switches for individual sensors, e.g. LAMSR2, LGMI, LSSMIS etc. For all-sky AMSU-A and MHS, which can run in parallel to clear-sky assimilation, there is a separate switch `LAMSUA_ALLSKY` or `LMHS_ALLSKY`. Comprehensive scientific documentation of the all-sky approach can be found in Bauer *et al.* (2010), Geer *et al.* (2010), Geer and Bauer (2011), Geer and Bauer (2012) and Geer *et al.* (2014).

#### (a) Observation operator

Code for the all-sky observation operator is prefixed by 'mwave' and located either in `IFS/MWAVE` or `SATRAD/MWAVE`. The observation operator wrapper `IFS/MWAVE/mwave_wrapper` is called from `IFS/OP_OBS/OBSOP_RAD`. The same wrapper function is called whether in direct, TL or AD mode, and the required TL or AD functionality is driven by optional arguments. Lower down, there are separate observation operator routines for each mode: (`IFS/MWAVE/mwave_obsop`, `mwave_obsop_tl` or `mwave_obsop_ad`). In the screening trajectory, `IFS/MWAVE/mwave_screen` is called instead. Inputs to the observation operator are the profiles of model variables (passed in via a structure of `mwave_phys_type`) and any observation-related information (passed via a structure of `mwave_rad_type`). The observation-related information has been read from the ODB by `IFS/MWAVE/mwave_get`, `mwave_get_tl` or `mwave_get_ad`. Outputs from the observation operator (such as the simulated brightness temperatures, and the observation error) are returned in a similar way and are written to the ODB by `IFS/MWAVE/mwave_put` or `mwave_put_tl`. This approach is slightly different to that of other observation operators and is a result of the code's former location in the model physics.

The main function of the observation operator code in `IFS/MWAVE` and `SATRAD/MWAVE` is simply to provide the correct inputs and initialisations to run `RTTOV_SCATT`. However, there is code for quality control, to produce diagnostic output, and to determine the observation error, which is not constant, but a function of hydrometeor amount, as described in Geer and Bauer (2011). VarQC (see part II), VarBC (see part II), blacklisting and background quality control (all in Chapter 4) are done largely as for other radiance observations. The internal IFS thinning routines are completely bypassed, however, because a suitable thinning has already been achieved during the superobbing.



A number of initialisation tasks are performed in `IFS/MWAVE/mwave_setup`, including reading the namelist `NAMMWAVE` for configuration flags. An array of `mwave_ids` structures is created, one for each satellite and sensor combination that will pass through the all-sky operators. In this private table are stored things like the instrument zenith angle, observation error specifications, and the ID numbers used in the rest of the IFS (e.g. sensor, satellite and bufr IDs).

(b) *External files*

Observation error definitions for completely clear and completely cloudy skies are stored in files with names like `mwave_error_<satellite>_<instrument>.dat`. These are read by `IFS/MWAVE/mwave_setup`.

Some configuration options are specified in the `NAMMWAVE` namelist in `SCRIPTS/GEN/ifsmn` and `ifstraj`.

(c) *Diagnostics*

The consistency of the TL and adjoint operators can be tested by setting `ldmwave_test = .true.` in the `NAMMWAVE` namelist in the `SCRIPTS/GEN/ifsmn` script. This causes `IFS/MWAVE/mwave_obsop_test` to be called during the minimisation with the real TL input values for each observation. The results of the test are written to the IFS logfiles, prefixed by 'MWAVE\_OBSOP\_TEST AD:'. The first number gives the TL / AD inaccuracy in multiples of machine precision. Typically this should be substantially less than 100 but it will go over 1000 for a few observations.

A number of diagnostics are stored in the ODB in the `allsky` or `allsky_body` table:

`DATUM_TBFLAG` - This is a bitfield which records quality control decisions for the all-sky observations. It is an additional diagnostic on top of the usual status and event flags, and it only records decisions made internally in the all-sky observation operator. A value of 1 indicates an OK observation; all other values indicate rejection. However, even if the observation is considered OK by the all-sky observation operator, it may subsequently be rejected by the other IFS screening processes (e.g. blacklisting, thinning, VarQC, background QC), so always check the 'status@hdr' and 'status@body' too. Binary arithmetic can be used to decipher the `tbflag` bitfield. For example, if `DATUM_TBFLAG = 33 = 25 + 20`, that means bits 5 and 0 have been set. Bit 5 indicates contamination by sea-ice. `20` is equal to 1; this would have indicated "OK" if no other bit had been set. The full structure of the `DATUM_TBFLAG` bitfield is described in `IFS/MODULE/yommwave`.

`DATUM_TBCLLOUD` - this is a bitfield recording the status of diagnostic cloud and rain identification tests performed on observed and simulated brightness temperatures by `IFS/OP_OBS/mwimager_cloud` and further documented in the code and in [Geer et al. \(2008\)](#). The bitfield structure is documented in `IFS/MODULE/yommwave`. The lowest 2 bits give the results of the FG cloud test. With AND representing the bitwise boolean operator, `(DATUM_TBCLLOUD AND 2) / 2` will give the result of the test for cloud in the FG, with 1 indicating a cloudy scene. `(DATUM_TBCLLOUD AND 1) / 1` will give the result for the observation.

There are also a number of diagnostics relating to FG and analysis model state. These are valid at the time and location of the observation, giving information that is not otherwise archived. These values include the surface rain and snow rate, in  $\text{kg m}^{-2} \text{ s}^{-1}$ , and the total columns of water vapour, cloud water, cloud ice, rain and snow, in  $\text{kg m}^{-2}$ .

### 3.3.4 Clear-sky limb radiances

Assimilation of clear-sky limb radiances has been implemented in the IFS for experimental purposes. The radiances are assimilated using the `RTLIMB` radiative transfer model which is an extension of `RTTOV` to the limb geometry. Details of the radiative transfer model and the assimilation of limb radiances can be found in [Bormann et al. \(2005\)](#); [Bormann and Healy \(2006\)](#); [Bormann and Thépaut \(2007\)](#); [Bormann et al. \(2007\)](#). Many aspects have been primarily developed for the assimilation of MIPAS limb radiances; the assimilation of radiances from other sensors is likely to require additional coding.

Limb radiances fall under obstype 10 "Limb observations", codetype 251. The general approach mirrors that used for clear-sky nadir radiances, i.e., the assimilation uses spatially interpolated vertical profile(s) of model variables. However, setup routines, the radiative transfer code, and the interface routines are different from the clear-sky nadir radiance assimilation.

The routine **SULIMB** sets up a limb group table (defined and stored in module **YOMLIMB**), for each satellite, sensor, and codetype, along the lines of the satellite group table set up in **SURAD**. Limb radiances are treated together with GPS radio occultation observations here. **SULIMB** calls the routine **RTL\_SETUP** which includes the interface routine to the satrad library to read the **RTLIMB** coefficient files. Note that in contrast to the setup for nadir radiances, the code is set up to use fixed pressure levels, reference and limit profiles that are specific to the RT-coefficient files. This information is stored in the limb group table. **RTL\_SETUP** also reads a channel selection file into the channel selection structure **Y\_LIMB\_CHAN\_SEL** in the module **YOMLIMB**. Observation errors and constant, channel-specific biases are also read here from auxiliary files and stored in dedicated variables **YOMLIMB**.

Setting of observation errors and biases and screening of clear-sky limb radiances is performed from **OBSOP\_LIMB\_RAD** in the routines **RTL\_OBERROR** and **RTL\_SCREEN**. The latter applies the channel selection previously stored in **Y\_LIMB\_CHAN\_SEL** in module **YOMLIMB**, and it performs cloud screening.

The actual assimilation happens under the routine **HOP** via **OBSOP\_LIMB\_RAD**. **OBSOP\_LIMB\_RAD** calls the routine **RTL\_HOP\_1D** which performs the following tasks: it interpolates the model profiles in the vertical to the fixed pressure levels (using the standard interpolation routines), does a simple extrapolation above the model top if required (based on a fixed mesospheric lapse rate for temperature, and holding humidity or ozone constant), and it checks the model profiles against the validity limits provided with the **RTLIMB** coefficient file. Finally, **RTL\_HOP\_1D** calls **RTLIMB\_HAT** to enter the satrad library and perform the radiance computations.

The routine **RTL\_HOP\_1D** is used when local horizontal homogeneity is to be assumed for the radiative transfer computations. Alternatively, the radiative transfer computations can take the horizontal structure in the limb-viewing plane into account by providing a series of profiles covering the limb-viewing plane. In this case, profiles provided by 2D GOMs are used, and the routine **RTL\_HOP\_2D** is called from **HOP** instead of **RTL\_HOP\_1D**. The two-dimensional facility is switched on by specifying **NOBSPROFS(10) > 1** for obstype 10 in the namelist **NAMNPROF**. Note that this means GPS radio occultation bending angles present in the assimilation will also take horizontal structure into account.

### 3.4 GPS RADIO OCCULTATION BENDING ANGLES

The subroutine **GPSRO\_OP** is called from **OBSOP\_GPSRO** and it simulates GPS radio occultation bending angles using the one-dimensional model outlined in [Healy and Thépaut \(2006\)](#). The subroutine evaluates a profile of bending angles,  $\alpha$  as function of impact parameter,  $a$ , at each observation location by evaluating the integral

$$\alpha(a) = -2a \int_a^{\infty} \frac{\frac{d \ln n}{dx}}{(x^2 - a^2)^{1/2}} dx \quad (3.52)$$

where  $n$  is the refractive index and  $x = nr$ , the product of the refractive index and  $r$ , a radial coordinate value. The pressure, temperature, specific humidity and geopotential on the model levels (**ZPRESF5**, **ZTF5**, **ZQF5** and **ZGEOPF5**, respectively) are the inputs to **GPSRO\_OP**. The observation operator calculates the refractivity (defined as  $N = 10^{-6}(n - 1)$ ) on the full model levels using the pressure, temperature and specific humidity profiles. It then converts the geopotential heights to geometric heights and then radius values. The bending angle integral is evaluated assuming that the refractivity,  $N$ , varies exponentially between the model levels.

The bending angle observation errors are set in **GPSRO\_OBERROR**. Entries in the JO tables are set in **SULIMB**.

The routine **GPSRO\_OP** is used when local horizontal homogeneity is to be assumed for the bending angle computations. Alternatively, the ray-tracing can take the horizontal structure in the limb-viewing plane into account by providing a series of profiles covering the limb-viewing plane. In this case, profiles provided by 2D-GOMs are used, and the routine **GPSRO\_2DOP** is called from instead of **GPSRO\_OP**. The 2d facility is switched on by specifying **NOBSPROFS(10) > 1** for obstype 10 in the namelist **NAMNPROF**. Note that this means any limb radiances present in the assimilation will also take horizontal structure into account.

### 3.5 GROUND-BASED RADAR PRECIPITATION COMPOSITES

This enables the assimilation of NEXRAD rain radar and rain gauges. The model-equivalent precipitation accumulations are computed inside the model physics and then stored directly to ODB. Here, the observation

---

operator first accumulates the model surface precipitation fields at each time step over the same period (NPRACCL) as the observed precipitation composites. This accumulation is currently performed inside the model physics (**EC\_PHYS**). Model precipitation amounts are then converted to  $\log(\text{RR}[\text{mm/h}]+1)$  space, to be consistent with observations (in **GBRAD\_OBSOP**). Scientific details can be found in [Lopez \(2011\)](#).

### 3.6 ATMOSPHERIC COMPOSITION

No documentation currently available.



# Chapter 4

## Screening

### Table of contents

- 4.1 Introduction**
- 4.2 The structure of the observation screening**
  - 4.2.1 The incoming observations
  - 4.2.2 The screening run
  - 4.2.3 General rationale of the observation screening
  - 4.2.4 3D-Var versus 4D-Var screening
- 4.3 Screening decisions made in observation operators**
  - 4.3.1 Satellite radiances
  - 4.3.2 Ground-based radar precipitation composites
- 4.4 Generic independent observation screening decisions**
  - 4.4.1 Preliminary check of observations
  - 4.4.2 Blacklisting
  - 4.4.3 Background quality control
- 4.5 The dependent observation screening decisions**
  - 4.5.1 Update of the observations
  - 4.5.2 Global time–location arrays
  - 4.5.3 Vertical consistency of multilevel reports
  - 4.5.4 Removal of duplicated reports
  - 4.5.5 Redundancy check
  - 4.5.6 Thinning
  - 4.5.7 Compression of the ODB
- 4.6 Parallel aspects**
- Appendix A**
  - A.1 Bad reporting practice of SYNOP and TEMP reports
  - A.2 Revised background quality control for selected observations

### 4.1 INTRODUCTION

This chapter describes the observation screening in the ECMWF 3D/4D-Var data assimilation. A more general description can be found in [Järvinen and Undén \(1997\)](#). The purpose of the observation screening is to select a clean array of observations to be used in the data assimilation. This selection involves quality checks, removal of duplicated observations, thinning of their resolution etc.. The current selection algorithm has been operational since September 1996 and was to a large extent designed to reproduce the functionalities of the corresponding codes in the ECMWF OI analysis ([Lönnerberg and Shaw, 1985, 1987](#); [Lönnerberg, 1989](#)). Figure 4.1 illustrates the dataflow during the screening.

### 4.2 THE STRUCTURE OF THE OBSERVATION SCREENING

#### 4.2.1 The incoming observations

The ‘extended’ ODB data base (the ECMA) contains all the observational information for the data window as required for 3D/4D-Var as well as all data that are going to be monitored. The next step is that the

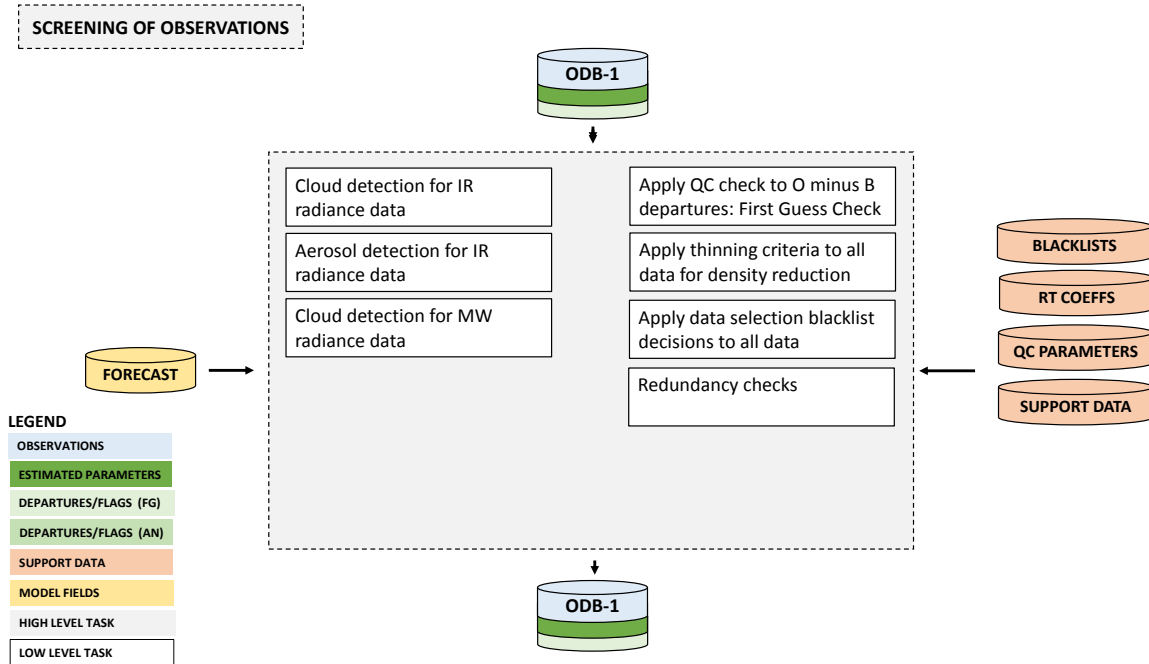


Figure 4.1 Simplified IFS flow diagram for screening. This is an illustrative, rather than comprehensive, description of the processing. See Fig. 1.1 for the wider observation processing context.

observations are compared to the model as it is integrated for the length of the assimilation window. The observation minus model differences (the departures) are computed as described in Part II and stored in the ODB. These departures are an important input to the data selection procedures as many quality-control decisions depend on the magnitude of the departure. The collection of routines that perform data selection are jointly referred to as ‘the screening’. The purpose of the observation screening is to select the best quality observations, to detect duplicates, and reduce data redundancy through thinning.

#### 4.2.2 The screening run

The ECMWF 3D/4D-Var data assimilation system makes use of an incremental minimization scheme, as described in Part II. The sequence of jobs starts with the first (high resolution) trajectory run. During this run the model counterparts for all the observations are calculated through the non-linear observation operators, and the observation minus model difference (the departures) are calculated. As soon as these background departures are available for all observations, the screening can be performed. Prior to the screening the model fields are deallocated (dealmod) as most of the information necessary in the screening is stored in the observation data base (ODB). For the observation screening, the background errors (available as grid data in the ‘errgrib’ file, see Part II) are interpolated to the observation locations for the observed variables (INIFGER, SUFGER and GEFGER - see Chapter 2, section 2.6).

Technically, the final result of the observation screening is a pair of ODBs. The original ‘extended’ observation data base now contains observations complemented by the background departures, together with quality control information for most of the observations. This ECMA ODB remains on disc for later use in feedback creation. The compressed ODB, the CCMA, is a subset of the original observations, and is passed for the subsequent minimization job. The CCMA contains only those observations that are to be used in the minimization.

#### 4.2.3 General rationale of the observation screening

The general logic in the 3D/4D-Var observation screening algorithm is to make the *independent* decisions first, i.e. the ones that do not depend on any other observations or decisions (DECIS). One example is the background quality control for one observed variable. These can be carried out in any order without affecting the result of any other independent decision. The rest of the decisions are considered as mutually *dependent*

on other observations or decisions, and they are taken next, following a certain logical order. For instance, the horizontal thinning of radiance reports is only performed for the subset of reports that passed the background quality control. Finally, the CCMA database is created for the minimization in such a way that it only contains the data that will be used.

#### 4.2.4 3D-Var versus 4D-Var screening

In the original 3D-Var assimilation system the screening rules were applied once, for the complete set of observations spanning a six-hour period. In the early implementation of the 4D-Var assimilation system, the same data selection approach called '3D-screening' was applied over the 6-hour long 4D-Var time window, which resulted in essentially the same screening decisions as in 3D-Var.

In summer 1997, a new screening procedure called 4D-screening was implemented that took into account the temporal distribution of the observations. The time window is divided into time-slots of typically half-hour length (15 minutes for the first and the last time slots). The 3D-screening algorithm was then applied separately to observations within each time-slot. This allowed more data to be used by 4D-Var, for instance, all messages from an hourly reporting station can now be used, whereas only one (closest to central time) would have been allowed by the redundancy check in the 3D-screening. The 4D-screening behaviour is activated by switch LSCRE4D; it is meant to be used in conjunction with time correlation of observation errors where appropriate, as explained in [Järvinen et al. \(1999\)](#) and in Part II.

### 4.3 SCREENING DECISIONS MADE IN OBSERVATION OPERATORS

Many screening decisions are easiest to make in the observation operator itself, and are performed under the condition LSCREEN=.TRUE.

#### 4.3.1 Satellite radiances

##### (a) *Cloud and rain rejection for clear-sky observations*

For data assimilated through the clear-sky route in the IFS, observations contaminated by significant cloud or rain signals must be removed before being supplied to the 4D-Var minimization in the clear-sky assimilation scheme. Microwave radiances that are assimilated in all-sky conditions are not subject to cloud or rain rejection.

For clear-sky microwave radiances (e.g. ATMS) cloud/rain screening is performed in the routine `MW_CLEARSKY_SCREEN`. This requires observation departures and is presently called from `DEPARTURE_JO`. In addition to departures in window channels, it also uses retrievals of liquid water path or scatter indices derived from the observations.

For infrared radiances the test for clouds is done in routine `CLOUD_DETECT` for AIRS/IASI and routine `HIRS_CLD` for HIRS. The former is based on the algorithm described in [McNally and Watts \(2003\)](#). The latter is described in [Krzeminski et al. \(2009b\)](#). In both cases the aim is to identify which infrared channels can be used in a particular scene and which must be rejected.

For both the microwave and infrared data, if an observation is rejected due to cloud contamination, the `contam_cld_flag` is set in the `datum_event1` field in the ODB. These observations will not influence any aspects of the analysis including bias parameter evolution in the VARBC.

There is a special case of infrared cloud contamination that does not lead to channels being rejected. In parallel to the setting of clear and cloudy flags, simplified cloud parameters (cloud top pressure and effective cloud fraction) are estimated from the infrared data (HIRS, AIRS and IASI) in routine `CLOUD_ESTIMATE`. In the case that a pixel is diagnosed as completely overcast and subject to some additional restrictions placed upon the altitude of the diagnosed cloud (e.g. that it is not within 100hPa of the surface), the rejection flags are NOT set. All channels in that pixel are then assimilated with the estimated cloud parameters passed to the forward operator and further evolved as local extensions to the control vector in the minimization. The additional use of overcast infrared radiances can be disabled by setting the logical variable `LCLDSINK` to false.

(b) *All-sky radiances*

Most data selection decisions for all-sky radiances are made within the observation operator code under `MWAVE_SCREEN` and recorded in the ODB column `DATUM_TBFLAG` (see [Chapter 3](#)).

### 4.3.2 Ground-based radar precipitation composites

Some additional screening is performed inside the observation operator for the NCEP Stage IV surface precipitation observations (routine `GBRAD_SCREEN`). Both sea points and points likely to be affected by the occurrence of atmospheric ducting are flagged as rejected. Ducting which leads to the undesirable deflection of radar beams towards the ground is diagnosed from vertical gradients of atmospheric refractivity, as computed from model temperature and moisture fields in routine `GBRAD_REFRACT` ([Lopez, 2011](#)). In addition, points with background departures exceeding 1.5 in  $\log(\text{RR}[\text{mm/h}]+1)$  space are also discarded from the assimilation.

## 4.4 GENERIC INDEPENDENT OBSERVATION SCREENING DECISIONS

### 4.4.1 Preliminary check of observations

The observation screening begins with a preliminary check of the completeness of the reports (`PRECH`). None of the following values should be missing from a report: observed value, background departure, observation error and vertical coordinate of observation. Also a check for a missing station altitude is performed for SYNOP, TEMP and PILOT reports. The reporting practice for SYNOP and TEMP mass observations (surface pressure and geopotential height) is checked (`REPRA`), as explained in [Appendix A](#). At this stage also, the observation error for SYNOP geopotential observations is inflated if the reported level is far from the true station level (`ADDOER`). The inflation is defined as a proportion of the difference between the reported level and the true station altitude by adding 2% of the height difference to the observation error.

### 4.4.2 Blacklisting

Next, the observations are scanned through for blacklisting (subroutine `BLACK`). At the set-up stage the blacklist interface is initialized (`BLINIT`) to the external blacklist library. The blacklist files consist formally of two parts. Firstly, the selection of variables for assimilation is specified in the 'data selection' part of the blacklist file. This controls which observation types, variables, vertical ranges etc. will be selected for the assimilation. Some more complicated decisions are also performed through the data selection file; for instance, an orographic rejection limit is applied in the case of the observation being too deep inside the model orography. This part of the blacklist also provides a handy tool for experimentation with the observing system, as well as with the assimilation system itself. Secondly, a 'monthly monitoring' blacklist file is provided for discarding the stations that have recently been reporting in an excessively noisy or biased manner compared with the ECMWF background field.

Most data selection criteria are coded in so called *blacklist files*, written in a convenient, readable blacklist language (see the Blacklist Documentation, [Järvinen et al., 1996](#)). The blacklist mechanism is very flexible and allows nearly complete control of which data to use/not use in the assimilation. The 'monthly blacklist' is the part of the blacklist that is based on operational data monitoring results, and it is maintained by the Meteorological Operations Section. The blacklist is consulted in the screening job. The interface is set up in `BLINIT`, in such a way that a number of named items from the header ([Table 4.1](#)) and body ([Table 4.2](#)) parts of the observation report can be passed to the blacklist software. Depending on the blacklisting criteria flags are communicated to the routine `BLACK`, and those are written to the ECMA ODB data base. Blacklist-rejected data are subsequently excluded from the CCMA ODB and will not be present in the minimisation job steps. Data selection rules should be coded in the blacklist files whenever possible rather than in the IFS code itself. The operational blacklist history is kept in an archive.

(a) *Scatterometer blacklisting decisions*

In order to screen on sea-ice contamination, scatterometer data are removed (within the blacklist mechanism) whenever the model sea-ice fraction exceeds 1% or the model sea-surface-temperature analysis is below 273.15 K. Land is removed by imposing that the model land-sea mask should not exceed 10%.



**Table 4.1** Header variables in the ifs/blacklist interface. Exact contents may change - see [black.F90](#).

Index	Name	Description
1	OBSTYP	observation type
2	STATID	station identifier
3	CODTYP	code type
4	INSTRM	instrument type
5	DATE	date
6	TIME	time
7	LAT	latitude
8	LON	longitude
9	STALT	station altitude
10	LINE_SAT	line number (atovs)
11	RETR_TYP	retrieval type
12	QL1	quality indicator 1
13	QL2	quality indicator 2
14	QL3	quality indicator 3
15	MODORO	model orography
16	LSMASK	land-sea mask (integer)
17	RLSMASK	land-sea mask (real)
18	MODPS	model surface pressure
19	MODTS	model surface temperature
20	MODT2M	model 2-metre temperature
21	MODTOP	model top level pressure
22	SENSOR	satellite sensor indicator
23	FOV	field of view index
24	SATZA	satellite zenith angle
25	NANDAT	analysis date
26	NANTIM	analysis time
27	SOE	solar elevation
28	QR	quality of retrieval
29	CLC	cloud cover
30	CP	cloud top pressure
31	PT	product type
32	SONDE_TYPE	sonde type
33	SPECIFIC	amsua specific
34	SEA_ICE	model sea ice fraction

**Table 4.2** Body variables for the ifs/blacklist interface. Exact contents may change - see [black.F90](#)

Index	Name	Description
1	VARIAB	variable name
2	VERT_CO	type of vertical coordinate
3	PRESS	pressure, height or channel number
4	PRESS_RL	reference level pressure
5	PPCODE	SYNOP pressure code
6	OBS_VALUE	observed value
7	FG_DEPARTURE	first guess departure
8	OBS-ERROR	observation error
9	FG_ERROR	first-guess error
10	WINCHAN_DEP	window channel departure
11	OBS_T	observed temperature

**Table 4.3** The predefined limits for the background quality control, given in terms of multiples of the expected variance of the normalized background departure.

Variable	Flag 1	Flag 2	Flag 3
u, v	9.00	16.00	25.00
z, ps	12.25	25.00	36.00
dz	x	x	x
T	9.00	16.00	25.00
rh, q	9.00	16.00	25.00

Flag values are denoted by 1 for a probably correct, 2 for a probably incorrect and 3 for an incorrect observation. The variables are denoted by u and v for wind components, z for geopotential height, ps for surface pressure, dz for thickness, T for temperature, rh for relative humidity and q for specific humidity, respectively.

(b) *Satellite radiances*

Like for any other observations, decisions are made to use or not use a particular radiance observation in the blacklist. These fall into two distinct types: The first is the usual a priori type decision which takes no account of the actual value of the observation. Examples for radiances include the exclusion of data measured by new instruments which we do not yet wish to use, data measured by bad/failed instruments, data measured at extreme scan positions, exclusion of data measured over land or high orography and the exclusion of data at certain times of year when solar intrusions may cause problems (there are others). The second type of test is particular to radiances and is a run-time decision based on the observed values (or more correctly the radiance departure from the background).

Depending on the magnitude of the radiance departure in key window channels, individual or combinations of microwave and infrared channels may be rejected. In some respects this may be considered an additional first-guess check that takes place in the blacklists. It can equally well be considered as an additional cloud/rain detection check that takes place in the blacklist as it exclusively involves window channels. No attempt is made here to document the particular test and threshold which are applied to each channel on every instrument and the user is referred to the data selection blacklists files for details. For both types of test applied in the blacklists environment, if it is failed there are two options for what then results. The setting of a FAIL(CONSTANT) flag means that the observations will be rejected and take no further part in the analysis. The setting of a FAIL(EXPERIMENTAL) flag means that the observation will enter the main analysis in such a way that it cannot force increments of e.g. temperature or humidity, but it can influence the calculation and evolution of bias correction coefficients inside VARBC. An example of when the latter is used would be for a new satellite for which we do not wish to actively assimilate the data, but wish to establish an accurate bias correction. Another application of the FAIL(EXPERIMENTAL) facility is its use for window channels used in the quality control of other data.

For some window channel microwave radiances over land, another setting of the blacklisting decision can be FAIL(USE\_EMISKF\_ONLY). This means that the observation will not be used for the atmospheric analysis in a similar way as FAIL(CONSTANT) rejects the observation, but the observation is used to influence the emissivity Kalman Filter atlas, described in section 3.3.2.

#### 4.4.3 Background quality control

The background quality control (FIRST) is performed for all the variables that are intended to be used in the assimilation. The procedure is as follows. The variance of the background departure  $y - H(\chi_b)$  can be estimated as a sum of observation and background-error variances  $\sigma_o^2 + \sigma_b^2$ , assuming that the observation and the background errors are uncorrelated. After normalizing with  $\sigma_b$ , the estimate of variance for the normalized departure is given by  $1 + \sigma_o^2/\sigma_b^2$ . In the background quality control, the square of the normalized background departure is considered as suspect when it exceeds its expected variance more than by a predefined multiple

(**FGCHK**, **SUFGLIM**). For the wind observations, the background quality control is performed simultaneously for both wind components (**FGWND**). In practice, there is an associated background quality-control flag with four possible values, namely 0 for a correct, 1 for a probably correct, 2 for a probably incorrect and 3 for an incorrect observation, respectively (**SUSCRE0**). [Table 4.3](#) gives the predefined limits for the background quality control in terms of multiples of the expected variance of the normalized background departure. These values are set in DEFRUN and can be changed in namelist **NAMJO**. For SATOB winds the background error limits are modified as explained in [Appendix A](#).

There is also a background quality control for the observed wind direction (**FGWND**). The predefined error limits of 60°, 90° and 120° apply for flag values 1, 2 and 3, respectively. The background quality control for the wind direction is applied only above 700 hPa for upper-air observations for wind speeds larger than 15 ms<sup>-1</sup>. If the wind-direction background quality-control flag has been set to a value that is greater than or equal to 2, the background quality-control flag for the wind observations is increased by 1.

There is no first-guess check for scatterometer data. It is demanded, though, that neither scatterometer nor model wind speed should exceed 35 ms<sup>-1</sup>, since that marks the range of validity for scatterometer wind inversion.

## 4.5 THE DEPENDENT OBSERVATION SCREENING DECISIONS

### 4.5.1 Update of the observations

Just before performing the dependent screening decisions, the flag information gathered so far is converted into a status of the reports, namely: **active**, **passive**, **rejected** or **blacklisted**, and also into a status of the data in the reports (**FLGTST**). The reports with a RDB report flag value 2 (probably incorrect) or higher for latitude, longitude, date and time are rejected. For the observed data there are RDB datum flags for the variable and for the pressure, i.e. the pressure level of the observation. The rejection limits for these are as follows: all data are rejected for the maximum RDB datum flag value 3 (incorrect), non-standard-level data are rejected for the maximum RDB datum flag value 2, and for the pressure RDB datum flag the rejection limit is 1 (probably correct). The background quality control rejection limits are flag value 3 for all the data, and flag value 2 for the non-standard-level data.

### 4.5.2 Global time–location arrays

Some of the dependent decisions require a global view to the data which is not available as the memory is distributed. Therefore *ad hoc* global time–location arrays are formed and broadcast in order to provide this view (GLOBA, DISTR).

### 4.5.3 Vertical consistency of multilevel reports

The first dependent decisions are the vertical-consistency check of multilevel reports (**VERCO**), and the removal of duplicated levels from the reports. The vertical-consistency check of multilevel reports is applied in such a way that if four consecutive layers are found to be of suspicious quality, even having a flag value one, then these layers are rejected, and also all the layers above these four are rejected in the case of geopotential observations. These decisions clearly require the quality-control information, and they are therefore 'dependent' on the preceding decisions.

### 4.5.4 Removal of duplicated reports

The duplicated reports will be removed next. That is performed (**MISCE**, **DUPLI**, **REDSL**) by searching pairs of collocated reports of the same observation types, and then checking the content of these reports. It may, for instance, happen that an airep report is formally duplicated by having a slightly different station identifier but with the observed variables inside these reports being exactly the same, or partially duplicated. The pair-wise checking of duplicates results in a rejection of some or all of the content of one of the reports.

#### 4.5.5 Redundancy check

The redundancy check of the reports, together with the level selection of multi-level reports, is performed next for the active reports that are collocated and that originate from the same station (REDUN). In 3D-screening, this check applies to the whole observation time window. In 4D-screening (LSCRE4D = .TRUE.), this check applies separately in each timeslot.

For **LAND SYNOP** and **PAOB** reports, the report closest to the analysis time with most active data is retained, whereas the other reports from that station are considered as redundant and are therefore rejected from the assimilation (REDRP, REDMO). For **SHIP SYNOP** and **DRIBU** observations the redundancy check is done in a slightly modified fashion (REDGL). These observations are considered as potentially redundant if the moving platforms are within a circle with a radius of 1° latitude. Also in this case only the report closest to the analysis time with most active data is retained. All the data from the multilevel **TEMP** and **PILOT** reports from same station are considered at the same time in the redundancy check (REDOR, SELEC). The principle is to retain the best quality data in the vicinity of standard levels and closest to the analysis time. One such datum will, however, only be retained in one of the reports. A wind observation, for instance, from a sounding station may therefore be retained either in a TEMP or in a PILOT report, depending on which one happens to be of a better quality. A **SYNOP** mass observation, if made at the same time and at the same station as the TEMP report, is redundant if there are any TEMP geopotential height observations that are no more than 50 hPa above the SYNOP mass observation (REDSM).

#### 4.5.6 Thinning

Finally, a horizontal thinning is performed for the AIREP, radiances (ATOVS,AIRS,IASI), GEOS, SATOB, ERS and SCAT SCAT reports. The horizontal thinning of reports means that a predefined minimum horizontal distance between the nearby reports from the same platform is enforced. For AIREP reports the free distance between reports is currently enforced to about 60 km (Cardinali *et al.*, 2003). The thinning of the AIREP data is performed with respect to one aircraft at a time (MOVPL, THIAIR). Reports from different aircraft may however be very close to each other. In this removal of redundant reports the best quality data is retained as the preceding quality controls are taken into account. In vertical, the thinning is performed for layers around model levels, thus allowing more reports for ascending and descending flight paths.

Thinning of radiances, GRAD, SATOB, ERS and ASCAT SCAT reports are each done in two stages controlled by THINN. For radiances (THINNER), a minimum distance of about 70 km is enforced and, thereafter, a repeat scan is performed to achieve the final separation of roughly 250 km or 120 km between reports from one platform. This is controlled through settings in DEFRUN, that can also be modified through namelist (NAMSCC). The thinning algorithm is the same as used for AIREPs except that for radiances a different preference order is applied: a sea sounding is preferred over a land one, a clear sounding is preferred over a cloudy one and, finally, the closest observation time to the analysis time is preferred. For geostationary water vapour radiances, a similar thinning in two stages is applied with currently about 70 km minimum distance and about 125 km final separation (THINNER). During the thinning, preference is given to data having the largest fraction of clear sky in the clear-sky radiance average, high infrared brightness temperature (for GOES data) and, finally, a small standard deviation of brightness temperatures within the CSR mean. A similar thinning technique is applied to SATOB high-density data (THINNER). Note that prior to assimilation a coarser pre-thinning may take place already during observation pre-processing in order to reduce otherwise excessive data volumes.

The screening of SATOB data has been extended for atmospheric motion wind observations, including individual quality estimate. The quality information from the quality control performed by the producer at extraction time is appended to each wind observation. This Quality Indicator (QI) is introduced as an additional criterion in the thinning step; priority is given to the observation with the highest QI value.

For ERS and ASCAT scatterometer data, the above described thinning algorithm is only applied along track. In across-track direction, backscatter data from these platforms are provided into wind-vector cells (WVC) with a spatial resolution of 25 km. In this direction, data is thinned by selecting predefined wind-vector cells (subroutine SCAQC). For ERS, from 19 cells, only 3, 7, 11, 15 and 19 are regarded (cells 1 and 2 are of known lower quality). For ASCAT, from 42 cells (two swaths of 21 cells each) only cells 1, 5, 9, 13, 17, 21, 22, 26, 30, 34, 38 and 42 are used. After this across-track thinning, the generic thinning algorithm is applied to the

remaining cells in along-track direction. QuikSCAT data (also provided on a 25 km grid) are not thinned. Instead, a 50 km wind product is determined from backscatter data from four underlying 25 km cells, each given a reduced weight of one fourth.

Scatterometer winds are besides thinning subject to a high-wind rejection test with an upper-wind speed limit set to  $35 \text{ ms}^{-1}$  to both the scatterometer and background winds (FGWND).

#### 4.5.7 Compression of the ODB

After the observation screening roughly a fraction of 1/10 of all the observed data are active and so the compressed observation ODB (the CCMA) for the minimization run only contains those data. The large compression rate is mainly driven by the number of radiance data, since after the screening there are only 10–20% of the radiance reports left, whereas for the conventional observations the figure is around 40%. As a part of the compression, the observations are re-sorted amongst the processors for the minimization job in order to achieve a more optimal load balancing of the parallel computer.

### 4.6 PARALLEL ASPECTS

As mentioned earlier, in the observation screening there are the two basic types of decision to be made. Independent decisions, on one hand, are those where no information concerning any other observation or decision is needed. In a parallel-computing environment these decisions can be happily made by different processors fully in parallel. For dependent decisions, on the other hand, a global view of the observations is needed which implies that some communication between the processors is required. The observation array is, however, far too large to be copied for each individual processor. Therefore, the implementation of observation screening at the ECMWF is such that only the minimum necessary information concerning the reports is communicated globally.

The global view of the observations is provided in the form of a global 'time–location' array for selected observation types. That array contains compact information concerning the reports that are still active at this stage. For instance, the observation time, location and station identifier as well as the owner processor of that report are included. The time–location array is composed at each processor locally and then collected for merging and redistribution to each processor. After the redistribution, the array is sorted locally within the processors according to the unique sequence number. Thus, every processor has exactly the same information to start with, and the dependent decisions can be performed in a reproducible manner independently of the computer configuration.

The time–location array is just large enough for all the dependent decisions, except for the redundancy checking of the multilevel TEMP and PILOT reports. This is a special case, in the sense that the information concerning each and every observed variable from each level is needed. Hence, the whole multilevel report has to be communicated. The alternative to this would be to force the observation clusters of the multilevel reports always into one processor without splitting them. In that case the codes responsible for the creation of the observation arrays for assimilation would need to ensure the geographical integrity of the observation arrays distributed amongst the processors. This is, however, not possible in all the cases, and the observation screening has to be able to cope with this. Currently, it is coded in such a way that only a limited number of multilevel TEMP and PILOT reports, based on the time–location array, are communicated between the appropriate processors as copies of these common stations.

## APPENDIX A

### A.1 Bad reporting practice of SYNOP and TEMP reports

The way the synoptic surface stations report mass observations (pressure or geopotential height) is considered as bad if:

- station altitude is above 800 m and station reports mean sea level pressure
- station altitude is above 800 m and station reports 1000 hPa level
- station altitude is above 1700 m and station reports 900 hPa level
- station altitude is below 300 m and station reports 900 hPa level

- station altitude is above 2300 m and station reports 850 hPa level
- station altitude is below 800 m and station reports 850 hPa level
- station altitude is above 3700 m and station reports 700 hPa level
- station altitude is below 2300 m and station reports 700 hPa level
- station altitude is below 3700 m and station reports 500 hPa level

The reporting practice is also considered as bad if the station reports 500 gpm, 1000 gpm, 2000 gpm, 3000 gpm or 4000 gpm level pressure, respectively, and station altitude is more than 800 m different from the reported level.

For TEMP geopotentials the reporting practice is considered as bad if:

- station altitude is above 800 m and station reports 1000 hPa level
- station altitude is above 2300 m and station reports 850 hPa level
- station altitude is above 3700 m and station reports 700 hPa level

## A.2 Revised background quality control for selected observations

The background quality-control rejection limits are applied more strictly for some observation types than stated in [Table 4.3](#). The special cases are the following ones.

- AIREP wind observations with zero wind speed are rejected if the background wind exceeds  $5 \text{ m s}^{-1}$ .
- For AIREP and DRIBU wind observations the rejection limit is multiplied by 0.5, and for PILOT wind by 0.8.
- For SATOB wind observations the rejection limit is multiplied by 0.1, except below 700 hPa level where it is multiplied by 0.2.
- No background quality control is applied for SCAT winds.
- For DRIBU surface pressure observations the rejection limit is multiplied by 0.9, and for PAOB surface pressure by 0.7.
- For AIREP temperature observations the rejection limit is multiplied by 1.6.

## Chapter 5

# Deprecated areas

### Table of contents

- 5.1 Introduction**
- 5.2 Continuous Observation Processing Environment (COPE) transition**
- 5.3 MKCMARPL tasks and functions [DEPRECATED]**
  - 5.3.1 Basic observation processing setup [DEPRECATED]
  - 5.3.2 Invoking, initializing and controlling the MKCMARPL [DEPRECATED]
  - 5.3.3 MKCMARPL [DEPRECATED]
  - 5.3.4 Basic observation handling routines [DEPRECATED]

### 5.1 INTRODUCTION

This section is for deprecated parts of the observation code, things which have increasingly little relevance to understanding the modern system. Unfortunately, the deprecated code still performs a few important tasks, otherwise it would have already been removed. This documentation is not kept up to date but it is still useful for understanding those few remaining tasks, especially for those people whose job it will be to replace them completely.

The main deprecated area is 'Make CMA replacement' or **MKCMARPL** which once performed most of the pre-processing tasks in the IFS. Nowadays, pre-processing for conventional in-situ observations has largely been superseded by COPE (what remains is Meteo-France specific). However, a number of other observation types still rely on **MKCMARPL** in important ways, or just in annoying ways that make it hard to simply delete what is apparently useless code. For example:

- AMVs require variable conversion from windspeed and direction to horizontal wind components *u* and *v*. More pointlessly, they also need to set up an (unused) initial observation error using the deprecated **OBSERR** routines. This error needs to be present in the ODB to prevent rejection during screening, even though it is not used.
- For some satellite radiances, channel numbering is reassigned. There may or may not be anything else useful going on under **LEVEL1CGEOS.OB**. for example, there are checks on longitudes, latitudes and times, but these are likely duplicates of checks elsewhere in the pre-processing.
- Scatterometer processing still relies on the MKCMARPL. The retrieval from backscatter to winds, and re-ordering of the observation body elements.
- Ozone observations still rely on MKCMARPL. Among other things they set up observation errors here.

### 5.2 CONTINUOUS OBSERVATION PROCESSING ENVIRONMENT (COPE) TRANSITION

The following is an alphabetical list of all subroutines, modules and module variables that have been deprecated and that are planned to be removed from IFS in one of the future cycles, or have already been removed:

**AIREPBE, AIREPIN, AWPRFIN, BIASCOR\_ODB, CONVENTIONAL\_OB, DRIBUBE, DRIBUIN, ERR-STAT, EWPRFIN, FINOEREV, FIXERR, GET\_NEW\_RS\_TRH\_BIAS, GET\_RS\_T\_BIAS, HATBIASC, LNDYIN, METARIN, NEW\_RS\_TRH\_BIAS, OBINSTP, OBSERR, PGPSIN, PILOTBE, PILOTIN, PRLMCHK, PTENDCOR, REPSEL, RH2Q, RS\_BIAS\_VALIDITY, SHIPIN, SONDE\_COUNTRY\_DB\_MATCH,**

SULEVLAY, SUOBSERR, SYNOPBE, SYNOPIN, TEMPBE, TEMPIN, YOMLVLY, YOMMKODB:LCD[0-9]\*, YOMMKODB:NMKCMVSE, YOMOERR, YOMOBS:LMKCMARPL, YOMRSTRHBIAS, Z2PICAO.

Note that some of these (for example **OBSERR** and **ERRSTAT**) are still used by, for example, the AMVs.

Additionally, some of the subroutines considered to be completely obsolete were not reimplemented in COPE framework. These include **PTENDCOR** formerly used for ship surface pressure adjustment (Subsection 2.4.3) and subroutines **GET\_RS\_T\_BIAS**, **HATBIASC**, **BIASCOR\_ODB**, **RS\_BIAS\_VALIDITY** and **BIASCOR** used for old style radiosonde temperature and humidity bias correction. These subroutines are not likely to be reimplemented in COPE unless there is a specific need to do so.

The following listing should give some pointers as to where to find particular **MKCMARPL** functionalities within the COPE framework. On the left side (red font) are former IFS Fortran subroutines and, on the right (bold font), their corresponding counterparts in COPE framework. Note that this is only represents a loose mapping where applicable:

- **AIREPIN** — **airep.json**
- **DRIBUIN** — **dribu.json**
- **TEMPIN** — **temp.json**
- **PILOTIN** — **pilot.json**
- **PGPSIN** — **pgps.json**
- **LNSYIN** — **synop.json**
- **SHIPIN** — **ship.json**
- **AWPRFIN** — **awp.json**
- **EWPRFIN** — **ewp.json**
- **PRLMCHK** — **DateTimeValidator, LocationValidator**
- **YOMOERR, SUOBSERR** — **error\_statistics.csv**
- **YOMLVLY, SULEVLAY, ERRSTAT, OBSERR, FIXERR** — **PrescribedErrorAssigner**
- **FINOEREV** — **FinalErrorAssigner**
- **RH2Q** — **SpecificHumidityAssigner**
- **OBINSTP** — **InstrumentTypeAssigner**
- **Z2PICAO** — **HeightToPressureConverter**
- **YOMRSTRHBIAS, GET\_NEW\_RS\_TRH\_BIAS, SONDE\_COUNTRY\_DB\_MATCH, NEW\_RS\_TRH\_BIAS** — **RadiosondeBiasCorrector**

As can be seen in the listing above, there is nearly one to one correspondence between the former **MKCMARPL** worker Fortran subroutines **[A-Z]\*IN** and **[a-z]\*.json** configuration files. This is not by coincidence since preserving the former logical structure makes the transition to new framework more transparent. The JSON configuration files describe processing pipeline for the given observation type in declarative way. This allows to modify or even construct new pipelines at runtime, reusing existing filters, without having to recompile the source. Conceptually, every pipeline is composed of a chain of filters that are sequentially applied on each observation report. All JSON configuration files can be found in the standard IFS scripts directory.

## 5.3 MKCMARPL TASKS AND FUNCTIONS *[DEPRECATED]*

### 5.3.1 Basic observation processing setup *[DEPRECATED]*

In order to perform the observation processing functions, a number of basic observation processing setups are carried out at the very beginning of initialising the IFS. This is done by calling several routines in addition to all other routines needed to setup the IFS.

- Program **MASTER** calls **CNT0** which in turn calls **SU0YOMA**.
- **SU0YOMA** calls (among other routines) **SUOAF** from which **SUCMOCTP**, **SUEVENTS**, **SUCODES**, **SUFLTXT** and **SUCMA** are called. **SUCMOCTP** defines the ODB observation types and code types, and **SUEVENTS**, **SUCODES** and **SUFLTXT** define analysis events, various codes used and flags naming conventions.
- **SUCMA** calls **SUCMAF** which then calls several subroutines: **SUCMAD1**, **SUCMAD2**, **SUCMAHFP**, **SUCMAHOP**, **SUCMBDFP** and **SUCMBDTP**. These routines define the structure of ODB Data



Descriptor Records (DDRs) as well as the ODB packing patterns (bit structure) employed for header and body respectively.

### 5.3.2 Invoking, initializing and controlling the MKCMARPL [DEPRECATED]

The MKCMARPL run is initiated by the **MKCMARPL** subroutine. This routine is only invoked in the SCREENING run of the IFS. It is called, together with some of its additional setup routines via subroutine SUOBS. The additional setup routines called at this level are: **SUANCT**, **DEFRUN**, **SULIM**, **SULEVLAY**, **SUSATRET**, **SUVNMB**, **SUSCREO**, **SUOBSORT**, **SETCOM**, **DEPERERR**, **SUERRORS**, **INIERSCA**.

- **MKCMARPL** is namelist driven and in **DEFRUN** a logical variable LMKCMARPL is defined. By default LMKCMARPL = .TRUE. but it can be overwritten via namelist NAMOBS. Furthermore, many other parameters and switches are defined in **DEFRUN** and some of them can also be overwritten via namelists.
- **SUANCT** and **SULIM** define some additional analysis constants and limits.
- **SULEVLAY** and **SUSATRET** define analysis related level/layer and satellite retrieval parameters, respectively.
- **SUVNMB** declares variable numbers.
- **SUSCREO**, **SUOBSORT** and **SETCOM** define flag limits, identify ambiguous moving platforms, initialise observation sorting, and provide some general observation common variables.
- **DEPERERR** and **SUERRORS** deal with observation error statistics definitions. **SUERRORS** calls **SUPERERR** to define observation persistence errors and **SUOBSERR** to define prescribed observation errors.
- **INIERSCA** deals with initialising SCATT processing.

The next step is to find out if it is a SCREENING run and if so to check if it is a MKCMARPL run as well. In the case of a MKCMARPL run all aspects of the observation processing before the screening are dealt with by calling **MKCMARPL** (more about it in [Subsection 5.3.3](#)). After **MKCMARPL** has finished there are several ways to proceed. These depend on the status of LMKCMARPLO and LRPLSWAPOUT logical switches (NAMOBS namelist). If LRPLSWAPOUT = .TRUE. the ODB is swapped out and if LMKCMARPLO = .TRUE. the ODB is written out and the run terminated. Both of these options are not normally used and their use is for diagnostics/debugging purposes. Once the **MKCMARPL** work has been completed the remainder of SUOBS will execute as before. Thus, calls to **WRITEOBA**, **WINDAUX**, **OBATABS**, **SUAMV**, **SURAD**, **SULIMB**, **SUOBAREA**, **MKGLOBSTAB** and **SUREO3** are issued.

In the context of operational running, the **MKCMARPL** related switches are set:

```
LMKCMARPL = .TRUE.   LRPLSWAPOUT = .FALSE.   LMKCAMRPLO = .FALSE.
```

### 5.3.3 MKCMARPL [DEPRECATED]

**WARNING:** As of IFS cycle 41r1, majority of MKCMARPL tasks dealing with conventional observation pre-processing have been deprecated and their functionality has been migrated to COPE framework. Although the MKCMARPL has not been fully replaced yet, and can still be used, it is strongly recommended to do new developments in the area of conventional observations within the COPE framework. For more details, including a full list of deprecated subroutines, see [Section 5.2](#).

The main purpose of **MKCMARPL** is to control the IFS observation pre-processing. Observation pre-processing at this stage is done in groups of observations. At the moment there are six groups: CONVENTIONAL, SATOB, TOVS/RTOVS, SCATT, LEVEL1C/GEOSS and OZONE observations. For each group a separate subroutine is called: **CONVENTIONAL\_OB**, **SATOB\_OB**, **TOVSRTOVS\_OB**, **SCAT\_OB**, **LEVEL1CGOES\_OB** and **OZONE\_OB**. These routines are just cover or hat routines for the actual work to be carried out underneath. However, **TOVSRTOVS\_OB** is currently not called because it is obsolete.

Each cover routine would call the ODB to get the observations it wants to process. This is done by calling the ODB **GETDB** subroutine. As the observations are brought, in one or more worker routines would be called to perform the observation processing functions. Once the worker routines have finished the control is handed back to the cover routine. The next step in the cover routine is to return observations back to the ODB database. This is done by calling the ODB **PUTDB** routine. In some of these cover routines several calls to

**GETDB/PUTDB** might be issued. This is because there may be sufficient differences between similar data to justify a slightly different approach in their pre-processing. For example under the **CONVENTIONAL\_OB** routine there are two calls to a **GETDB** and **PUTDB** pair. The first call deals with all conventional observations except SATEMs; the second call deals with the SATEMs. As indicated earlier, between each **GETDB** and **PUTDB** a number of observations type or code type designed worker routines are called.

- **CONVENTIONAL\_OB** calls the following worker routines: **SYNOBIN**, **AIREBIN**, **DRIBUIN**, **TEMPIN**, **PILOTIN**, **EWPRFIN**, **AWPRFIN**, **PAOBIN** and **METARSIN**. A worker routine name indicates which observations it is dealing with.
- **SATOB\_OB** calls **SATOBIN** and **SATAMIN**.
- **SCAT\_OB** calls **ERS1IN**, **NSCATIN**, **ASCATIN** and **QSCATIN**.
- **LEVEL1CGEOS\_OB** calls **RAD1CIN** and **GOESRIN**.
- **OZONE\_OB** calls only **REO3SIN**.

### 5.3.4 Basic observation handling routines [DEPRECATED]

The observation pre-processing worker routines referred to in [Subsection 5.3.3](#), names of which always end with “IN”, are the basic observation handling routines. They all follow more or less the same logic. As an example consider **AIREBIN** which deals with AIREP observations.

The first thing which is done is to define the instrument specification (**OBINSTP**) followed by preliminary quality control check both at the report level (**PRLMCHK**) as well as at the data level (**GETSETE** and **AIREPBE**).

- **PRLMCHK** calls **REPSEL** and **TIMDIF** to do report selection according to preset criteria and to find out time difference between analysis time and the actual observation time, respectively.
- **GETSETE** makes a local copy of a given observation variable and its related parameters from an ODB supplied array.
- After updating the local copy, **AIREPBE** is called to return the updated local copy back to the ODB supplied array.

The preliminary quality control at the report level consists of making sure that observation position, date and time are reasonable. Furthermore, as there is a possibility of excluding certain observations via the NAMOBS namelist, a check is made of whether the observation is actually wanted at this stage. Once the report level check is passed attention is turned to the data itself. Each datum is checked against predefined list of expected data. If not in the list, datum is rejected and a warning message issued. At this stage it is also ensured that missing indicators used are unique.

After the preliminary phase attention is turned to getting data in the right form and shape for further usage. Thus, in the case of an AIREP observation, this is done in sections of available variables: wind and temperature.

- (i) **Wind.** There are four wind variables: wind direction (**DDD**), wind force (**FFF**),  $u$  and  $v$  components. For each of these variables the first thing which is done is to get a local copy of it together with its related parameters from an ODB supplied array (**GETSETE**). Once a variable is made available locally a check is made to ensure that the vertical coordinate is pressure; if instead of pressure a flight level is supplied it is converted into pressure by assuming a standard ICAO atmosphere (**Z2PICAO**). If the variable in question is either  $u$  or  $v$ , then **DDD** and **FFF** are converted into  $u$  and  $v$  wind components. Furthermore, for each of the four variables appropriate observation error statistics are assigned (**ERRSTAT**, **FINOERR**). Also, if any flags are set at this stage an appropriate word in the local copy is updated (**PPVAFL**). Finally, an updated local copy of an observed quantity and its related parameters are returned back into the ODB (**AIREPBE**).
- (ii) **Temperature.** In the case of temperature only one observed variable is dealt with. The pattern of making a local copy (**GETSETE**), ensuring that pressure is the vertical coordinate (**Z2PICAO**), assigning the observation error statistics (**ERRSTAT**), updating flags (**PPVAFL**) and returning an updated local copy back to the ODB (**AIREPBE**) is repeated.

As just mentioned **ERRSTAT** deals with assigning observation errors for a given observation variable. **ERRSTAT** first calls **OBSPERR** to assign observation persistence error; then it calls **OBSERR** which in turn calls **FIXERR**

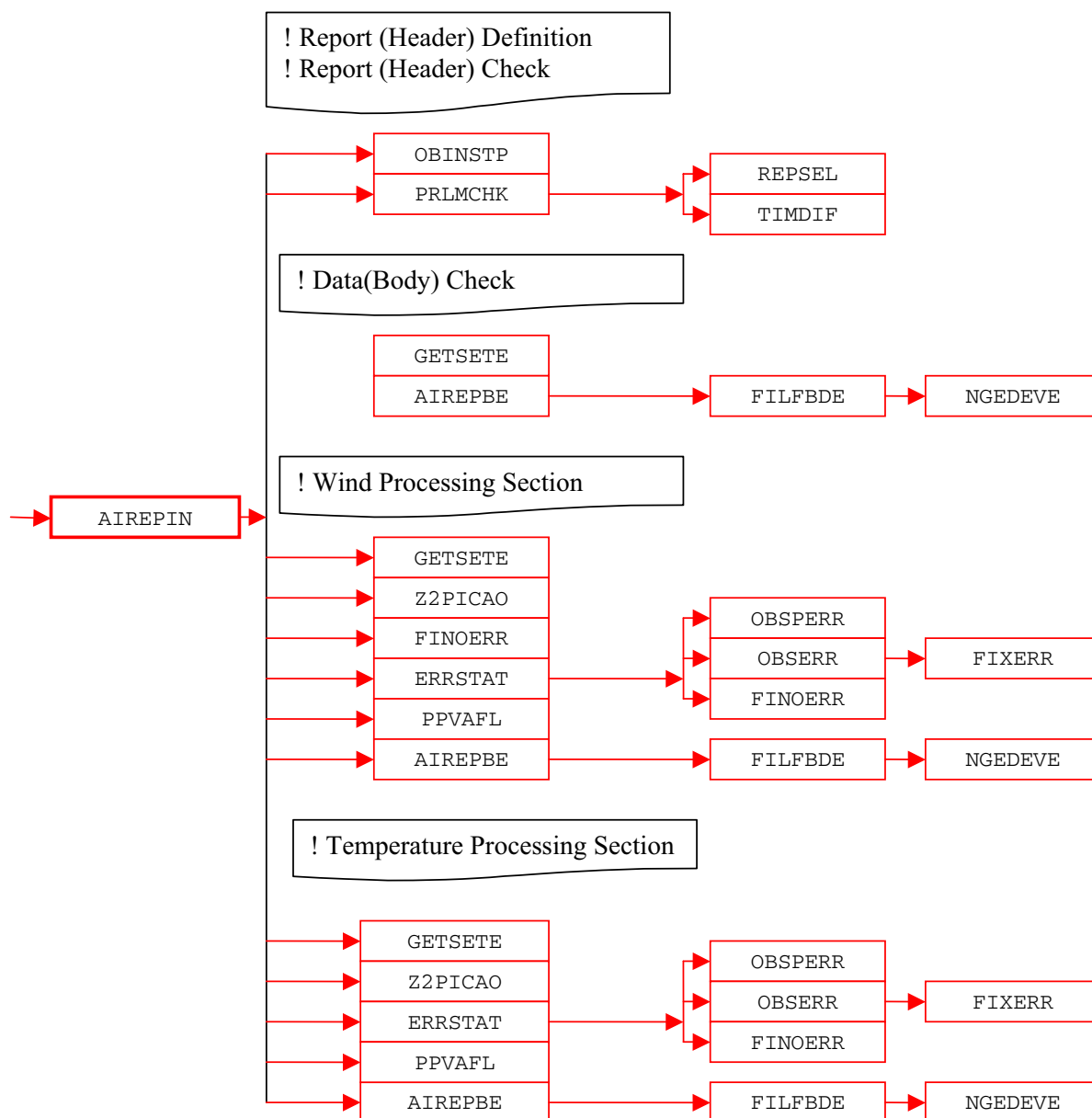


**Figure 5.1** Simplified IFS observation pre-processing flow diagram, with *AIREPIN* as an example. Colour coding scheme: routines in red boxes perform observation pre-processing.

to assign prescribed observation error. It is worth mentioning that observation errors themselves are already predefined at an earlier stage (*SU.ERRORS*).

The pattern of activities outlined for *AIREPIN* is repeated more or less in the other worker routines. However, the *SYNOBIN* routine is first split further into *SHIPIN*, *METARIN*, *PGPSIN* and *LANSYIN*. This is because SHIP, METAR, GPS and SYNOP LAND observations are sufficiently different to justify a separate worker routine. Furthermore, *LANSYIN* is somewhat more complicated than *AIREPIN*. One of the reasons for this is that we have to distinguish between low and high level stations.



## Chapter 6

# Tables, codes and flags

### Table of contents

- [6.1 Introduction](#)
- [6.2 BUFR observation types and subtypes](#)
- [6.3 Obstype and codetype](#)
- [6.4 Variable codes \(varno\)](#)
- [6.5 Conventional observation operator codes: NVAR and CVAR\\_NAME - \*\[DEPRECATED\]\*](#)
- [6.6 Observation characteristics: instrument specification and retrieval type](#)
- [6.7 Vertical coordinate: pressure, satellite ID and level ID codes](#)
- [6.8 ODB report status: events, flags and codes](#)
- [6.9 Datum status: events, RDB and analysis flags](#)

### 6.1 INTRODUCTION

Older versions of the IFS documentation have contained copious tables attempting to document all the codes, flags and groupings for observations in the IFS. If this was ever possible, in recent years the variety of observational data processing has mushroomed, these tables have in some places become hopelessly out of date and their true counterparts are too large to comfortably fit in such documentation. The truest record is the IFS source code, the ODB data archived to MARS, and the logfiles of the IFS. The ODB governance database at <http://apps.ecmwf.int/odbgov> is reasonably up-to-date but does not cover everything. Some of the old tables from the IFS documentation are provided here, although no longer kept up-to-date, as they are useful for illustration purposes, and as a guide to what these codes are for. See also Sec. 1.4.

### 6.2 BUFR OBSERVATION TYPES AND SUBTYPES

Although BUFR observation types and subtypes are not directly used in the IFS they are defined here. BUFR observation types and subtypes are mapped into ODB observation types and code types before the IFS (i.e. the **MERGEODB** step). Some example BUFR observation types and subtypes are listed in [Table 6.1](#). See WMO documentation for more, or the ODB governance tables <http://data-portal.ecmwf.int/odbgov/>

**Table 6.1** Some BUFR observation types and subtypes. See WMO documentation for the full set, or the ODB governance tables <http://data-portal.ecmwf.int/odbgov/>.

Observation Type		Subtype	
Code	Name	Code	Name
0	Land Surface	1	Land SYNOP
		3	Automatic Land SYNOP
		9	Abbreviated Land SYNOP
		110	GPS
		140	METAR
1	Sea Surface	9	SHIP
		11	SHIP
		13	Automatic SHIP
		19	Reduced SHIP
		21	DRIBU
		22	BATHY
2	Upper Air Sounding	91	Land PILOT
		92	SHIP PILOT
		95	Wind Profiler (American)
		96	Wind Profiler (European/Japanese)
		101	Land TEMP
		102	SHIP TEMPS
		103	DROP TEMP
		104	ROCOB
		105	SHIP ROCOB
		106	Mobile TEMP
3	Satellite Sounding	0	High Resolution TOVS
		51	High Resolution TOVS
		53	RTOVS
		54	ATOVS
		55	ATOVS
		57	ATOVS
		61	Low Level Temperature SATEM
		62	High Level SATEM
		63	PWC SATEM
		65	Merged SATEM
		71	Low Level TOVS
		72	High Level TOVS
		73	PWC TOVS
		75	Merged TOVS
		129	TRMM
130	TMI		
161	PAOB		
206	OZONE Retrieved Layers		

Table 6.1 *Continued.*

Observation Type		Subtype	
Code	Name	Code	Name
4	AIREP	142	AIREP
		143	COLBA
		144	AMDAR
		145	ACARS
5	SATOB	82	Temperature and Wind
		83	Wind Only
		84	Temperature only
		85	Temperature only
		86	High Resolution VIS Wind
		87	AMV
		89	Geostationary Clear Sky Radiances (GRAD)
12	SCATT/SSMI	189	Geostationary Clear Sky Radiances (GRAD)
		190	Geostationary All Sky Radiances (GRAD)
		122	ERS-1, ERS-2
		127	SSMI
		136	NSCAT
253	PAOB	137	QSCAT
		139	ASCAT
		161	PAOB

**Table 6.2** *Some ODB observation types and code types. See the ODB governance tables <http://data-portal.ecmwf.int/odbgov/> for a fuller and more up-to-date list*

Observation Type		Code Type	
Code	Name	Code	Name
1	SYNOP	11	Land SYNOP
		14	Automatic Land SYNOP
		16	French RADOME
		21	SHIP
		22	Abbreviated SHIP
		23	SHRED
		24	Automatic SHIP
		140	METAR
		110	GPS
		2	AIREP
141	AIREP		
142	Simulated AIREP		
144	AMDAR		
145	ACARS		
241	COLBA		
3	SATO	88	SATO
		89	High Resolution VIS wind
		90	AMV
		188	SST
4	DRIBU	63	BATHY
		64	TESAC
		160	ERS as DRIBU
		165	DRIBU
5	TEMP	35	Land TEMP
		36	SHIP TEMP
		37	Mobile TEMP
		39	ROCOB
		40	SHIP ROCOB
		135	DROP TEMP
		137	Simulated TEMP

### 6.3 OBSTYPE AND CODETYPE

There are also ODB 'observation types' and, as with BUFR, there are different number of code types for each of them. It is reasonable to question why the BUFR and ODB observation types and sub or code types are different. The answer is a historic one. The ODB observation types and code types have been used before BUFR came in to existence and as an international code it was difficult to impose our practice on the others. Also, there was not enough enthusiasm on our side to switch to the BUFR ones. Some ODB observation types and code types are listed in Table 6.2. See the ODB governance tables <http://data-portal.ecmwf.int/odbgov/> for a fuller and more up-to-date list. The coexistence of different codes used for BUFR and ODB observation types and the subtype and code type requires a mapping from one to another. The ODB governance tables also describe that mapping.



Table 6.2 *Continued.*

Observation Type		Code Type	
Code	Name	Code	Name
6	PILOT	32	Land PILOT
		33	SHIP PILOT
		34	American Wind Profiler
		131	Japanese Wind Profiler
		132	Mobile Wind Profiler
		134	European Wind Profiler
7	SATEM	86	GTS SATEM
		184	High Resolution Simulated TOVS
		185	High Resolution Simulated DWL SATEM
		186	High Resolution SATEM
		200	GTS BUFR SATEM 250km
		201	GTS BUFR Clear Radiances
		202	GTS BUFR Retrieved Profiles/Clear Radiances
		210	ATOVS/GRAD
		211	RTOVS
		212	TOVS
		215	SSMI
8	PAOB	164	PAOB
9	SCATTEROMETER	122	ERS-1, ERS-2
		210	NSCAT
		301	QuikSCAT
		139	ASCAT
10	RAW RADIANCE		

**Table 6.3** Some variables (VARNO) in the ODB. Check the ODB governance database <http://data-portal.ecmwf.int/odbgov/> for the latest information.

No.	Code	Name	Unit
1	3	Wind Component ( $u$ )	$\text{ms}^{-1}$
2	4	Wind Component ( $v$ )	$\text{ms}^{-1}$
3	1	Geopotential ( $Z$ )	$\text{m}^2\text{s}^{-2}$
4	57	Thickness ( $DZ$ )	$\text{m}^2\text{s}^{-2}$
5	29	Relative Humidity ( $RH$ )	numeric
6	9	Precipitable Water Content ( $PWC$ )	$\text{kgm}^{-2}$
7	58	2 m Relative Humidity ( $RH_{2m}$ )	numeric
8	2	Temperature	K
9	59	Dew Point	K
10	39	2 m Temperature ( $T_{2m}$ )	K
11	40	2 m Dew Point ( $Td_{2m}$ )	K
12	11	Surface Temperature ( $T_s$ )	K
13	30	Pressure Tendency ( $P_t$ )	Pa/3h
14	60	Past Weather ( $W$ )	WMO Code 4561
15	61	Present Weather ( $WW$ )	WMO Code 4677
16	62	Visibility ( $V$ )	WMO Code 4300
17	63	Type of High Clouds ( $C_H$ )	WMO Code 0509
18	64	Type of Middle Clouds ( $C_M$ )	WMO Code 0515
19	65	Type of Low Clouds ( $C_L$ )	WMO Code 0513
20	66	Cloud Base Height ( $N_h$ )	m
21	67	Low Cloud Amount ( $N$ )	WMO Code 2700
22	68	Additional Cloud Group Height ( $h_s h_s$ )	m
23	69	Additional Cloud Group Type ( $C$ )	WMO Code 0500
24	70	Additional Cloud Group Amount ( $N_s$ )	WMO Code 2700
25	71	Snow Depth ( $Sd$ )	m
26	72	State of Ground ( $E$ )	WMO Code 0901
27	73	Ground Temperature ( $T_g T_g$ )	K
28	74	Special Phenomena ( $S_p S_p$ )	WMO Code 3778
29	75	Special Phenomena ( $s_p s_p$ )	WMO Code 3778
30	76	Ice Code Type ( $R_s$ )	WMO Code 3551
31	77	Ice Thickness ( $E_s E_s$ )	WMO Code 1751
32	78	Ice ( $I_s$ )	WMO Code 1751
33	79	Time Period of Rain Information ( $t_r t_r$ )	hour
34	80	6 Hour Rain Amount	$\text{kgm}^{-2}$
35	81	Maximum Temperature ( $JJ$ )	K
36	82	Ship Speed ( $V_s$ )	$\text{ms}^{-1}$
37	83	Ship Direction ( $D_s$ )	degree
38	84	Wave Height ( $H_w H_w$ )	m
39	85	Wave Period ( $P_w P_w$ )	s
40	86	Wave Direction ( $D_w D_w$ )	degree
41	87	General Cloud Group	WMO Code

## 6.4 VARIABLE CODES (VARNO)

To provide easy recognition of ‘observed’ variables each of them is assigned a numerical code. These codes are then embedded in ODB reports. For illustrative purposes some historical codes are listed in Table 6.3 but for the latest information please check the subroutine or ideally the ODB governance database <http://data-portal.ecmwf.int/odbgov/>. The **VARNO\_MODULE** encodes these varnos in the IFS and is auto-generated from the ODB database. Note there is an additional indexing of varnos, given in the first column of Table 6.3, which is encoded in the routine **SUVNMB**. This additional ‘implied’ varno is DEPRECATED and will be eliminated in the next cycle.

Table 6.3 *Continued.*

No.	Code	Name	Unit
42	88	Relative Humidity from Low Clouds	numeric
43	89	Relative Humidity from Middle Clouds	numeric
44	90	Relative Humidity from High Clouds	numeric
45	91	Total Amount of Clouds	WMO Code 20011
46	92	6 Hour Snowfall	m
47	110	Surface Pressure ( $P_s$ )	Pa
48	111	Wind Direction	degree
49	112	Wind Force	$\text{ms}^{-1}$
50	119	Brightness Temperature ( $T_b$ )	K
51	120	Raw Radiance	K
52	121	Cloud Amount from Satellite	%
53	122	Backscatter ( $\sigma^0$ )	dB
54	5	Wind Shear ( $\partial u/\partial z$ )	$\text{s}^{-1}$
55	6	Wind Shear ( $\partial v/\partial z$ )	$\text{s}^{-1}$
56	41	$u_{10\text{m}}$	$\text{ms}^{-1}$
57	42	$v_{10\text{m}}$	$\text{ms}^{-1}$
58	19	Layer Relative Humidity	numeric
59	200	Auxiliary Variable	numeric
60	123	Cloud Liquid Water ( $Q_l$ )	$\text{kgkg}^{-1}$
61	124	Ambiguous v	$\text{ms}^{-1}$
62	125	Ambiguous u	$\text{ms}^{-1}$
63	7	Specific Humidity ( $Q$ )	$\text{kgkg}^{-1}$
64	126	Ambiguous Wind Direction	degree
65	127	Ambiguous Wind Speed	$\text{ms}^{-1}$
66	8	Vertical Speed	$\text{ms}^{-1}$
67	56	Virtual Temperature ( $T_v$ )	K
68	206	Ozone	$\text{kgm}^{-2}$
69	156	Height	m
70	215	SSM/I Pseudo Variable	$\text{kgm}^{-2}$
71	160	Past Weather	numeric
72	130	Pressure Tendency Characteristics	numeric
73	12	Sea Water Temperature	K
74	192	Radar Reflectivity	Db
75	128	Atmospheric Path Delay in Satellite Signal	m
76	162	Radio Occultation Bending Angle	Rad
77	187	Horizontal line-of-sight wind component	$\text{ms}^{-1}$
78	174	Aerosol optical depth at $0.55\mu\text{m}$ (AOD)	
79	163	Limb Radiances	
80	181	GEMS reactive gases, N02	
81	182	GEMS reactive gases, S02	
82	183	GEMS reactive gases, CO	
83	184	GEMS reactive gases	
84	185	GEMS reactive gases, G03	
85	175	Cloud optical depth (COD)	
86	176	Ratio of fine mode to total aerosol optical depth at $0.55\mu\text{m}$ (RAO)	
87	177	Aerosol reflectance multi-channel (RFA)	
88	178	Aerosol optical depth multi-channel (ODA)	
89	179	Normalized Soil Moisture	0-100%
90	180	Soil Moisture	$\text{kg}^3\text{kg}^{-3}$
91	186	GHG	
92	187	GHG	
93	195	Radar doppler wind	

**Table 6.4** Association between variable numbering and observation operator routines for some of the longstanding observation types. The CVAR-NAMEs also appear in the printed Jo-table in the log-file. For the full and up-to-date set of variable numbers see [yomcosjo.F90](#).

NVAR	CVAR_NAME	Observation operator routine	Description
1	U	PPUV	Upper air wind components
2	U10	PPUV10M	10-metre wind components
3	DD		Wind direction
4	FF	PPUV	Wind speed
5	H	PPRH	Relative humidity
6	H2	PPRH2M	2-metre relative humidity
7	T	PPT	Temperature
8	Z	PPGEOP	Geopotential
9	DZ	PPGEOP	Thickness
10	LH	PPRH	Layer mean RH (M-France)
11	T2	PPT2M	2-metre temperature
12	TS		Surface temperature (M-France)
13	RAD	RADTR/RADTR_ML	Radiance data
14	SN		Snow (M-France)
15	RR		Rain rate (M-France)
16	PS	PPPS	Surface pressure
17	CC	PPTCC	Cloud cover
18	CLW	PPCLW	Cloud liquid water
19	Q	PPQ	Specific humidity
20	FFF	PPUV10M	10-metre wind speed
21	S0		Sigma_0
22	X		Reserved
23	PWC	PPPWC	Layer water content or TCWV
24	TO3	PPPWC	Layer ozone content
25	TCW		Layer cloud water content
26	RFL	REFLSIM	Radar reflectivity
27	APD	GPSZEN_DELAY	GPS total zenith delay
28	RO	GPSRO_OP	GPS radio occultation
29	HLS	PP_UV(+conversion to HLOS in HOP)	Horizontal line-of-sight winds
30	AOD	AOD_OP	Aerosol optical depth
31	LRA	RTL_HOP_1D	Limb sound radiance

## 6.5 CONVENTIONAL OBSERVATION OPERATOR CODES: NVAR AND CVAR\_NAME - [DEPRECATED]

Each available conventional observation operator has been given a number (NVAR) and a short name (CVAR\_NAME, three characters), set in [YOMCOSJO](#) and linked to the varno through [MAP\\_VARNO\\_TO\\_NVAR](#). These codes are also used to structure the diagnostic Jo-table. Some of the traditional operator names are: U, U10, DD, FF, H, H2, T, Z, DZ, LH, T2, TS, RAD, SN, RR, PS, CC, CLW, Q, FFF, S0, X, PWC, TO3 and TCW, numbered sequentially in NVAR. Each number can be referenced by variables such as NVAR\_U(= 1), NVAR\_U10(= 2) and so on. See [table 6.4](#).

**Table 6.5** *SYNOP instrument specification.*

Type	Bit Position	No. of Bits	Value – Description
Instrument Specification	0	10	32 – SYNOP Instrument Code Type
Not Defined	10–30	21	Reserved

**Table 6.6** *AIREP instrument specification.*

Type	Bit Position	No. of Bits	Value – Description
Instrument Specification	0	10	23 – AIREP Instrument Code Type
Flight Information	10	4	BUFR Code Table 8004 – Flight Phase
Not Defined	10–30	21	Reserved

**Table 6.7** *SATOB instrument specification.*

Type	Bit Position	No. of Bits	Value – Description
Instrument Specification	0	10	60 – GOES 62 – METEOSAT 63 – Indian SATOB 68 – Japan
I1 (Country Name)	10	4	0 – Europe 1 – Japan 2 – USA 3 – USSR 4 – India
I2I2 (Satellite Indicator Figure)	14	8	4 – METEOSAT 177 – Pretoria 0 – GEOS 3 – Japan 20 – India
Not Defined	22–30	8	Reserved

**Table 6.8** *DRIBU instrument specification.*

Type	Bit Position	No. of Bits	Value – Description
Instrument Specification	0	10	Not Defined
K1	10	4	Not Defined
K2	14	4	Not Defined
K3	18	4	Not Defined
Not Defined	22–30	8	Reserved

## 6.6 OBSERVATION CHARACTERISTICS: INSTRUMENT SPECIFICATION AND RETRIEVAL TYPE

Where applicable, [Tables 6.5](#) to [6.11](#) describe in details how the ODB's instrument specification word is structured. Tables provided are for different observation types.

In [Table 6.12](#) the ODB's header retrieval word codes are described.

**Table 6.9** *TEMP instrument specification.*

Type	Bit Position	No. of Bits	Value – Description
Instrument Specification	0	10	Not Defined
Not Defined	10–30	21	Reserved

**Table 6.10** *PILOT instrument specification.*

Type	Bit Position	No. of Bits	Value – Description
Instrument Specification	0	10	Not Defined
A4	10	4	Not Defined
Not Defined	14–30	17	Reserved

**Table 6.11** *SATEM instrument specification.*

Type	Bit Position	No. of Bits	Value – Description
Instrument Specification	0	23	77 777 777B
I3	24	4	WMO Manual On Codes, vol II, section II-4-E-8
I4	28	4	Data processing technique. WMO Manual On Codes, vol II, section II-4-E-9
I2I2	32	7	Satellite name. WMO Manual on Codes, vol II, section II-4-E-7
I1	39	4	Country operating satellite. WMO code 1761
IS	43	7	Instrument specification code. Research Manual 5, Table 7.5
Not Defined	50	18	Reserved

**Table 6.12** *Satellite retrieval codes.*

Retrieval Codes	Description
1	Clear
2	Partly Clear
3	Cloudy

**Table 6.13** *Vertical coordinate.*

Vertical Coordinate Codes	Description
1	Pressure (Pa)
2	Height (GPM)
3	Satellite Channel (numeric)
4	Scatterometer Channel (numeric)

**Table 6.14** *Pressure codes.*

Pressure Codes	Description
0	Sea Level
1	Station Level
2	850 hPa Geopotential
3	700 hPa Geopotential
4	500 hPa Geopotential
5	1000 GPM Pressure
6	2000 GPM Pressure
7	3000 GPM Pressure
8	4000 GPM Pressure
9	900 hPa Geopotential
10	1000 hPa Geopotential
11	500 hPa Geopotential
12	925 hPa Geopotential

**Table 6.15** *Level ID.*

Bit Position	No. of Bits	Value – Description
0	1	1 – Max Wind Level
1	1	1 – Tropopause
2	1	1 – D Part
3	1	1 – C Part
4	1	1 – B Part
5	1	1 – A Part
6	1	1 – Surface Level
7	1	1 – Significant Wind Level
8	1	1 – Significant Temperature Level
9–31	24	Not Defined

## 6.7 VERTICAL COORDINATE: PRESSURE, SATELLITE ID AND LEVEL ID CODES

In the ODB the vertical coordinate is expressed by various codes, and [Table 6.13](#) describes those codes.

Also, the ODB pressure code word is expressed in terms of codes which are defined in [Table 6.14](#).

Upper air observations (TEMP and PILOT) have the level at which the observation was taken defined in terms what it is and that information is stored in the ODB. Details are given in [Table 6.15](#).

**Table 6.16** *Report Status.*

Bit Position	No. of Bits	Value – Description
0	1	1 – Report Active
1	1	1 – Passive Report
2	1	1 – Rejected Report
3	1	1 – Blacklisted Report

**Table 6.17** *Blacklist Events.*

Bit Position	No. of Bits	Value – Description
0	1	1 – Monthly Monitoring
1	1	1 – Constant Blacklisting
2	1	1 – Experimental Blacklisting
3	1	1 – Whitelisting
4	1	1 – Experimental Whitelisting
5	1	1 – Observation Type Blacklisting
6	1	1 – Station ID Blacklisted
7	1	1 – Code Type Blacklisted
8	1	1 – Instrument Type Blacklisted
9	1	1 – Date Blacklisted
10	1	1 – Time Blacklisted
11	1	1 – Latitude Blacklisted
12	1	1 – Longitude Blacklisted
13	1	1 – Station Altitude Blacklisted
14	1	1 – Blacklisted due to Land/Sea Mask
15	1	1 – Blacklisted due to Model Orography
16	1	1 – Blacklisted due to distance from reference point
17–30	14	Not Used

**Table 6.18** *Global report events.*

Bit Position	No. of Bits	Description (Value)
0	1	1 – No Data in Report
1	1	1 – All Data Rejected
2	1	1 – Bad Reporting Practice
3	1	1 – Rejected due to RDB Flag
4	1	1 – Redundant Report
5	1	1 – Missing Station Altitude
6	1	1 – Failed Quality Control
7	1	1 – Report Overcast IR

## 6.8 ODB REPORT STATUS: EVENTS, FLAGS AND CODES

The status of each ODB report is described in terms of being active, passive, rejected or blacklisted. For some microwave radiances, the additional flag `use_emiskf_only` is also used, see 3.3.2 and (b). The ODB report status word is packed with the 4 bits given in Table 6.16.

There is one, 31 bits packed, word for each ODB report to account for various blacklist events. Details are given in Table 6.17.

Each ODB report has two words to store report events. Each report event word uses 31 bits. These events are set during observation processing to describe in more details what happened with a report.

The first ODB report event word is described in Table 6.18.



**Table 6.19** *TEMP report events.*

Bit Position	No. of Bits	Value – Description
0	1	1 - Old Style Z Bias Correction Applied
1	1	1 - New Style T Bias Correction Applied
2	1	1 - RH Bias Correction Applied
3–30	28	Not Used

**Table 6.20** *PILOT report events.*

Bit Position	No. of Bits	Value – Description
0	1	1 - American Wind Profiler
1	1	1 - European Wind Profiler
2–30	29	Not Used

**Table 6.21** *SATEM report events.*

Bit Position	No. of Bits	Value – Description
0	1	1 - Thinned Report
1–30	30	Not Used

**Table 6.22** *SCAT report events.*

Bit Position	No. of Bits	Value – Description
0	1	1 - Report thinned in across-node direction
1	1	1 - Reported Wind Directions too Close
2	1	1 - Report in QuikScat outer swath
3	1	1 - Report Contaminated by Rain
4–30	29	Not Used

The second ODB report event word holds an additional set of events which are now dependent on observation type. Details are given in [Tables 6.19](#) to [6.22](#).

The ODB report RDB flag word ([DEPRECATED], probably unused) is 30 bits packed which contains flags for five report parameters: latitude, longitude, date, time and altitude. Each parameter occupies 6 bits with further stratification which is identical for every parameter as indicated in [Table 6.23](#).

**Table 6.23** RDB report (latitude, longitude, date, time and altitude) flags. [DEPRECATED], probably unused.

Parameter	No. of Bits	Bit Position	Bit Position	No. of Bits	Value – Description		
			0	1	0 – No Human Monitoring Substitution 1 – Human Monitoring Substitution		
Latitude	6	0+	+1	1	0 – No Q/C Substitution 1 – Q/C Substitution		
Longitude	6	6+					
Date	6	12+	+2	1	0 – Override Flag not Set 1 – Override Flag Set		
Time	6	18+					
Altitude	6	24+	+3	2	0 – Parameter Correct 1 – Parameter Probably Correct 2 – Parameter Probably Incorrect 3 – Parameter Incorrect		
					+5	1	0 – Parameter Flag Set by Q/C or not Checked 1 – Parameter Flag Set by Human Monitoring

**Table 6.24** *Datum status.*

Bit Position	No. of Bits	Value – Description
0	1	1 – Report Active
1	1	1 – Passive Report
2	1	1 – Rejected Report
3	1	1 – Blacklisted Report

**Table 6.25** *Global datum events.*

Bit Position	No. of Bits	Value – Description
0	1	1 – Missing Vertical Coordinate
1	1	1 – Missing Observed Value
2	1	1 – Missing Background (First Guess) Value
3	1	1 – Rejected due to RDB Flag
4	1	1 – Activated due to RDB Flag
5	1	1 – Activated by Whitelist
6	1	1 – Bad Reporting Practice
7	1	1 – Vertical Position out of Range
8	1	1 – Reference Level Position out of Range
9	1	1 – Too Big First Guess Departure
10	1	1 – Too Big Departure in Assimilation
11	1	1 – Too Big Observation Error
12	1	1 – Redundant Datum
13	1	1 – Redundant Level
14	1	1 – Report Over Land
15	1	1 – Report Over Sea
16	1	1 – Not Analysis Variable
17	1	1 – Duplicate Datum/Level
18	1	1 – Too Many Surface Data
19	1	1 – Multi Level Check
20	1	1 – Level Selection
21	1	1 – Vertical Consistency Check
22	1	1 – Vertical Coordinate Changed from Z to P
23	1	1 – Datum Rejected via Namelist
24	1	1 – Combined Flagging
25	1	1 – Datum Rejected due to Rejected Report
26	1	1 – Variational QC Performed
27	1	1 – Observation Error Increased
28	1	1 – Cloud Contamination
29	1	1 – Rain Contamination
30	1	1 – Aerosol Contamination
31	1	1 – Missing or Not Sensible Emissivity Values

## 6.9 DATUM STATUS: EVENTS, RDB AND ANALYSIS FLAGS

The status of each datum, like report status, is described in terms of being: active, passive, rejected or blacklisted. [Table 6.24](#) shows that the ODB datum status is a packed word with 4 bits used to describe its status.

There are two ODB words reserved for datum events. They both use 31 bits each to store relevant information. The first event word has the same structure for all observation types, whereas the second event word is observation type dependent. [Tables 6.25](#) to [6.28](#) describe the event words structures for the observation types that use them.

**Table 6.26** *SYNOP datum events.*

Bit Position	No. of Bits	Value – Description
0	1	1 – Bias Corrected Ps
1–30	30	Not Used

**Table 6.27** *DRIBU datum events.*

Bit Position	No. of Bits	Value – Description
0	1	1 – Bias Corrected Ps
1–30	30	Not Used

**Table 6.28** *TEMP datum events.*

Bit Position	No. of Bits	Value – Description
0	1	1 – Bias Corrected Value Used
1–30	30	Not Used

**Table 6.29** *Datum blacklist events.*

Bit Position	No. of Bits	Value – Description
0	1	1 – Pressure Blacklisted
1	1	1 – Variable Blacklisted
2	1	1 – Blacklisted due to Pressure Code
3	1	1 – Blacklisted due to Distance from Reference Point
4	1	1 – Blacklisted due to Type of Vertical Coordinate
5	1	1 – Blacklisted due to Observed Value
6	1	1 – Blacklisted due to First Guess departure
7–30	24	Not Used

Furthermore, each datum in the ODB has a blacklist event word. This word uses 31 bits to describe various blacklist events as indicated in [Table 6.29](#).

For each datum in ODB there is an RDB flag ([DEPRECATED], probably unused) word which holds flags for pressure (vertical coordinate) and the datum itself. This is packed word with 30 bits used – see [Table 6.30](#). Pressure and datum RDB flags use 15 bits each. Thus pressure RDB flag starts at bit position 0, whereas the datum flag starts at bit position 15. Each 15 bits structure is further stratified in exactly the same way for both parameters:

In addition to RDB datum flags there is a word in ODB to store analysis flags. There are five types of analysis flags: final analysis, first guess, departure, variational q/c and blacklist flags. Each flag occupies 4 bits and the exact description is given in [Table 6.31](#).

**Table 6.30** *RDB pressure (vertical coordinate) and datum flags. [DEPRECATED], probably unused.*

Parameter	No. of Bits	Bit Position	Bit Position	No. of Bits	Value – Description
			0	1	0 – No Human Monitoring Substitution 1 – Human Monitoring Substitution
Pressure	15	0+	+1	1	0 – No Q/C Substitution 1 – Q/C Substitution
Datum	15	15+	+2	1	0 – Override Flag not Set 1 – Override Flag Set
			+3	2	0 – Correct 1 – Probably Correct 2 – Probably Incorrect 3 – Parameter Incorrect
			+5	1	0 – Flag Set by Q/C or not Checked 1 – Flag Set by Human Monitoring
			+6	2	0 – Previous Analysis judged it correct 1 – Previous Analysis judged it probably correct 2 – Previous Analysis judged it probably incorrect 3 – Previous Analysis judged it incorrect
			+8	1	0 – Not used by previous analysis 1 – Used by previous analysis
			+9	5	Not Used

**Table 6.31** *Analysis flags. DEPRECATED, probably unused.*

Flag Type	Bit Position	No. of Bits	Value – Description
Final	0	4	0 – Correct 1 – Probably correct 2 – Probably incorrect 3 – Incorrect
First Guess	4	4	0 – Correct 1 – Probably correct 2 – Probably incorrect 3 – Incorrect
Departure	8	4	0 – Correct 1 – Probably correct 2 – Probably incorrect 3 – Incorrect
Variational Q/C	12	4	0 – Correct 1 – Probably correct 2 – Probably incorrect 3 – Incorrect
Blacklist	16	4	0 – Correct 1 – Probably correct 2 – Probably incorrect 3 – Incorrect
Not Defined	20	11	Reserved

## References

- Alduchov, O. A. and Eskridge, R. E. (1996). Improved Magnus form approximation of saturation vapor pressure. *J. Appl. Meteorol.*, **35**, 601–609.
- Andersson, E., Pailleux, J., Thépaut, J.-N., Eyre, J. R., McNally, A. P., Kelly, G. A. and Courtier, P. (1994). Use of cloud-cleared radiances in three/four-dimensional variational data assimilation. *Q. J. R. Meteorol. Soc.*, **120**, 627–653.
- Baordo, F. and Geer, A. J. (2016). Assimilation of SSMIS humidity-sounding channels in all-sky conditions over land using a dynamic emissivity retrieval. *Quarterly Journal of the Royal Meteorological Society*, doi: 10.1002/qj.2873.
- Bauer, P., Geer, A. J., Lopez, P. and Salmond, D. (2010). Direct 4D-Var assimilation of all-sky radiances: Part I. Implementation. *Q. J. R. Meteorol. Soc.*, **136**, 1868–1885.
- Blondin, C. (1991). Parametrization of land surface processes in numerical weather prediction. In T. J. Schmugge and J.-C. André (Eds), *Land Surface Evaporation: Measurement and Parametrization*, pp. 31–54, Springer-Verlag.
- Bonavita, M., Dahoui, M., Lopez, P., Prates, F., Holm, E., Chiara, G. D., Geer, A., Isaksen, L. and Ingleby, B. (2017). On the initialization of tropical cyclones. *ECMWF Tech. Memo. No. 810*.
- Bormann, N. (2014). Reformulation of the emissivity kalman filter atlas. *RD Internal Memorandum*, p. 14pp, available online: <http://intra.ecmwf.int/publications/library/do/references/show?id=1471>.
- Bormann, N. (2017). Slant path radiative transfer for the assimilation of sounder radiances. *Tellus A: Dynamic Meteorology and Oceanography*, **69**(1), 1272779.
- Bormann, N. and Bonavita, M. (2013). Spread of the ensemble of data assimilations in radiance space. *ECMWF Technical Memorandum 708*.
- Bormann, N., Bonavita, M., Dragani, R., Eresmaa, R., Matricardi, M. and McNally, A. (2016). Enhancing the impact of IASI observations through an updated observation-error covariance matrix. *Q. J. R. Meteorol. Soc.*, **142**, 1767–1780.
- Bormann, N. and Healy, S. (2006). A fast radiative-transfer model for the assimilation of MIPAS limb radiances: Accounting for horizontal gradients. *Q. J. R. Meteorol. Soc.*, **132**, 2357–2376.
- Bormann, N., Healy, S. and Hamrud, M. (2007). Assimilation of MIPAS limb radiances in the ECMWF system. Part II: Experiments with a 2-dimensional observation operator and comparison to retrieval assimilation. *Q. J. R. Meteorol. Soc.*, **133**, 329–346.
- Bormann, N., Matricardi, M. and Healy, S. (2005). A fast radiative transfer model for the assimilation of infrared limb radiances from MIPAS. *Q. J. R. Meteorol. Soc.*, **131**, 1631–1653.
- Bormann, N., Saarinen, S., Kelly, G. and Thépaut, J.-N. (2003). The spatial structure of observation errors in atmospheric motion vectors from geostationary satellite data. *Mon. Wea. Rev.*, **131**, 706–718.
- Bormann, N. and Thépaut, J.-N. (2007). Assimilation of MIPAS limb radiances in the ECMWF system. Part I: Experiments with a 1-dimensional observation operator. *Q. J. R. Meteorol. Soc.*, **133**, 309–327.

- Buck, A. L. (1981). New equations for computing vapor pressure and enhancement factor. *J. Appl. Meteorol.*, **20**, 1527–1532.
- Cardinali, C., Andersson, E., Viterbo, P., Thépaut, J.-N. and Vasiljevic, D. (1994). Use of conventional surface observations in three-dimensional variational data assimilation. *ECMWF Tech. Memo. No. 205*.
- Cardinali, C., Isaksen, L. and Andersson, E. (2003). Use and impact of automated aircraft data in a global 4D-Var data assimilation system. *Mon. Wea. Rev.*, **131**, 1865–1877.
- Courtier, P., Andersson, E., Heckley, W., Pailleux, J., Vasiljevic, D., Hamrud, M., Hollingsworth, A., Rabier, F. and Fisher, M. (1998). The ECMWF implementation of three dimensional variational assimilation (3D-Var). I: Formulation. *Q. J. R. Meteorol. Soc.*, **124**, 1783–1807.
- Deblonde, G. and English, S. (2001). Evaluation of the fastem-2 fast microwave oceanic surface emissivity model. In *Tech. Proc. ITSC-XI*, pp. 67–78, Budapest.
- Engelen, R. J., Andersson, E., Chevallier, F., Hollingsworth, A., Matricardi, M., McNally, A., Thépaut, J.-N. and Watts, P. (2004). Estimating atmospheric CO<sub>2</sub> from advanced infrared satellite radiances within an operational 4D-Var data assimilation system: Methodology and first results. *J. Geophys. Res.*, **109**, D19309.
- Eyre, J. R. (1991). A fast radiative transfer model for satellite sounding systems. *ECMWF Tech. Memo. No. 176*.
- Geer, A. J., Baordo, F., Bormann, N. and English, S. (2014). All-sky assimilation of microwave humidity sounders. *ECMWF technical memorandum, in preparation*.
- Geer, A. J. and Bauer, P. (2011). Observation errors in all-sky data assimilation. *Q. J. R. Meteorol. Soc.*, DOI: 10.1002/qj.830.
- Geer, A. J. and Bauer, P. (2012). Assimilating AMSU-A radiances sensitive to cloud and temperature using the all-sky approach. *ECMWF technical memorandum 670*.
- Geer, A. J., Bauer, P. and Lopez, P. (2008). Lessons learnt from the operational 1D+4D-Var assimilation of rain- and cloud-affected SSM/I observations at ECMWF. *Q. J. R. Meteorol. Soc.*, **134**, 1513–1525.
- Geer, A. J., Bauer, P. and Lopez, P. (2010). Direct 4D-Var assimilation of all-sky radiances: Part II. Assessment. *Q. J. R. Meteorol. Soc.*, **136**, 1886–1905.
- Geleyn, J.-F. (1988). Interpolation of wind, temperature and humidity values from the model levels to the height of measurement. *Tellus*, **40**, 347–351.
- Han, W. and Bormann, N. (2016). Constrained adaptive bias correction for satellite radiance assimilation in the ECMWF 4D-Var system. *ECMWF Tech. Memo. No. 783.*, doi:10.21957/rex0omex.
- Healy, S. and Thépaut, J.-N. (2006). Assimilation experiments with CHAMP GPS radio occultation measurements. *Q. J. R. Meteorol. Soc.*, **132**, 605–623.
- Hersbach, H. (2010a). Assimilation of scatterometer data as equivalent-neutral wind. *ECMWF Tech. Memo. No. 629*.
- Hersbach, H. (2010b). Comparison of c-band scatterometer cmod5.n equivalent neutral winds with ecmwf. *J. Atmos. Oceanic Technol.*, **27**, 721–736.
- Hersbach, H. (2011). Sea surface roughness and drag coefficient as functions of neutral wind speed. *J. Phys. Oceanogr.*, **41**, 247–251.
- Hersbach, H., Stoffelen, A. and de, S. H. (2007). An improved C-band scatterometer ocean geophysical model function: CMOD5. *J. Geophys. Res.*, **112**, doi:10.1029/2006JC003743.
- Hocking, J. (2014). Interpolation methods in the rttov radiative transfer model. *Forecast Research Technical Report No. 590*.



- Huddleston, J. N. and Stiles, B. W. (2000). Multidimensional histogram (MUDH) rain flag. *Product Description Version 2.1*, URL <http://podaac-www.jpl.nasa.gov/quikscat/>.
- Ingleby, B. (2015). Global assimilation of air temperature, humidity, wind and pressure from surface stations. *Q. J. R. Meteorol. Soc.*, **141**, 504–517.
- Isaksen, L. and Janssen, P. A. E. M. (2004). Impact of ERS scatterometer winds in ECMWF's assimilation. *Q. J. R. Meteorol. Soc.*, **130**, 1793–1814.
- Järvinen, H., Andersson, E. and Bouttier, F. (1999). Variational assimilation of time sequences of surface observations with serially correlated errors. *ECMWF Tech. Memo. No. 266*.
- Järvinen, H., Saarinen, S. and Undén, P. (1996). *User's Guide for Blacklisting*. Available on request from ECMWF, Shinfield Park, RG2 9AX, Reading, Berkshire, UK.
- Järvinen, H. and Undén, P. (1997). Observation screening and first guess quality control in the ECMWF 3D-Var data assimilation system. *ECMWF Tech. Memo. No. 236*.
- Karbou, F., Gérard, E. and Rabier, F. (2006). Microwave land emissivity and skin temperature for AMSU-A and -B assimilation over land. *Q. J. R. Meteorol. Soc.*, **132**, 2333–2355.
- Krzeminski, B., Bormann, N., Karbou, F. and Bauer, P. (2009a). Improved use of surface-sensitive microwave radiances at ECMWF. In *Proceedings of 2009 EUMETSAT Meteorological Satellite Conference*, Bath, United Kingdom.
- Krzeminski, B., Bormann, N., Kelly, G., McNally, A. and Bauer, P. (2009b). Revision of the HIRS cloud detection at ecmwf. *ECMWF/EUMETSAT fellowship reports No. 19*.
- Lean, K. and Bormann, N. (2021). Using model cloud information to reassign low level AMVs for NWP. *ECMWF/EUMETSAT fellowship reports No. 56*.
- Lean, P., Geer, A., Salmond, D. and Hague, J. (2016). The cost and scalability of observation processing in IFS; implications for future observation usage. *RD internal memo, RD16-045*.
- Leidner, S. M., Hoffman, R. N. and Augenbaum, J. (2000). *SeaWinds Scatterometer Real-Time BUFR Geophysical Data Product, User's Guide Version 2.3.0*. NOAA/NESDIS.
- Lönnerberg, P. (1989). Developments in the ECMWF analysis system. In *Proc. ECMWF Seminar on Data assimilation and the Use of Satellite Data*, pp. 75–119, Reading, 5–9 September 1988.
- Lönnerberg, P. and Shaw, D. (1985). Data selection and quality control in the ECMWF analysis system. In *ECMWF Workshop on The Use And Quality Control of Meteorological Observations*, pp. 225–254, Reading, 6–9 November 1984.
- Lönnerberg, P. and Shaw, D. (Eds) (1987). *ECMWF Data Assimilation Scientific Documentation, Research Manual 1*.
- Lopez, P. (2011). Direct 4d-var assimilation of NCEP stage IV radar and gauge precipitation data at ecmwf. *Monthly Weather Review*, **139**(7), 2098–2116.
- Lorenc, A. C. (1986). Analysis methods for numerical weather prediction. *Q. J. R. Meteorol. Soc.*, **112**, 1177–1194.
- Louis, J.-F. (1979). A parametric model of vertical eddy fluxes in the atmosphere. *Boundary-Layer Meteorol.*, **17**, 187–202.
- Louis, J.-F., Tiedtke, M. and Geleyn, J.-F. (1982). A short history of the PBL parametrization at ECMWF. In *Proc. ECMWF Workshop on Planetary Boundary Layer Parameterization*, pp. 59–80, Reading, 25–27 November, 1981.
- Lupu, C. and McNally, A. (2012). Assimilation of cloud affected radiances from meteosat-9 at ecmwf. *ECMWF/EUMETSAT fellowship reports No. 25*.

- Matricardi, M., Chevallier, F. and Tjemkes, S. (2001). An improved fast radiative transfer model for the assimilation of radiance observations. *ECMWF Tech. Memo. No. 345*.
- McNally, A. P. (2009). The direct assimilation of cloud affected satellite infrared radiances in the ecmwf 4d-var. *Q. J. R. Meteorol. Soc.*, **135**, 1214–1229.
- McNally, A. P., Andersson, E., Kelly, G. and Saunders, R. W. (1999). The use of raw TOVS/ATOVS radiances in the ECMWF 4D-Var assimilation system. *ECMWF Newsletter No. 83*, pp. 2–7.
- McNally, A. P. and Watts, P. D. (2003). A cloud detection algorithm for high spectral resolution infrared sounders. *Q. J. R. Meteorol. Soc.*, **129**, 3411–3423.
- Munro, R., Köpken, C., Kelly, G., Thépaut, J.-N. and Saunders, R. (2004). Assimilation of Meteosat radiance data within the 4D-Var system at ECMWF: Data quality monitoring, bias correction and single-cycle experiments. *Q. J. R. Meteorol. Soc.*, **130**, 2293–2313.
- Pailleux, J. (1990). A global variational assimilation scheme and its application for using TOVS radiances. In *Proc. WMO International Symposium on Assimilation of Observations in Meteorology and Oceanography*, pp. 325–328, Clermont-Ferrand, France.
- Saunders, R. W. and Matricardi, M. (1998). A fast forward model for ATOVS (RTATOV). In *Tech. Proc. 9th International TOVS Study Conference*, p. 11 pp, Igls, Austria, 20–26 February, 1997.
- Sherlock, V. J. (1999). ISEM-6: Infrared Surface Emissivity Model for RRTOV-6. *Forecasting Research Technical Report No. 299*, available from Met Office, London Road, Bracknell, Berkshire RG12 2SZ, UK.
- Simmons, A. J. and Burridge, D. (1981). An energy and angular momentum conserving vertical finite difference scheme and hybrid coordinate. *Mon. Wea. Rev.*, **109**, 758–766.
- Simmons, A. J. and Chen, J. (1991). The calculation of geopotential and the pressure gradient in the ECMWF atmospheric model: Influence on the simulation of the polar atmosphere and on temperature analyses. *Q. J. R. Meteorol. Soc.*, **117**, 29–58.
- Stoffelen, A. and Anderson, D. (1997). Ambiguity removal and assimilation of scatterometer data. *Q. J. R. Meteorol. Soc.*, **123**, 491–518.
- Tomassini, M., LeMeur, D. and Saunders, R. W. (1998). Near-surface satellite wind observations of hurricanes and their impact on ECMWF model analyses and forecasts. *Mon. Wea. Rev.*, **126**, 1274–1286.
- Vasiljevic, D., Cardinali, C. and Undén, P. (1992). ECMWF 3D-Variational assimilation of conventional observations. In *Proc. ECMWF Workshop on Variational Assimilation with Emphasis on Three-dimensional Aspects*, Reading, 9–12 November 1992.
- Wattrelot, E., Caumont, O. and Mahfouf, J.-F. (2014). Operational implementation of the 1D+3D-Var assimilation method of radar reflectivity data in the AROME model. *Monthly Weather Review*, **142**(5), 1852–1873.